# Radiative Corrections to Hadron Production in $e^+e^-$ Annihilations at DAΦNE Energies

D I S S E R T A T I O N

zur Erlangung des akademischen Grades
doctor rerum naturalium
(Dr. rer. nat.)
im Fach Physik

eingereicht an der
Mathematisch-Naturwissenschaftlichen Fakultät I
der Humboldt-Universität zu Berlin

von
Dipl.-Phys. Axel Hoefer
geboren am 10.02.1970 in Ekeren (Belgien)

Präsident der Humboldt-Universität zu Berlin:
Prof. Dr. J. Mlynek

Dekan der Mathematisch-Naturwissenschaftlichen Fakultät I:
Prof. Dr. B. Ronacher

Gutachter:

1. Prof. Dr. F. Jegerlehner
2. Prof. Dr. U. Wolff
3. Prof. Dr. J. Fleischer

eingereicht am 26. Oktober 2001
Tag der mündlichen Prüfung: 8. März 2002

**Abstract**

Radiative corrections to low energy hadron production as measured at the $e^+e^-$–colliders DA$\Phi$NE and VEPP-2M are investigated. The goal of this work is to provide the theoretical condition for extracting hadronic cross sections undressed from QED corrections from the measured data with a precision of per mill level. High precision hadronic data are required to reduce the theoretical error of the running fine structure constant $\alpha(s)$ and the muon anomalous magnetic moment $a_\mu$ and therefore represent a key to a possible discovery of "new physics". Especially the channel of charged pion pair production $e^+e^- \to \pi^+\pi^-$ below 1 GeV appears to be of great importance. To this process the complete $O(\alpha)$ QED initial state, final state and initial–final state interference corrections are calculated. Analytic formulae are given for the virtual and for the real photon corrections. The total cross section ($\sigma$), the pion angular distribution ($d\sigma/d\cos\Theta$) and the $\pi^+\pi^-$ invariant mass distribution ($d\sigma/ds'$) are investigated in the regime of experimentally realistic kinematical cuts. It is shown that in addition to the full $O(\alpha)$ corrections also the $O(\alpha^2)$ and leading log $O(\alpha^3)$ photonic corrections as well as the contributions from IS $e^+e^-$ pair production have to be taken into account if at least per cent accuracy is required. For the data analysis I focus on an inclusive treatment of all photons. The theoretical error concerning this treatment of radiative corrections is then estimated to be 2 per mill for both the measurement of the total cross section and the $\pi^+\pi^-$ invariant mass distribution. In addition the model uncertainty due to the pion substructure is discussed. To be able to extract the pion form factor from the experimental data with the desired accuracy a dedicated Fortran program was written which allows to take into account experimentally realistic kinematical cuts. Altogether the precision of the theoretical prediction matches the requirements of low energy $e^+e^-$ experiments like the ones at DA$\Phi$NE and VEPP-2M.

**Keywords:**
QED Corrections, hadronic cross sections, DA$\Phi$NE physics, Standard Model

**Zusammenfassung**

Strahlungskorrekturen zur Hadronproduktion bei niedrigen Energien, wie man sie an den $e^+e^-$-Beschleunigern DA$\Phi$NE und VEPP-2M misst, werden untersucht. Ziel dieser Arbeit ist es, die von QED–Korrekturen befreiten hadronischen Wirkungsquerschnitte aus den hadronischen Daten mit einer Präzision auf Promille–Niveau zu extrahieren.

Hadronische Präzisionsdaten werden benötigt, um den theoretischen Fehler zur laufenden Feinstrukturkonstanten $\alpha(s)$ und zum anomalen magnetischen Moment des Myons $a_\mu$ zu senken und sie stellen daher einen Schlüssel zur möglichen Entdeckung "neuer Physik" dar. Insbesondere die Paarproduktion geladener Pionen $e^+e^- \to \pi^+\pi^-$ unterhalb einer Energie von 1 GeV ist von grosser Wichtigkeit. Zu diesem Prozess werden die vollständigen $O(\alpha)$–QED–Korrekturen zum Anfangszustand, Endzustand sowie die Interferenzkorrekturen berechnet. Analytische Formeln zu den virtuellen und reellen photonischen Korrekturen werden angegeben. Der totale Wirkungsquerschnitt ($\sigma$), die Pion–Winkelverteilung ($d\sigma/d\cos\Theta$) und die Invariantemasseverteilung des Pionpaars ($d\sigma/ds'$) werden für den Fall realistischer kinematischer Schnitte untersucht. Es wird gezeigt, dass zusätzlich zu den vollständigen $O(\alpha)$–Korrekturen zusätzlich die photonischen Anfangszustandskorrekturen der Ordnung $O(\alpha^2)$ und führende Photonbeiträge der Ordnung $O(\alpha^3)$ sowie Beiträge zur $e^+e^-$-Paarabstrahlung vom Anfangszustand berücksichtigt werden müssen wenn mindestens eine Genauigkeit auf Prozent–Niveau verlangt wird. Für die Datenanalyse wird der Schwerpunkt auf eine inklusive Behandlung aller Photonen gelegt. Die Messung sowohl des totalen Wirkungsquerschnitts als auch der $\pi^+\pi^-$–Invariantemasseverteilung betreffend wird der theoretische Fehler dieser Behandlung der Strahlungskorrekturen mit 2 Promille abgeschätzt. Ausserdem wird die Modellunsicherheit als Folge der Pion–Substruktur diskutiert. Um den Formfaktor mit der gewünschten Präzision aus den experimentellen Daten extrahieren zu können, wurde ein auf diese Fragestellung zugeschnittenes Fortran-Programm geschrieben, welches die Berücksichtigung realistischer kinematischer Schnitte erlaubt. Insgesamt erfüllt die Genauigkeit der theoretischen Vorhersagen die Erfordernisse der Niedrigenergie–$e^+e^-$–Experimente wie diejenigen bei DA$\Phi$NE oder VEPP-2M.

**Schlagwörter:**
QED-Korrekturen, hadronische Wirkungsquerschnitte, DA$\Phi$NE-Physik, Standardmodell

# Contents

# List of Figures

# List of Tables

# Chapter 1

# Introduction and Motivation

The goal of high energy physics research is to understand nature on the most fundamental level. The questions to be answered are "what are the basic constituents of matter?" and "what are the fundamental interactions that govern all processes in nature?". Thanks to the theoretical, experimental and technical progress throughout the last century it became possible to test theoretical predictions in experiment with increasing precision.

In 1949 Tomonaga, Schwinger and Feynman [1, 2, 3, 4, 5, 6] showed how to extract meaningful physical predictions from quantum electrodynamics (QED). This lead to very precise calculations of electromagnetic effects at subatomic scales like the evaluation of the anomalous magnetic moment of the electron $a_e$ up to fourth order in the electromagnetic fine structure constant $\alpha$ [7, 8]. Experimentally the theoretical result was confirmed with an accuracy of one part in $10^8$ [9]. The measured value of $a_e$ currently provides the best determination of the fine structure constant[1] [11]:

$$\alpha^{-1} = 137.03599958(52) \; . \tag{1.1}$$

Another variable which can be precisely evaluated as well as accurately measured is the muon anomalous magnetic moment $a_\mu$. Only recently, by an analysis of the '98 and '99 data, taken at the E821 muon experiment at the Brookhaven National Laboratory (BNL) [12], the experimental error of $a_\mu$ could be reduced by about a factor 0.18 compared to the previous value from the muon experiment at CERN [13]. Averaging the results of the two experiments leads to the so far best experimental value for the muon anomalous magnetic moment:

$$a_\mu^{exp} \;\; = \;\; (1165920.23 \pm 1.51) \times 10^{-9} \; . \tag{1.2}$$

Although this is less accurate by about a factor 350 than the experimental value for $a_e$, the measurement of $a_\mu$ appears to be much better suited for probing short distance effects. This is because for $a_\mu$ these effects are in general enhanced by a factor

[1] The best determination of $\alpha$ *not* depending on $a_e$ is coming from quantum Hall effect measurements [10].

$m_\mu^2/m_e^2 \simeq 40000$ in respect to $a_e$ ($m_\mu$ and $m_e$ being the muon and electron mass). This enhancement clearly overcompensates for the larger experimental error of $a_\mu$. The present situation is going to be improved even further when the experimental error is reduced to its target value[2] of $4 \times 10^{-10}$ which is more accurate than the present theoretical value [14, 15, 16, 17, 18, 19, 20, 21, 22, 23, 24, 25, 26, 27, 28]:

$$\begin{aligned} a_\mu^{th} &= a_\mu^{\rm QED} + a_\mu^{\rm had} + a_\mu^{\rm weak} + a_\mu^{\rm NEW} \\ &= (1165847.06 \pm 0.03 \ + \ 68.03 \pm 1.1 \ + \ 1.51 \pm 0.04 + ? \ ) \ \times 10^{-9} \\ &= (1165916.6 \pm 1.1) \times 10^{-9} \ . \end{aligned} \tag{1.3}$$

In eq. (1.3) the contributions $a_\mu^{\rm QED}$, $a_\mu^{\rm had}$ and $a_\mu^{\rm weak}$ are due to the pure electromagnetic, the strong[3] and the weak interaction, respectively. $a_\mu^{\rm NEW}$ corresponds to yet unknown contributions from physics beyond the standard model. From the comparison of the experimental and theoretical value, given in eq. (1.2) and (1.3), one finds that

1. the measurement of $a_\mu$ is highly sensitive to QCD effects (for recent discussions see e.g. [29, 30, 31]),

2. the theoretical error is dominated by the error of the hadronic contribution which is of the same order as the complete electroweak contribution,

3. $a_\mu^{exp}$ and $a_\mu^{th}$ do not agree within the given error when only taking standard model contributions into account [$a_\mu^{exp} - a_\mu^{th} = (3.63 \pm 1.87) \times 10^{-9}$], which is evidence for new physics[4],

4. the new physics effects appear to be about three times larger than the weak interaction contributions.

Assuming that the deviation of $a_\mu^{exp}$ from the standard model value is due to a true physical effect it is still possible to think of many different scenarios which could be responsible for it. In the past the impact of supersymmetric models on $a_\mu$ was discussed by several authors [36, 37, 38, 39, 40, 41, 42, 43, 44]. Recent attempts to explain the data can be found e.g. in [32] and several other publications like [45, 46, 47, 48, 49, 50, 51, 52, 53, 54, 55].

Clearly, to catch up with the increasing experimental precision, a reduction of the theoretical error of $a_\mu^{\rm had}$ is absolutely mandatory. By far the dominant contribution to $a_\mu^{\rm had}$ (more than 97%) corresponds to the 2-loop vertex correction diagram

[2] This is expected to be achieved soon, when the E821 data of the 2000 run and the 2001 run are included into the analysis.

[3] $a_\mu^{\rm had}$ contains the first and second order hadronic vacuum polarization contribution as well as the contribution from light-by-light scattering.

[4] Hence the evidence for new physics is estimated to be a $2\,\sigma$ effect which is smaller than the estimated $2.6\,\sigma$ effect in [32]. This is because in eq. (1.3) the more conservative value for $a_\mu^{\rm had}$ given in [19] was taken while in [32] the value given in [33] was used (see also [34, 35]).

with a hadronic vacuum polarization insertion into the photon propagator, which is shown in Fig. 1.1. Here the hadronic "blob" includes all quark contributions to the photon propagator. Photonic vacuum polarization effects lead to a screening of the electromagnetic charge. Hence the electromagnetic coupling strength becomes a function of the energy scale. This can be expressed by a running effective fine structure constant:

$$\alpha(s) \;=\; \frac{\alpha}{1-\Delta\alpha(s)}\,, \tag{1.4}$$

where $\sqrt{s}$ is the invariant mass of the virtual photon. $\Delta\alpha$ is the sum of approximately equal contributions from hadronic and leptonic vacuum polarization effects:

$$\Delta\alpha(s) = \Delta\alpha_{\rm lep}(s) + \Delta\alpha_{\rm had}(s) \;=\; -4\pi\alpha\;\Re e\left[\Pi'_\gamma(s) - \Pi'_\gamma(0)\right]\,, \tag{1.5}$$

$\Pi'_\gamma(s)$ being the irreducible photon vacuum polarization which is defined via the time-ordered current correlator function:

$$i\int d^4x\, e^{iq\cdot x}\langle 0|{\rm T} j^\mu_{em}(x) j^\nu_{em}(0)|0\rangle \;=\; -(q^2 g^{\mu\nu} - q^\mu q^\nu)\Pi'_\gamma(q^2)\,. \tag{1.6}$$

Here $j^\mu_{em}$ is the electromagnetic current. The leptonic contribution $\Delta\alpha_{\rm lep}$ can be evaluated in a straight forward way by using perturbation theory. This is not possible for the hadronic contribution $\Delta\alpha_{\rm had}$ since perturbative QCD is not applicable at low energies. Fortunately $\Delta\alpha_{\rm had}$ can be related to the total cross section for hadron production in $e^+e^-$ collisions $\sigma_{\rm had}(s) = \sigma(e^+e^- \to \gamma^* \to \text{hadrons})$, when taking into account analyticity and unitarity[5] [56, 57]. $\Delta\alpha_{\rm had}$ can then conveniently be expressed in terms of a dispersion integral [58, 59]:

$$\Delta\alpha_{\rm had}(s) = -\frac{\alpha s}{3\pi}{\rm Re}\int_{4m_\pi^2}^\infty ds' \frac{R(s')}{s'(s'-s-i\epsilon)}\,, \tag{1.7}$$

$R(s)$ being the $e^+e^-$ cross section for the production of a hadronic final state normalized to the total cross section for muon pair production at the $e^+e^-$ center of mass energy $\sqrt{s}$:

$$R(s) = \frac{\sigma(e^+e^- \to \gamma^*(s) \to \text{hadrons})}{\sigma(e^+e^- \to \gamma^*(s) \to \mu^+\mu^-)}\,. \tag{1.8}$$

While the high energy tail of the dispersion integral (1.7) can be calculated within perturbative QCD, at low $s$ the cross section ratio $R(s)$ has to be determined from experimental data. Hence our knowledge of $\Delta\alpha(s)$ depends on precise measurements of low energy hadronic cross sections.

[5] Analyticity is a consequence of causality. It implies the dispersion relation which relates the imaginary part of an analytic complex function to its real part. Unitarity implies the optical theorem which here can be used to relate the total hadronic cross section to the imaginary part of the hadronic vacuum polatization.

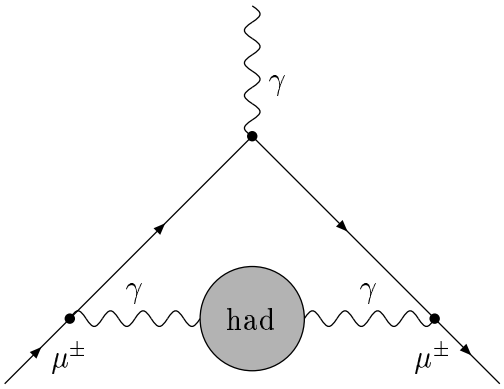


Figure 1.1: leading contribution to $a_\mu^{\rm had}$

Also the hadronic contribution to $a_\mu$ corresponding to the Feynman diagram in Fig. 1.1 can be expressed by a dispersion integral over the cross section ratio $R(s)$, although with a different kernel [57, 60, 18, 61, 33, 62]:

$$a_\mu^{\rm had(1)} \;=\; \Big(\frac{\alpha m_\mu}{3\pi}\Big)^2 \int_{4m_\pi^2}^{\infty} ds\, \frac{R(s)\hat{K}(s)}{s^2}\,. \tag{1.9}$$

In eq. (1.9) $\hat{K}(s)$ is a bounded function in $s$ ($0.63 \leq \hat{K}(s) < 1$ for $4m_\pi^2 \leq s < \infty$). Note that the integrand in (1.9) contains two powers of $s$ in the denominator. It is therefore strongly peaked for small energies. As a consequence most important for the accurate evaluation of $a_\mu^{\rm had}$ is the precise knowledge of low energy hadronic cross sections which account for the major contribution to the dispersion integral (see Table 1.1 which was taken from [62]). In fact more than 70 % of $a_\mu^{\rm had}$ is related to hadronic processes with center of mass energies below 1 GeV. This is mainly the region of the $\rho/\omega$ resonance. A more precise measurement of $\sigma_{\rm had}$ at low energies would also reduce the theoretical error of the fine structure constant at the Z-boson resonance $\alpha(M_Z^2)$. This is necessary to get stronger constraints on the parameters of the standard model.

Since cross sections at low energies cannot be obtained by using perturbative QCD they have to be measured in $e^+e^-$ collision experiments. A recent update [19] of a detailed analysis by Eidelman and Jegerlehner [18] includes new low energy hadronic data from VEPP-2M [63, 64, 65] and BES II [66] which reduces the error of $a_\mu^{\rm th}$ by about a factor[6] 2/3. Nonetheless the main task remains a more precise determination of the cross section $\sigma(e^+e^- \to \rho, \omega \to \pi^+\pi^-)$ for the production of a charged pion pair via a $\rho/\omega$ intermediate state[7]. Alemany, Davier and Höcker [61] used additional data from $\tau$ decays which can be related to the above cross section

[6] This is the error given in eq. (1.3).

[7] A recent analysis of four pion production which is important at energies above 1 GeV was presented in [67].

| channel | $\tilde{a}_\mu^{\rm had}$ | acc. | channel | $\tilde{a}_\mu^{\rm had}$ | acc. |
|---|---|---|---|---|---|
| $\rho, \omega \to \pi^+\pi^-$ | 506 | 0.3% | $3\pi$ | 4 | 10% |
| $\omega \to 3\pi$ | 47 | $\sim 1\%$ | $K^+K^-$ | 4 | $\downarrow$ |
| $\phi$ | 40 | $\downarrow$ | $K_SK_L$ | 1 | $\cdot$ |
| $\pi^+\pi^-\pi^0\pi^0$ | 24 | $\cdot$ | $\pi^+\pi^-\pi^+\pi^-\pi^0$ | 1.8 | $\cdot$ |
| $\pi^+\pi^-\pi^+\pi^-$ | 14 | $\cdot$ | $\pi^+\pi^-\pi^+\pi^-\pi^+\pi^-$ | 0.5 | $\cdot$ |
| $\pi^+\pi^-\pi^+\pi^-\pi^0\pi^0$ | 5 | 10% | $p\bar{p}$ | 0.2 | $\cdot$ |
| 2 GeV $\leq E \leq M_{J/\psi}$ | 22 | | | | |
| $M_{J/\psi} \leq E \leq M_\Upsilon$ | 20 | | | | |
| $M_\Upsilon < E$ | $\lesssim 5$ | | | | |

Table 1.1: Contribution to $\tilde{a}_\mu^{\rm had} = a_\mu^{\rm had} \times 10^{10}$ from exclusive hadronic channels and the desired accuracy for the measurement of the corresponding hadronic cross sections

by isospin symmetry. Isospin, however, is violated by the electromagnetic interaction, leading to a systematic error which is hard to estimate. A precise theoretical prediction of $a_\mu$ therefore still has to be based on $e^+e^-$ data. To reduce the error of $a_\mu^{th}$ to a level which is comparable to what can be reached by the E821 experiment one would have to measure $\sigma_{\rm had}(\sqrt{s} \leq 1\,{\rm GeV})$ with an accuracy of 0.3 %[8][18]. The experiments best suited for this job appear to be the KLOE experiment at the DAΦNE collider in Frascati as well as the experiments SND and CMD-2 at the VEPP-2M collider in Novosibirsk. While at VEPP-2M the hadronic data for the different center of mass energies are taken via an energy scan [63], at the DAΦNE collider, which will be running on the Φ resonance for the next few years [68, 69, 70], the radiative return due to initial state radiation is used to measure $\sigma_{\rm had}$ below the Φ peak ($\sqrt{s} = 1.02\,{\rm GeV}$)[9]. Although by this method statistics is reduced by about two orders of magnitude this handicap can be compensated by virtue of the high luminosity of the DAΦNE collider[10]. Furthermore, since at DAΦNE the collision energy is fixed at 1.02 GeV, the energy calibration has to be done only once which leads to a reduction of the systematic error. One therefore can expect that $\sigma_{\rm had}(\sqrt{s} \leq 1\,{\rm GeV})$ will be determined with the desired precision within the next few years.

Note that the hadronic cross section which is observed experimentally is not the quantity that is needed for the dispersion integral (1.7) and (1.9) for which the

[8] As an intermediate goal reaching a precision of 1 % for center of mass energies $\sqrt{s} \leq 1.4\,{\rm GeV}$ could already reduce the theoretical error of $a_\mu^{\rm had}$ substantially to about $7 \times 10^{-10}$.

[9] The radiative return phenomenon also allows to measure low energy cross sections at the $B$-factories BABAR/SLAC and BELLE/KEK [71]. At higher energies $R(s)$ measurements are performed by the BES Collaboration at BEPC [72, 73]. Future plans attempt to remeasure $R(s)$ in the range $M_\Phi < E_{\rm cm} < M_{J/\psi}$ (PEP-N project at SLAC).

[10] The design luminosity of DAΦNE is $L = 5 \times 10^{32}{\rm cm}^{-2}{\rm s}^{-1}$. In December '00 a peak luminosity of $L = 1.8 \times 10^{31}{\rm cm}^{-2}{\rm s}^{-1}$ could be reached. This value is expected to be improved even further in the near future.

following definition has been adopted:

$$R(s) \;=\; \sigma^{(0)}_{\rm had}(s)/\frac{4\pi\alpha^2}{s}\,. \tag{1.10}$$

This is the undressed hadronic cross section

$$\sigma^{(0)}_{\rm had}(s) = \sigma_{\rm had}(s)(\alpha/\alpha(s))^2 \tag{1.11}$$

in terms of the lowest order $\mu$-pair production cross section at $s \gg m_\mu^2$ [18]. The observed cross section in contrast is distorted by radiative effects due to real and virtual initial state (IS) and final state (FS) photons. Hence the measured hadronic cross sections have to be undressed from radiative corrections. Here IS bremsstrahlung represents the dominant contribution which can easily account for an effect of several percent, depending on the respective center of mass energy. But also FS corrections can lead to sizable contributions which can exceed 1% of the measured total cross section. Concerning the measurement of the hadron invariant mass distribution $d\sigma/ds'$ as done at DAΦNE the contribution due to final state photons[11] can exceed 10%.

Hence to reach the desired per mill accuracy for $\sigma_{\rm had}(\sqrt{s} \leq 1\,{\rm GeV})$ a careful treatment of QED corrections is needed. This includes above all the complete calculation of the massive $O(\alpha)$ corrections to the process $e^+e^- \to \rho, \omega \to \pi^+\pi^-$. In addition higher order IS photonic corrections up to $O(\alpha^3)$ and contributions from initial state fermion pair production show significant effects in case of a radiative return measurement of the invariant mass distribution of the hadronic final state $d\sigma/ds'$. Thus they also have to be included into the analysis. Furthermore, bearing in mind the experimental situation, realistic kinematical cuts have to be taken into account. This can be done in the most flexible way by a dedicated computer program by which the phase space integrations are carried out numerically.

At DAΦNE the experimental analysis is currently based on events with a tagged photon [74, 75, 76, 77, 78, 79]. This has the advantage that hereby the background due to competing processes like $e^+e^- \to \pi^+\pi^-\pi^0$ can be reduced more easily. Furthermore, by applying strong cuts to the angle between the tagged photon and the final state pions, the contribution from FS corrections can be reduced considerably. Through this the model dependence concerning the undressing procedure can be reduced [76]. On the other hand, selecting events with a tagged photon reduces statistics considerably. More seriously, the complete initial state $O(\alpha^2)$ QED corrections are known only for the case that the radiated photons are treated inclusively [80]. Hence, concerning the undressing procedure, at present it appears to be hardly possible to reach a higher precision than of percent level when using the tagged photon method only.

[11] Note that, due to the non-perturbative behaviour of QCD at low energies, how to apply radiative corrections to the hadronic final state is not determined in a non-ambiguous way by theory. Hence there remains a residual model dependence concerning the procedure of undressing the observed cross sections from radiative corrections which is due to the final state photons.

In contrast to previous investigations in the present analysis the emphasis is laid on an inclusive treatment of all photons, including those that materialize into anything non-hadronic. To reach the desired precision the complete massive $O(\alpha)$ initial state, final state and initial-final state interference corrections to the production channel $e^+e^- \to \pi^+\pi^-$ are calculated. Taking furthermore into account the photonic and IS fermion pair production contributions up to $O(\alpha^3)$, the total cross section $\sigma$, the $\pi^+\pi^-$ pair invariant mass distribution $d\sigma/ds'$ and the pion angular distribution $d\sigma/d\cos\theta$ are then investigated for experimentally realistic kinematical cuts. A strategy to extract the undressed hadronic cross section from the experimental data, which is needed for the dispersion integrals (1.7) and (1.9), is developed and discussed. Finally the precision of this strategy is estimated, including a consideration of the model uncertainty which is related to the non-perturbative QCD effects of the $\pi^+\pi^-$ final state.

The goal of this work is to provide the theoretical condition to extract the undressed hadronic cross sections from the measured data at low energy hadronic experiments like DAΦNE and VEPP-2M with a precision at per mill level.

# Chapter 2

# Some Remarks about Radiative Corrections

In the following the QED corrections to low energy hadron production in $e^+e^-$ collisions will be considered. After a general model-independent treatment of the initial state corrections I will focus on the production channel of a charged pion pair ($e^+e^- \to \pi^+\pi^-$). Analytic formulae for the complete massive $O(\alpha)$ corrections will be presented. These include the real and virtual corrections to the final state as well as the real and virtual interference corrections. The hadronic structure of the pions will be parametrized by the pion form factor $F_\pi$. The pion angular distribution and cross sections with kinematical cuts are treated numerically, using the Fortran program A$\phi\rho\omega$DITE [81]. They will be considered in chapter 4.

When calculating QED corrections to scattering processes in perturbation theory one usually has to deal with infrared (IR) divergent expressions (infinities that appear in the limit of zero momentum) and ultraviolet (UV) divergent expressions (infinities that appear in the limit of infinite momentum).

The IR divergences are due to the fact that the incoming and outgoing particles of a scattering process are treated as asymptotically free states in perturbation theory. Concerning electrically charged particles such free states are unphysical since the field quanta of QED, the photons, are massless and therefore can have arbitrarily small energies. An electrically charged particle is therefore always "dressed" by a cloud of very low energy photons. For a given scattering process adding the real and virtual photonic corrections cancels the IR poles which appear in both contributions. These poles are a consequence of the artificial separation of real and virtual photonic corrections in perturbation theory and it was proven that the cancellation happens in each order of the perturbative expansion [82, 83]. Considering the exclusive measurement of a real photon which is emitted from a charged particle, restricting the real photon phase space to a small photon energy $E_\gamma < \Lambda$, a straightforward calculation would lead to an IR divergent result in the limit $\Lambda \to 0$ which is obviously unphysical. This is the case for contributions of each order in the perturbative expansion. There is, however, a systematic way of getting rid of this unphysical

behavior by adding contributions of all orders [83]. This leads to an exponentiation of the in the limit $\Lambda \to 0$ IR singular terms such that the observables are well behaved for low photon energies.

In calculations of subleading corrections in perturbative QED we have to deal with loop integrals which are UV divergent in four spacetime dimensions. To regularize the UV divergences it is possible to introduce a formal UV cutoff, e.g. by switching from 4 to $4-\varepsilon_{UV}$ spacetime dimensions (dimensional regularization). Since observables are finite quantities in four spacetime dimensions we need a procedure of removing the UV cut off while keeping the observables finite. In renormalizable theories this can be achieved by a redefinition of the parameters (charges and masses) and fields, thus absorbing the UV cutoff by switching from bare to renormalized parameters and fields. Since QED is a renormalizable theory [1] it is possible to rewrite the QED-Lagrangian in terms of renormalized fields and parameters by introducing a finite number of renormalization constants which allow for a cancellation of the UV divergences to each order of the perturbative expansion. For further details on the renormalization procedure see e.g. [84, 85, 86, 87].

Consider now the process of low energy hadron production in an $e^+e^-$ collision experiment. The dynamics of such a process is determined by a Lagrangian $\mathcal{L}$ which is the sum of an electron contribution $\mathcal{L}_e$, a hadronic contribution $\mathcal{L}_h$ and a pure gauge contribution $\mathcal{L}_\gamma$:

$$\mathcal{L} \;=\; \mathcal{L}_e + \mathcal{L}_h + \mathcal{L}_\gamma \; . \tag{2.1}$$

The hadronic part of the Lagrangian depends on the specific hadronic channel under consideration. The electron contribution and the pure gauge contribution read

$$\begin{aligned} \mathcal{L}_e \;&=\; \bar{\psi}\left(i\partial\!\!\!/ - eA\!\!\!/\right)\psi - m_e\bar{\psi}\psi + (Z_2-1)\,\bar{\psi}i\partial\!\!\!/\psi - (Z_0-1)\,m_e\bar{\psi}\psi \\ &\quad - (Z_1-1)\,e\bar{\psi}A\!\!\!/\psi \; , \end{aligned} \tag{2.2}$$

$$\mathcal{L}_\gamma \;=\; -\frac{1}{4}F_{\mu\nu}F^{\mu\nu} - \frac{1}{2\xi}\left(\partial_\mu A^\mu\right)^2 - (Z_3-1)\,\frac{1}{4}F_{\mu\nu}F^{\mu\nu} \; . \tag{2.3}$$

Here the Lagrangian is written in terms of the renormalized quantities like the renormalized Dirac field of the electron $\psi$, the renormalized photon field $A^\mu$, the renormalized electron mass $m_e$ and the renormalized electromagnetic charge $e$. The terms containing the renormalization constants $Z_i$ (i=0,1,2,3) - the counter terms - lead to a cancellation of the UV divergences in the physical observables. $Z_3$ is related to the photon self energy which after Dyson summation of the irreducible photon self energy contributions leads to the running of the electromagnetic coupling $[\alpha \to \alpha(s)]$[1]. $Z_0$, $Z_1$ and $Z_2$ are related to the electron self energy $\Sigma^e$ and the electron vertex correction $\Lambda_\mu$, respectively.

To obtain the next to leading order (NLO) total cross section $\sigma_{NLO}$ for the process under consideration one has to take into account all contributions including one

[1] In fact the running of $\alpha$ is a consequence of the renormalization group equation.

additional real or virtual photon. Hence the cross section can be written as the sum of two terms, one corresponding to the virtual and the other to the real photon $O(\alpha)$ corrections ($F$ is the flux factor):

$$\sigma_{NLO} \;=\; \frac{1}{F}\int dLips\;|\mathcal{M}_0+\mathcal{M}_1|^2+\frac{1}{F}\int dLips_\gamma\;|\mathcal{M}_\gamma|^2\;. \tag{2.4}$$

In eq. (2.4) $\mathcal{M}_0$ is the Born amplitude, $\mathcal{M}_1$ is the sum of the amplitudes of all virtual correction contributions ($\mathcal{M}_1=\sum_i \mathcal{M}_{1i}$, with the summation index $i$ running over all 1-loop amplitudes) and $\mathcal{M}_\gamma$ is the lowest order amplitude for the process with one additional photon in the final state. The integration measure $dLips$ ($dLips_\gamma$) corresponds to the Lorentz invariant phase space integrations.

Expanding the squared 1 loop amplitude yields

$$|\mathcal{M}_0+\mathcal{M}_1|^2 \;=\; |\mathcal{M}_0|^2+\sum_i 2\Re e(\mathcal{M}_0\mathcal{M}_{1i}^*)+O(\alpha^2)\;. \tag{2.5}$$

Corrections of higher order can be neglected in a NLO calculation. Hence the NLO differential cross section can be written as the sum of the 1-loop corrected Born cross section and the lowest order cross section of the process with one additional real photon in the final state:

$$\left(\frac{d\sigma}{d\Omega}\right)_{NLO} \;=\; \left(\frac{d\sigma}{d\Omega}\right)_0(1+\sum_i\delta_i)+\left(\frac{d\sigma}{d\Omega}\right)_\gamma\;. \tag{2.6}$$

As before the sum is taken over all virtual correction contributions corresponding to all 1-loop Feynman diagrams, where

$$\delta_i \;=\; \frac{2\Re e(\mathcal{M}_0\mathcal{M}_{1i}^*)}{|\mathcal{M}_0|^2}\;. \tag{2.7}$$

Note that there are additional NLO corrections coming from wave function renormalization of the fields corresponding to the in- and out-going particles (external leg corrections). These corrections can also be written in the form of eq. (2.7) and have to be included.

When integrating $d\sigma/d\Omega$ over the angles the real and virtual initial-final state interference (IFS) correction contributions drop out which is a consequence of charge conjugation invariance of the electromagnetic interaction. The NLO correction to the total cross section is therefore determined by the correction factors $\delta_i$ corresponding to the initial state (IS) and final state (FS) corrections only. The same is true for the invariant mass distribution $d\sigma/ds'$ of the hadronic final state. As we will see later it can be written as

$$\frac{d\sigma}{ds'} \;=\; \sigma_0(s')\;\rho_{\rm ini}(s,s')+\sigma_0(s)\;\rho_{\rm fin}(s,s')\;, \tag{2.8}$$

where $\rho_{\rm ini}(s,s')$ and $\rho_{\rm fin}(s,s')$ are the IS and FS radiator function corresponding to the real and virtual IS and FS QED corrections, respectively. The form of eq. (2.8) can be kept when higher order photonic corrections and IS pair production contributions are included.

# Chapter 3

# Initial State Corrections to $e^+e^- \to X$

## 3.1 The Born Cross Section

The Born amplitude for the production of an arbitrary $N$-particle final state $X$ in $e^+e^-$ collisions can be written as a Lorentz contraction of a vector current, corresponding to the initial $e^+e^-$ state, with a final state rank 1 tensor $H^\mu$:

$$\mathcal{M}_0 = \bar{v}_{s_2}(p_2)(-\imath e\gamma_\mu)u_{s_1}(p_1)\, H^\mu(q)\,, \quad (q \equiv p_1 + p_2)\,. \tag{3.1}$$

In eq. (3.1) $p_1$, $p_2$ are the momenta and $s_1$, $s_2$ are the spins of the initial state electron $e^-$ and positron $e^+$, respectively. $H^\mu$ corresponds to the final state $X$ and therefore depends on the final state masses $m_1$, $m_2 \ldots m_N$, the final state momenta $k_1$, $k_2 \ldots k_N$ and the final state spins $t_1$, $t_2 \ldots t_N$. The total Born cross section is then obtained by integrating the squared Born amplitude (which is summed over the final spins and averaged over the initial spins) over the complete $N$-particle phase space:

$$\sigma_0(s) \;=\; \frac{1}{2s\beta_e}\int\prod_{i=1}^{N}\frac{d^3k_i}{(2\pi)^3 2E_i}\,(2\pi)^4\delta^{(4)}(q-\sum_{i=1}^{N}k_i)\,\overline{|\mathcal{M}_0|}^2\,, \tag{3.2}$$

with

$$s \;\equiv\; q^2\,, \quad \beta_e \;=\; \sqrt{1-\frac{4m_e^2}{s}}\,, \tag{3.3}$$

$$\overline{|\mathcal{M}_0|}^2 \;=\; \frac{1}{4}\sum_{s_1,s_2,t_i}\mathcal{M}_0\mathcal{M}_0^\dagger := E^0_{\mu\nu}F^{\mu\nu}(q)\,. \tag{3.4}$$

In (3.4) the squared Born amplitude is written as a contraction of the Born initial state tensor $E^0_{\mu\nu}$ and the final state tensor $F^{\mu\nu}$ which are defined as

$$\begin{aligned} E^0_{\mu\nu} &= \frac{1}{4}\sum_{s_1 s_2}\Big[\bar{v}_{s_2}(p_2)(-\imath e\gamma_\mu)u_{s_1}(p_1)\Big]\Big[\bar{v}_{s_2}(p_2)(-\imath e\gamma_\nu)u_{s_1}(p_1)\Big]^\dagger \\ &= e^2\left(p_{1\mu}p_{2\nu}+p_{2\mu}p_{1\nu}-\frac{s}{2}g_{\mu\nu}\right)\,, \qquad (3.5) \\ F^{\mu\nu}(q) &= \sum_{t_i} H^\mu(q)H^{*\nu}(q)\,. \qquad (3.6) \end{aligned}$$

Integrating $F^{\mu\nu}$ over the complete $N$-particle phase space leads to the integrated final state tensor

$$\begin{aligned} \mathcal{F}^{\mu\nu}(q) &= \int\prod_{i=1}^N \frac{d^3k_i}{(2\pi)^3 2E_i}\,(2\pi)^4\delta^{(4)}(q-\sum_{i=1}^N k_i)\;F^{\mu\nu}(q) \\ &= A(s)g^{\mu\nu}+B(s)q^\mu q^\nu, \qquad (3.7) \end{aligned}$$

which only depends on the sum of all final state momenta $q$ as well as on the Lorentz invariant quantities $s$ and the final state masses $m_i$ $(i=1\ldots N)$. The second equality is a consequence of Lorentz covariance. With these definitions the Born cross section reads

$$\sigma_0(s)=\frac{1}{2s\beta_e}E^0_{\mu\nu}\mathcal{F}^{\mu\nu}(q)=\frac{1}{2s\beta_e}A(s)\;\mathrm{tr}\left(E^{0\nu}_{\ \ \mu}\right)=-e^2\;\frac{s+2m_e^2}{2s\beta_e}\;A(s)\,. \qquad (3.8)$$

In eq. (3.8) gauge invariance has been used which implies the Ward identity:

$$q^\mu E^0_{\mu\nu}=0\,. \qquad (3.9)$$

Taking also for the final state tensor gauge invariance into account, $\mathcal{F}^{\mu\nu}$ becomes transverse:

$$q_\mu\mathcal{F}^{\mu\nu}(q)=0 \quad\Longrightarrow\quad \mathcal{F}^{\mu\nu}(q)=-\frac{\sigma_0(s)}{e^2}\frac{2s\beta_e}{s+2m_e^2}\left(g^{\mu\nu}-\frac{q^\mu q^\nu}{s}\right). \qquad (3.10)$$

This relation between the integrated final state tensor and the Born cross section will be used when applying radiative corrections to the initial $e^+e^-$ state.

## 3.2 Initial State Bremsstrahlung

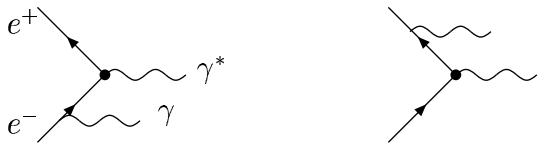


Consider now the case that a real photon $\gamma(k,\lambda)$ is radiated off either the initial state electron or the initial state positron ($k$ is the photon momentum and $\lambda$ the photon helicity). The corresponding amplitude reads (with $q' = q - k = \sum k_i$)

$$\begin{aligned}\mathcal{M}_{\gamma_i} &= \Big\{\bar{v}_{s_2}(p_2)(-\imath e\gamma_\mu)\left[\imath\frac{(\not{p}_1 - \not{k}) + m_e}{(p_1-k)^2 - m_e^2 + i\epsilon}\right](-\imath e\gamma_\rho)u_{s_1}(p_1) \\ &+ \bar{v}_{s_2}(p_2)(-\imath e\gamma_\rho)\left[\imath\frac{-(\not{p}_2 - \not{k}) + m_e}{(p_2-k)^2 - m_e^2 + i\epsilon}\right](-\imath e\gamma_\mu)u_{s_1}(p_1)\Big\} \\ &\times \epsilon^{*\rho}_\lambda(k)\, H^\mu(q')\ . \end{aligned} \tag{3.11}$$

Integrating the squared amplitude over the complete $N+1$ particle phase space leads to the related total cross section (with $s' \equiv q'^2$):

$$\begin{aligned}\sigma_{\gamma_i}(s) &= \frac{\mu_{IR}^{4-n}}{2s\beta_e}\int\frac{d^{n-1}k}{(2\pi)^{n-1}2|\vec{k}|}\prod_{i=1}^{N}\frac{d^3k_i}{(2\pi)^3 2E_i}\,(2\pi)^4\delta^{(4)}(q-k-\sum_{i=1}^{N}k_i)\,\overline{|\mathcal{M}_\gamma|}^2 \\ &= \frac{\mu_{IR}^{4-n}}{2s\beta_e}\int ds'\int\frac{d^{n-1}k}{(2\pi)^{n-1}2|\vec{k}|}\frac{d^3q'}{2q'^0}\,\delta^{(4)}(q-q'-k) \\ &\times\int\prod_{i=1}^{N}\frac{d^3k_i}{(2\pi)^3 2E_i}\,(2\pi)^4\delta^{(4)}(q'-\sum_{i=1}^{N}k_i)\,\overline{|\mathcal{M}_\gamma|}^2\ , \end{aligned} \tag{3.12}$$

where eq. (C.7) in App. C was used. Note that the integral over the photon momentum $k$ is IR divergent in $n = 4$ spacetime dimensions. To regularize the IR divergence a soft photon cut off is introduced. Here this is achieved by dimensional regularization, thus by switching from 4 to $n = 4 + \varepsilon_{IR}$ dimensions. As for the Born case also the squared amplitude for initial state bremsstrahlung can be written as a contraction of an initial state tensor $E^\gamma_{\mu\nu}$ and the final state tensor $F^{\mu\nu}$ as defined in eq. (3.6):

$$\overline{|\mathcal{M}_\gamma|}^2 = \frac{1}{4}\sum_{s_1,s_2,\lambda,t_i}\mathcal{M}_\gamma\mathcal{M}_\gamma^\dagger := E^\gamma_{\mu\nu}F^{\mu\nu}(q')\ . \tag{3.13}$$

In contrast to the Born case the initial state tensor now includes the contribution from the bremsstrahlung photon that is radiated by the initial state electron or

positron:

$$
\begin{aligned}
E^{\gamma}_{\mu\nu} &= \frac{1}{4}\sum_{s_1,s_2,\lambda}\left\{\bar{v}_{s_2}(p_2)(-\imath e\gamma_\mu)\left[\imath\frac{(\not{p}_1-\not{k})+m_e}{(p_1-k)^2-m_e^2+i\epsilon}\right](-\imath e\gamma_\rho)u_{s_1}(p_1)\right. \\
&+ \left.\bar{v}_{s_2}(p_2)(-\imath e\gamma_\rho)\left[\imath\frac{-(\not{p}_2-\not{k})+m_e}{(p_2-k)^2-m_e^2+i\epsilon}\right](-\imath e\gamma_\mu)u_{s_1}(p_1)\right\} \\
&\times\left\{\bar{v}_{s_2}(p_2)(-\imath e\gamma_\nu)\left[\imath\frac{(\not{p}_1-\not{k})+m_e}{(p_1-k)^2-m_e^2+i\epsilon}\right](-\imath e\gamma_{\rho'})u_{s_1}(p_1)\right. \\
&+ \left.\bar{v}_{s_2}(p_2)(-\imath e\gamma_{\rho'})\left[\imath\frac{-(\not{p}_2-\not{k})+m_e}{(p_2-k)^2-m_e^2+i\epsilon}\right](-\imath e\gamma_\nu)u_{s_1}(p_1)\right\}^{\dagger} \\
&\times \epsilon^{\rho'}_{\lambda}(k)\epsilon^{*\rho}_{\lambda}(k)\ . \qquad (3.14)
\end{aligned}
$$

Again, as a consequence of gauge invariance, the initial state tensor obeys the Ward identity:

$$
q'^{\mu}E^{\gamma}_{\mu\nu} = 0\ . \qquad (3.15)
$$

Using the relation between the integrated final state tensor and the Born cross section in eq. (3.10) it is possible to write the total cross section corresponding to the process including one IS photon as a convolution integral:

$$
\sigma_{\gamma_i}(s) = \int ds'\sigma_0(s')\rho_{\rm ini}(s,s')\ , \qquad (3.16)
$$

where

$$
\rho_{\rm ini}(s') = -\frac{\mu_{IR}^{4-n}}{s\beta_e^2}\,\frac{s'\beta_e(s')}{s'+2m_e^2}\int\frac{d^{n-1}k}{(2\pi)^{n-1}2|\vec{k}|}\,\delta(q'^2-s')\mathrm{tr}\left(E^{\gamma\nu}_{\mu}\right) \qquad (3.17)
$$

is the regularized initial state radiator function. Note that $\rho_{\rm ini}$ does not contain any information about the final state since only the trace of the initial state tensor appears. It is therefore the same for any final state.

A straightforward calculation yields

$$
\begin{aligned}
\mathrm{tr}\left(E^{\gamma\nu}_{\mu}\right) &= -e^2\left\{(s+2m_e^2)\left[\frac{s-2m_e^2}{(p_1k)(p_2k)}-\frac{m_e^2}{(p_1k)^2}-\frac{m_e^2}{(p_2k)^2}\right]\right. \\
&- 2(s-3m_e^2)\left[\frac{1}{p_1k}+\frac{1}{p_2k}\right] + 2m_e^2\left[\frac{p_2k}{(p_1k)^2}+\frac{p_1k}{(p_2k)^2}\right] \\
&+ \left.2\left[\frac{p_2k}{p_1k}+\frac{p_1k}{p_2k}\right]\right\}\ . \qquad (3.18)
\end{aligned}
$$

The terms with two powers of the photon momentum $k$ in the denominator become singular in the limit $n\to 4$ when integrating over the photon phase space. Since these divergences occur in the soft photon limit,

$$
E_\gamma = \frac{s-s'}{2\sqrt{s}} \longrightarrow 0\ , \qquad (3.19)
$$

the convolution integral in eq. (3.16) is usually divided into a low energy part ($E_\gamma \leq \Lambda$) which demands IR regularization and the rest ($E_\gamma > \Lambda$) which is IR finite for $n = 4$:

$$\begin{aligned}\sigma_{\gamma_i}(s) &= 2\sqrt{s}\left[\int_0^\Lambda dE_\gamma\ \sigma_0(E_\gamma)\ \rho_{\rm ini}(E_\gamma) + \int_\Lambda^{E_0} dE_\gamma\ \sigma_0(E_\gamma)\ \rho_{\rm ini}(E_\gamma)\right] \\ &\equiv \sigma^S_{\gamma_i}(s,\Lambda) + \sigma^H_{\gamma_i}(s,\Lambda)\ . \end{aligned} \tag{3.20}$$

$E_0$ is the maximum photon energy. $\Lambda$ is the soft photon cut off energy, depending on the choice where to draw the boundary between soft photons ($E_\gamma \leq \Lambda$) and hard photons ($E_\gamma > \Lambda$), with the requirement that $\Lambda$ is small, which means that

$$\sigma_0(E_\gamma = 0) \simeq \sigma_0(E_\gamma = \Lambda)\ . \tag{3.21}$$

The initial state radiator function can be written as the sum of two contributions:

$$\rho_{\rm ini}(E_\gamma) = \rho^{(1)}_{\rm ini}(E_\gamma) + \rho^{(2)}_{\rm ini}(E_\gamma)\ , \tag{3.22}$$

where $\rho^{(1)}_{\rm ini}$ is the contribution with two powers of $k$ in the denominator. It is therefore the dominant contribution to $\rho_{\rm ini}$ at low photon energies $E_\gamma$. The $E_\gamma$ integral over $\rho^{(1)}_{\rm ini}$ becomes IR divergent for $n \to 4$.

From eq. (3.21) follows that the soft photon correction factorizes. Thus the Born cross section is multiplied by a soft photon correction factor:

$$\sigma^S_{\gamma_i}(s,\Lambda) = \sigma_0(s)\ \delta^S_{\rm ini}(s,\Lambda)\ , \tag{3.23}$$

with

$$\begin{aligned}\delta^S_{\rm ini}(s,\Lambda) &= \int_{soft} ds'\ \rho^{(1)}_{\rm ini}(s,s') \\ &= e^2\ \mu_{IR}^{4-n} \int_{soft} \frac{d^{n-1}k}{(2\pi)^{n-1} 2|\vec{k}|}\ \left[\frac{s-2m_e^2}{(p_1k)(p_2k)} - \frac{m_e^2}{(p_1k)^2} - \frac{m_e^2}{(p_2k)^2}\right]. \end{aligned} \tag{3.24}$$

The index "soft" indicates that the integral is taken in the soft photon range $0 \leq E_\gamma \leq \Lambda$. Replacing the total cross section by the differential cross section ($\sigma \to d\sigma/d\Omega$) the soft photon factor $\delta^S_{\rm ini}$ stays the same. The calculation of the soft photon integral which is presented in App. B. yields

$$\begin{aligned}\delta^S_{\rm ini}(s,\Lambda) &= \frac{\alpha}{\pi}\ \left\{\left[-1 + \frac{s-2m_e^2}{s\beta_e}\ \log\left(\frac{1+\beta_e}{1-\beta_e}\right)\right]\right. \\ &\times \left[\frac{2}{\varepsilon_{IR}} + \log\left(\frac{\Lambda^2}{4\pi\mu_{IR}^2}\right) + \gamma_E + 2\log 2\right] + \frac{1}{\beta_e}\ \log\left(\frac{1+\beta_e}{1-\beta_e}\right) \\ &\left. -\frac{s-2m_e^2}{s\beta_e}\ \frac{1}{2}\ \log^2\left(\frac{1+\beta_e}{1-\beta_e}\right) - 2\ \frac{s-2m_e^2}{s\beta_e}\ {\rm Li}_2\left(\frac{2\beta_e}{1+\beta_e}\right)\right\}\ . \end{aligned} \tag{3.25}$$

To obtain the hard photon contribution $\sigma_{\gamma_i}^H$ the integral in eq. (3.17) has to be calculated which yields the initial state radiator function $\rho_{\rm ini}(s,s')$.

The integration can easily be carried out in the $e^+e^-$ center of mass system which is the same as the laboratory system. Since the integral is finite in 4 dimensions no regularization is required. The integration yields

$$\begin{aligned}\rho_{\rm ini}(s,s') &= \frac{\alpha}{\pi}\,\frac{1}{s\beta_e}\,\frac{s'\beta_e(s')}{s'+2m_e^2}\left\{\,2\,\left[1-\frac{s-2m_e^2}{s\beta_e}\,\log\left(\frac{1+\beta_e}{1-\beta_e}\right)\right]\right.\\ &\left.\times\left(1-\frac{s+2m_e^2}{s-s'}\right)\,-\,\frac{s-s'}{s}\left[1-\frac{1}{\beta_e}\,\log\left(\frac{1+\beta_e}{1-\beta_e}\right)\right]\right\}\,. \qquad (3.26)\end{aligned}$$

To lowest order the inclusive cross section corresponding to photon emission from the initial state with $E_\gamma \geq \Lambda$ therefore reads

$$\sigma_{\gamma_i}^H = \int_{s-2\sqrt{s}E_0}^{s-2\sqrt{s}\Lambda} ds'\,\sigma_0(s')\rho_{\rm ini}(s,s')\,. \qquad (3.27)$$

Concerning hadron production in $e^+e^-$ collisions at DAΦNE energies the electron mass is much smaller than the center of mass energy ($s \gg m_e^2$). In this limit the initial state radiator function in eq. (3.26) becomes

$$\rho_{\rm ini}(s,s') = \frac{\alpha}{\pi}\,\frac{s^2+s'^2}{s^2(s-s')}\,\left[\log\left(\frac{s}{m_e^2}\right)-1\right], \qquad (3.28)$$

which agrees with eq. (9) in the paper by Bonneau and Martin [88].

## 3.3 The Vertex Correction

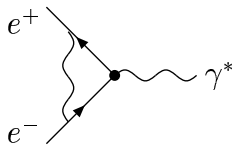


The amplitude corresponding to the initial state vertex correction can be written in a similar form as the Born amplitude:

$$\mathcal{M}_V^e = \bar{v}_{s_2}(p_2)\left[-ie\Lambda_\mu(q^2)\right]u_{s_1}(p_1)\,H^\mu(q)\,. \qquad (3.29)$$

The vertex correction $\Lambda_\mu$ in (3.29) is given by the following 3-point integral:

$$\Lambda_\mu(q^2) = i(-ie)^2\mu^{4-n}\int\frac{d^nk}{(2\pi)^n}\,\frac{N}{D} + (Z_1-1)^{(1)}\gamma_\mu\,, \qquad (3.30)$$

where the numerator $N$ and the denominator $D$ of the integrand read:

$$\begin{aligned} N &= \gamma_\alpha(-\not{p}_2 + \not{k} + m_e)\gamma_\mu(\not{p}_1 + \not{k} + m_e)\gamma^\alpha \,, && (3.31)\\ D &= \left[(p_1+k)^2 - m_e^2 + i\epsilon\right]\left[(p_2-k)^2 - m_e^2 + i\epsilon\right]\left[k^2 + i\epsilon\right] \,. && (3.32) \end{aligned}$$

The vertex correction in (3.30) corresponds to the renormalized Lagrangian $\mathcal{L}_e$ given in eq. (2.2). In (3.30) the 1-loop counter term $[(Z_1-1)^{(1)}\gamma_\mu]$ leads to a cancellation of the UV divergence of the integral. Using the following identities for the gamma matrices in $n$ dimensions:

$$\{\gamma^\mu, \gamma^\nu\} = 2g^{\mu\nu} \,, \quad \gamma_\mu\gamma^\mu = n \,, \tag{3.33}$$

and taking into account the on-shell conditions for the initial state electron and positron, the numerator $N$ can be simplified:

$$\begin{aligned} N &= \gamma_\mu\left[-4p_1p_2 + 4(p_1-p_2)k + (n-2)k^2\right] - 4\,(p_{1\mu} - p_{2\mu})\,\not{k} \\ &\quad + k_\mu\left[4m_e - 2(n-2)\not{k}\right] \,. \end{aligned} \tag{3.34}$$

$\Lambda_\mu$ can now be written as the sum of a contribution which is IR divergent in $n = 4$ dimensions ($\Lambda_\mu^{IR}$), an IR and UV finite contribution ($\Lambda_\mu^{\text{fin}}$) and a contribution containing the UV divergent integral as well as the counter term ($\Lambda_\mu^{UV}$):

$$\Lambda_\mu = \Lambda_\mu^{IR} + \Lambda_\mu^{\text{fin}} + \Lambda_\mu^{UV} \,. \tag{3.35}$$

To regularize $\Lambda_\mu^{IR}$ an IR cut off has to be introduced. As for the soft photon case this is achieved by treating the IR divergent integral in $n = 4 + \varepsilon_{IR}$ dimensions. $\Lambda_\mu^{UV}$ on the other hand can be regularized by switching to $n = 4 - \varepsilon_{UV}$ dimensions. The contributions to the initial state vertex correction can then be written in terms of the master integrals $I_{3S}$, $I_{3V}^\alpha$ and $I_{3T}^{\alpha\beta}$ [see App. A, eq. (A.50), eq. (A.68) and eq. (A.73)]:

$$\begin{aligned} \Lambda_\mu^{IR} &= i(-ie^2)\,\mu_{IR}^{-\varepsilon_{IR}}\,\gamma_\mu(-4p_1p_2)\,I_{3S}(-p_1,p_2,k) \,, && (3.36)\\ \Lambda_\mu^{\text{fin}} &= i(-ie^2)\,4\left[\gamma_\mu(p_{1\alpha}-p_{2\alpha}) - (p_{1\mu}-p_{2\mu})\gamma_\alpha + 4g_{\mu\alpha}m_e\right] \\ &\quad \times I_{3V}^\alpha(-p_1,p_2,k) \,, && (3.37)\\ \Lambda_\mu^{UV} &= i(-ie^2)\,\mu_{UV}^{\varepsilon_{UV}}\,(2-\varepsilon_{UV})\left[\gamma_\mu g_{\alpha\beta} - 2g_{\mu\alpha}\gamma_\beta\right] I_{3T}^{\alpha\beta}(-p_1,p_2,k) \\ &\quad + (Z_1-1)^{(1)} \,. && (3.38) \end{aligned}$$

As a consequence of Lorentz covariance and gauge invariance the vertex correction contributions can be expressed as a linear combination of two rank-1 tensors. $\Lambda_\mu$ can then be parametrized by the form factors $F_1$ and $F_2$:

$$\Lambda_\mu^x = \gamma^\mu F_1^x(q^2) - \frac{i\sigma^{\mu\nu}q_\nu}{2m_e}F_2^x(q^2) \,, \quad \text{with} \quad x = \text{IR, fin, UV} \,. \tag{3.39}$$

Summing all three contributions yields

$$\Lambda_\mu(q^2) \;=\; \gamma_\mu\, F_1(q^2) - \frac{i\sigma_{\mu\nu}q^\nu}{2m_e}\, F_2(q^2)\;, \tag{3.40}$$

where

$$F_1(q^2) \;=\; F_1^{IR}(q^2) + F_1^{\rm fin}(q^2) + F_1^{UV}(q^2)\;, \tag{3.41}$$
$$F_2(q^2) \;=\; F_2^{\rm fin}(q^2) + F_2^{UV}(q^2)\;. \tag{3.42}$$

When taking the classical limit, the form factors $F_1$ and $F_2$ appear to be related to the coupling to an electric or a magnetic field. $F_1 \equiv G_e$ and $F_1 + F_2 \equiv G_m$ are therefore called the electric and magnetic form factor of the electron, respectively[1]. The vertex correction to the Born amplitude can be written as a contraction of an initial state tensor $E^{Vertex}_{\mu\nu}$, corresponding to the initial state vertex correction with the final state tensor $F^{\mu\nu}$, given in (3.6):

$$\frac{1}{4}\sum_{s_1,s_2,t_i} 2\Re e\left[\mathcal{M}_0(q)\mathcal{M}_V^{e*}(q)\right] := E^{Vertex}_{\mu\nu}(q)F^{\mu\nu}(q)\;, \tag{3.43}$$

where

$$E^{Vertex}_{\mu\nu}(q) \;=\; e^2\left\{ 2\Re e\left[F_1(q^2)\right]\;\left( p_{1\mu}p_{2\nu} + p_{2\mu}p_{1\nu} - \frac{s}{2}g_{\mu\nu}\right)\right.$$
$$\left. +\Re e\left[F_2(q^2)\right]\;\left(\, q_\mu q_\nu - s\; g_{\mu\nu}\,\right)\right\}.$$

The tensor structure of $E^{Vertex}_{\mu\nu}$ reflects gauge invariance:

$$q^\mu E^{Vertex}_{\mu\nu} \;=\; 0\;. \tag{3.44}$$

The initial state vertex correction contribution to the total cross section $\sigma_{V_i}$ is obtained by integration over the complete phase space, thus by replacing the final state tensor by the integrated final state tensor and multiplying with the flux factor:

$$\sigma_{V_i}(s) \;=\; \frac{1}{2s\beta_e}E^{Vertex}_{\mu\nu}\mathcal{F}^{\mu\nu}(q) \;=\; -\frac{1}{e^2}\,\frac{1}{s+2m_e^2}\,\sigma_0(s)\;{\rm tr}\left[E^{\nu(Vertex)}_\mu\right]$$
$$=\; \left\{\, 2\Re e\left[F_1(q^2)\right] \;+\; 3\Re e\left[F_2(q^2)\right]\;\frac{s}{s+2m_e^2}\,\right\}\,\sigma_0(s)\;. \tag{3.45}$$

The form factor $F_2$ is of $O(m_e^2/s)$ and therefore can be neglected[2] The initial state vertex correction tensor is then proportional to the Born initial state tensor:

$$E^{Vertex}_{\mu\nu}(q) \;=\; 2\Re e[F_1(q^2)]\;E^0_{\mu\nu}(q)\;. \tag{3.46}$$

[1] Switching from the s-channel process to the t-channel process, $F_2(t=0)$ is exactly the anomalous magnetic moment of the electron.

[2] At the $g-2$ experiments the t-channel process is measured, where the electron or muon interacts with a classical magnetic field. The momentum transfer from the magnetic field is therefore very small ($t \simeq 0$). $F_2(t=0) \equiv (g-2)/2$ then becomes an experimentally measurable quantity.

Hence the initial state vertex correction is obtained simply by multiplying the differential or total Born cross section by the factor $2\Re e F_1(q^2)$. Inserting the results of the master integrals given in App. B into eq. (3.36), (3.37), (3.38) and using the Gordon decomposition,

$$\bar{v}(p_2)\gamma^\mu u(p_1) = \bar{v}(p_2)\left[\frac{p_1^\mu - p_2^\mu}{2m_e} - \frac{i\sigma^{\mu\nu}q_\nu}{2m_e}\right]u(p_1)\,, \tag{3.47}$$

a straightforward calculation leads to the following results for the form factor contributions:

$$\begin{aligned}
F_1^{IR}(q^2) &= \frac{\alpha}{\pi}\,\frac{s-2m_e^2}{s\beta_e}\left\{\frac{1}{\varepsilon_{IR}}\left\{-\log\left(\frac{1+\beta_e}{1-\beta_e}\right)+\pi i\right\}\right. \\
&+ \frac{1}{2}\left\{\left[\log\left(\frac{1+\beta_e}{1-\beta_e}\right)-\pi i\right]\left[\log\left(\frac{4\pi\mu_{IR}^2}{s}\right)-\gamma_E\right]\right. \\
&- \frac{1}{2}\log\left(\frac{1+\beta_e}{1-\beta_e}\right)\left[\log\left(\frac{1-\beta_e^2}{4}\right)+2\log(\beta_e)\right] \\
&- \log\left(\frac{1+\beta_e}{2\beta_e}\right)\log\left(\frac{1-\beta_e}{2\beta_e}\right)-2\mathrm{Li}_2\left(-\frac{1-\beta_e}{2\beta_e}\right) \\
&+ \left.\left.\frac{2}{3}\pi^2+2\pi i\log(\beta_e)\right\}\right\}\,, \qquad (3.48)\\
F_1^{\mathrm{fin}}(q^2) &= \frac{\alpha}{\pi}\,\beta_e\,\left[\log\left(\frac{1+\beta_e}{1-\beta_e}\right)-\pi i\right]\left[1+\frac{2m_e^2}{s\beta_e^2}\right]\,, \qquad (3.49)\\
F_2^{\mathrm{fin}}(q^2) &= -\frac{\alpha}{\pi}\,\beta_e\,\left[\log\left(\frac{1+\beta_e}{1-\beta_e}\right)-\pi i\right]\,\frac{2m_e^2}{s\beta_e^2}\,, \qquad (3.50)\\
F_1^{UV}(q^2) &= \frac{\alpha}{4\pi}\left\{\log\left(\frac{\mu_{\overline{MS}}^2}{s}\right)-\log\left(\frac{1-\beta_e^2}{4}\right)\right. \\
&\qquad \left.-\frac{1}{\beta_e}\,\left[\log\left(\frac{1+\beta_e}{1-\beta_e}\right)-\pi i\right]\right\}\,, \qquad (3.51)\\
F_2^{UV}(q^2) &= \frac{\alpha}{\pi}\,\frac{m_e^2}{s\beta_e}\,\left[\log\left(\frac{1+\beta_e}{1-\beta_e}\right)-\pi i\right]\,. \qquad (3.52)
\end{aligned}$$

Here $F_2^{UV}$ is given in the $\overline{MS}$ scheme. Hence the counter term reads

$$(Z_1-1)^{(1)} = -\frac{\alpha}{4\pi}\left\{\frac{2}{\varepsilon_{UV}}+\log(4\pi)+\log\left(\mu_{UV}^2\right)-\gamma_E-\log\left(\mu_{\overline{MS}}^2\right)\right\}. \tag{3.53}$$

## 3.4 Self Energies

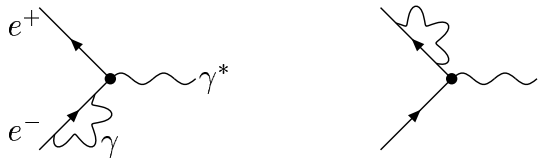


How to apply the 1-loop self energy corrections to the external legs can be seen when the S-matrix element to the process $e^+e^- \to X$ is written as a function of the on-shell-truncated, renormalized Green's function in momentum space $\tilde{G}_{R,tr}$ (see e.g. [84]):

$$\langle k_1, \dots k_N|S|p_1, p_2\rangle \;=\; \prod_{i=1}^{2+N}(1-\Sigma_1^i)^{-1/2}\;\tilde{G}_{R,tr}(k_1,...,k_N;p_1,p_2)\;. \tag{3.54}$$

The running parameter $i$ corresponds to the two initial state and $N$ final state particles. For an external fermion ($i = f$) with momentum $p_f$, the term $\Sigma_1^i$ reads

$$\Sigma_1^f \;=\; \frac{\partial\Sigma^f(\not{p}_f)}{\partial\not{p}_f}\Big|_{\not{p}_f=m_f^{ph}}\;, \tag{3.55}$$

where $\Sigma^f(\not{p}_f)$ is the renormalized irreducible self energy and $m_f^{ph}$ is the physical mass of the fermion, defined as the pole of its propagator. Since only the 1-loop corrections will be taken into account it is possible to neglect terms of $O(\alpha^2)$, thus

$$(1-\Sigma_1^f)^{-1/2} \;=\; 1+\frac{1}{2}\,\Sigma_{1\alpha}^f+O(\alpha^2)\;, \tag{3.56}$$

$$m_f^{ph} \;=\; m_f+O(\alpha^2)\;, \tag{3.57}$$

where $m_f$ is the renormalized mass, corresponding to the renormalized Lagrangian in eq. (2.2). $\Sigma_{1\alpha}^f$ is the $O(\alpha)$ contribution to $\Sigma_1^f$. Hence the amplitude corresponding to the 1-loop initial state $e^+e^-$ self energy correction reads (with $\Sigma^f \equiv \Sigma^e$, $\Sigma_{1\alpha}^f \equiv \Sigma_1^e$, $m_f \equiv m_e$)

$$\mathcal{M}_{S_i} \;=\; \mathcal{M}_0\,\Sigma_1^e\;. \tag{3.58}$$

The 1-loop self energy $\Sigma^e$ is the sum of an UV divergent integral which is regularized in $n = 4-\varepsilon_{UV}$ dimensions and the 1-loop counter terms which contains the 1-loop renormalization constants $(Z_0-1)^{(1)}$ and $(Z_2-1)^{(1)}$. The counter terms lead to a cancellation of the UV divergences such that the result is finite:

$$\begin{aligned}-i\Sigma^e(\not{p}) \;&=\; \mu^{4-n}(-ie)^2\int\frac{d^nk}{(2\pi)^n}\frac{(2-n)(\not{p}+\not{k})+nm_e}{[(p+k)^2-m_e^2+i\epsilon]\,[k^2+i\epsilon]}\\ &\quad + im_e(Z_0-1)^{(1)}\mathbf{1}+i(Z_2-1)^{(1)}\not{p}\\ &=\; -i\left[A(p^2)\mathbf{1}+B(p^2)\not{p}\right]\;,\end{aligned}$$

where the functions $A(p^2)$ and $B(p^2)$ can be expressed in terms of the master integrals $I_{2S}(p,k)$ and $I^{\alpha}_{2V}(p.k)$, given in App. A.

$$A(p^2) = -ie^2\, n\, m_e\, I_{2S}(p,k) - m_e\, (Z_0-1)^{(1)}\,, \tag{3.59}$$

$$B(p^2) = -ie^2\, (2-n)\left[I_{2S}(p,k) + \frac{p_\alpha I^{\alpha}_{2V}(p,k)}{p^2}\right] - (Z_2-1)^{(1)}\,. \tag{3.60}$$

Inserting now the expression for $I_{2S}$ and $I^{\alpha}_{2V}$ [eq. (A.18), (A.19)] and expanding in $\varepsilon_{UV}$ yields

$$\begin{aligned} A(p^2) &= \frac{\alpha}{\pi}\, m_R \left\{ \frac{2}{\varepsilon_{UV}} - \gamma_E + \log\left(4\pi\mu^2\right) - \frac{1}{2} \right. \\ &- \left. \int_0^1 dx\, \log\left[p^2x^2 - x\left(p^2 - m_e^2\right) - i\epsilon\right] \right\} - m_e\,(Z_0-1)^{(1)}\,, \end{aligned} \tag{3.61}$$

$$\begin{aligned} B(p^2) &= -\frac{\alpha}{4\pi} \left\{ \frac{2}{\varepsilon_{UV}} - \gamma_E + \log\left(4\pi\mu^2\right) - 1 \right. \\ &- \left. 2\int_0^1 dx\, (1-x)\, \log\left[p^2x^2 - x\left(p^2 - m_e^2\right) - i\epsilon\right] \right\} - (Z_2-1)^{(1)}\,. \end{aligned} \tag{3.62}$$

In the $\overline{MS}$ scheme the counter terms read

$$(Z_0-1)^{(1)} = \frac{\alpha}{\pi}\left\{ \frac{2}{\varepsilon_{UV}} - \gamma_E + \log\left(4\pi\mu^2\right) - \log\left(\mu^2_{\overline{MS}}\right) \right\}\,, \tag{3.63}$$

$$(Z_2-1)^{(1)} = -\frac{\alpha}{4\pi}\left\{ \frac{2}{\varepsilon_{UV}} - \gamma_E + \log\left(4\pi\mu^2\right) - \log\left(\mu^2_{\overline{MS}}\right) \right\}\,. \tag{3.64}$$

The UV poles are canceled and $A(p^2)$ and $B(p^2)$ are therefore UV finite:

$$A(p^2) = -\frac{\alpha}{\pi}\, m_R \left\{ \frac{1}{2} + \int_0^1 dx\, \log\left[ \frac{p^2x^2 - x\,(p^2-m_e^2) - i\epsilon}{\mu^2_{\overline{MS}}} \right] \right\}\,, \tag{3.65}$$

$$B(p^2) = \frac{\alpha}{2\pi} \left\{ \frac{1}{2} + \int_0^1 dx\, (1-x)\, \log\left[ \frac{p^2x^2 - x\,(p^2-m_e^2) - i\epsilon}{\mu^2_{\overline{MS}}} \right] \right\}\,. \tag{3.66}$$

$\Sigma^e_1$ can now be expressed in terms of $A(p^2)$ and $B(p^2)$:

$$\Sigma^e_1(\not{p}) = \left.\frac{\partial A(p^2)}{\partial p^2}\right|_{\not{p}=m_e} 2m_e + \left.\frac{\partial B(p^2)}{\partial p^2}\right|_{\not{p}=m_e} 2m_e^2 + B\left(m_e^2\right)\,. \tag{3.67}$$

The derivatives of $A$ and $B$ are IR divergent. They are regularized in $n = 4 + \varepsilon_{IR}$ dimensions and can be expressed in terms of the derivatives of the corresponding

2-point integrals that are presented in App. A [eq. (A.23), (A.24)]:

$$\begin{aligned}
\left.\frac{\partial A(p^2)}{\partial p^2}\right|_{\not{p}=m_e} &= -ie^2(4+\varepsilon_{IR})\,\frac{\partial I_{2S}(p,k)}{\partial p^2}\,m_e \\
&= \frac{\alpha}{\pi}\frac{1}{m_e}\left\{\frac{1}{\varepsilon_{IR}}-\frac{1}{2}\left[-\gamma_E+\log\left(\frac{4\pi\mu_{IR}^2}{m_e^2}\right)+\frac{3}{2}\right]\right\}, \qquad (3.68)\\
\left.\frac{\partial B(p^2)}{\partial p^2}\right|_{\not{p}=m_e} &= ie^2(2+\varepsilon_{IR})\left[\frac{\partial I_{2S}(p,k)}{\partial p^2}+\frac{\partial}{\partial p^2}\left(\frac{p_\alpha I_{2V}^\alpha}{p^2}\right)\right] \\
&= -\frac{\alpha}{2\pi}\frac{1}{m_e^2}\left\{\frac{1}{\varepsilon_{IR}}-\frac{1}{2}\left[-\gamma_E+\log\left(\frac{4\pi\mu_{IR}^2}{m_e^2}\right)+2\right]\right\}. \qquad (3.69)
\end{aligned}$$

Together with

$$B(m_e^2) = \frac{\alpha}{4\pi}\left[\log\left(\frac{m_e^2}{\mu_{\overline{MS}}^2}\right)-2\right] \qquad (3.70)$$

the result for the initial state self energy correction becomes:

$$\Sigma_1^{\overline{MS}} = \frac{\alpha}{\pi}\left[\frac{1}{\varepsilon_{IR}}+\frac{1}{2}\gamma_E+\frac{1}{2}\log\left(\frac{m_e^2}{4\pi\mu_{IR}^2}\right)-1+\frac{1}{4}\log\left(\frac{m_e^2}{\mu_{\overline{MS}}^2}\right)\right]. \qquad (3.71)$$

Hence the analytic results for the $O(\alpha)$ IS QED corrections are complete. IS corrections of higher order will be considered together with the FS and IFS interference corrections in chapter 4.

# Chapter 4

# Complete $O(\alpha)$ Corrections to $e^+e^- \longrightarrow \pi^+\pi^-$

Consider now the production of a charged pion pair $[e^-(p_1)e^+(p_2) \to \pi^-(k_1)\pi^+(k_2)]$ which is the dominant hadronic channel for center of mass energies below 1 GeV. Like any QED process pion pair production is always accompanied by the emission of photons which can be either radiated off the initial $e^+e^-$ state or the final $\pi^+\pi^-$ state. Here the major difficulty is how to apply radiative corrections to the final state. Since perturbative QCD breaks down at low energies it is not possible to treat the final state pions in terms of their constituent quarks. On the other hand hard photons that participate in the scattering process can probe the pion sub structure. Treating the pions as point-like particles by simply applying scalar QED is therefore also not a solution to the problem. What makes things even more complicated is the fact that the pion pair does not couple directly to the virtual photon but e.g. via an intermediate $\rho$ or $\omega$ resonance which are highly non-perturbative phenomena.

Usually the $\pi^+\pi^-$ data are represented in terms of the pion form factor $F_\pi(s)$. The absolute square of $F_\pi(s)$ can be expressed as the Born cross section including photon vacuum polarization contributions devided by the lowest order cross section for point-like pions which can be evaluated in scalar QED:

$$|F_\pi(s)|^2 \;=\; \frac{\sigma_{\pi\pi}(s)}{\sigma_{\pi\pi}^{\text{point}}(s)} \qquad \text{with} \qquad \sigma_{\pi\pi}^{\text{point}}(s) \;=\; \frac{\pi}{3}\frac{\alpha^2\beta_\pi^3}{s}\,. \tag{4.1}$$

Here $\beta_\pi = (1 - 4m_\pi^2/s)^{1/2}$ is the pion velocity and $F_\pi(s)$ is the dressed form factor which thus includes the photon vacuum polarization. To obtain the undressed form factor $F_\pi^{(0)}(s)$ we can proceed as in eq. (1.11):

$$|F_\pi^{(0)}(s)|^2 = |F_\pi(s)|^2\,(\alpha/\alpha(s))^2\,. \tag{4.2}$$

The cross section ratio $R(s)$ as defined in eq. (1.10) corresponding to pion pair production can then be expressed in terms of the undressed form factor:

$$R_{\pi\pi}(s) = \frac{\beta_\pi^3}{4}|F_\pi^{(0)}(s)|^2\,. \tag{4.3}$$

To apply radiative corrections to the lowest order cross section the procedure will be the following: first the QED corrections for pointlike pions will be considered. These results can then be extended to the case of physical pions by multiplying with a form factor; graphically: plus one, two or more virtual and/or real photons

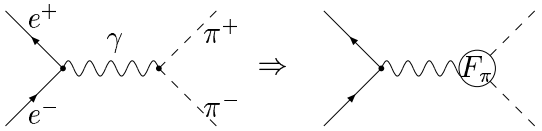


attached in all ways to the charged lines.

Why can this procedure be trusted? There are two main points which convince us that the model ambiguity of the FS radiation cannot be too large, although it is hard to give a solid estimate of the uncertainty. The first point is that the FS QED corrections are ultraviolet (UV) finite in our case. This is in contrast, for example, to the weak leptonic decays of pseudo-scalar mesons, where the QED corrections to the effective Fermi interaction depends on an UV cut-off, which in the SM corresponds to a large logarithm which probes the short distance (SD) structure of the hadron. There is no corresponding SD sensitivity in our case. This is confirmed by a recent analysis of the radiative correction to the pion form factor at low energies within the frame work of chiral perturbation theory [89]. In fact the correction does not depend on any chiral low energy parameter, which would encode an eventual SD ambiguity. The second important point is that the FS correction turns out to be large (of order 10 %) in regions which are dominated by soft photon emission where the treatment of the pions as point particles is actually justified. The question of the model uncertainty will be discussed later in more detail.

The hadronic contribution to the Lagrangian $\mathcal{L}_h \equiv \mathcal{L}_\pi$ [see eq. (2.1)] is now taken to be the gauge invariant, renormalized QED Lagrangian of charged point-like particles which correspond to the complex scalar field $\Phi$:

$$\begin{aligned}\mathcal{L}_\pi &= (\partial_\mu\Phi)(\partial^\mu\Phi^*) - ie(\Phi^*\partial_\mu\Phi - \Phi\partial_\mu\Phi^*)A^\mu + e^2 g_{\mu\nu}\Phi\Phi^* A^\mu A^\nu - m_\pi^2\Phi^*\Phi \\ &+ (Z_2^{(\pi)} - 1)(\partial_\mu\Phi)(\partial^\mu\Phi^*) - (Z_1^{(\pi t)} - 1)ie(\Phi^*\partial_\mu\Phi - \Phi\partial_\mu\Phi^*)A^\mu \\ &+ (Z_1^{(\pi q)} - 1)e^2 g_{\mu\nu}\Phi\Phi^* A^\mu A^\nu - (Z_0^{(\pi)} - 1)m_\pi^2\Phi^*\Phi\ . \qquad (4.4)\end{aligned}$$

From eq. (4.4) follows that the pions can couple via two different vertices to the electromagnetic field. The Feynman rules for the vertices are the following:

**1.** Write $-ie(p+p')^\mu$ for a negatively charged pion with the incoming momentum $p$ and the outgoing momentum $p'$ which couples to a photon via a triple vertex,

**2.** Write $2ie^2 g_{\mu\nu}$ for a pion which couples via a quartic vertex to a photon[1].

[1]The factor 2 for the vertex is a consequence of the fact that the photon field is a real field. Therefore two identical Wick contractions with external photon operators have to be taken into account when deriving the Feynman rules. In addition there is a factor $i$ which has to be taken into account if the pion propagator is also multiplied with $i$.

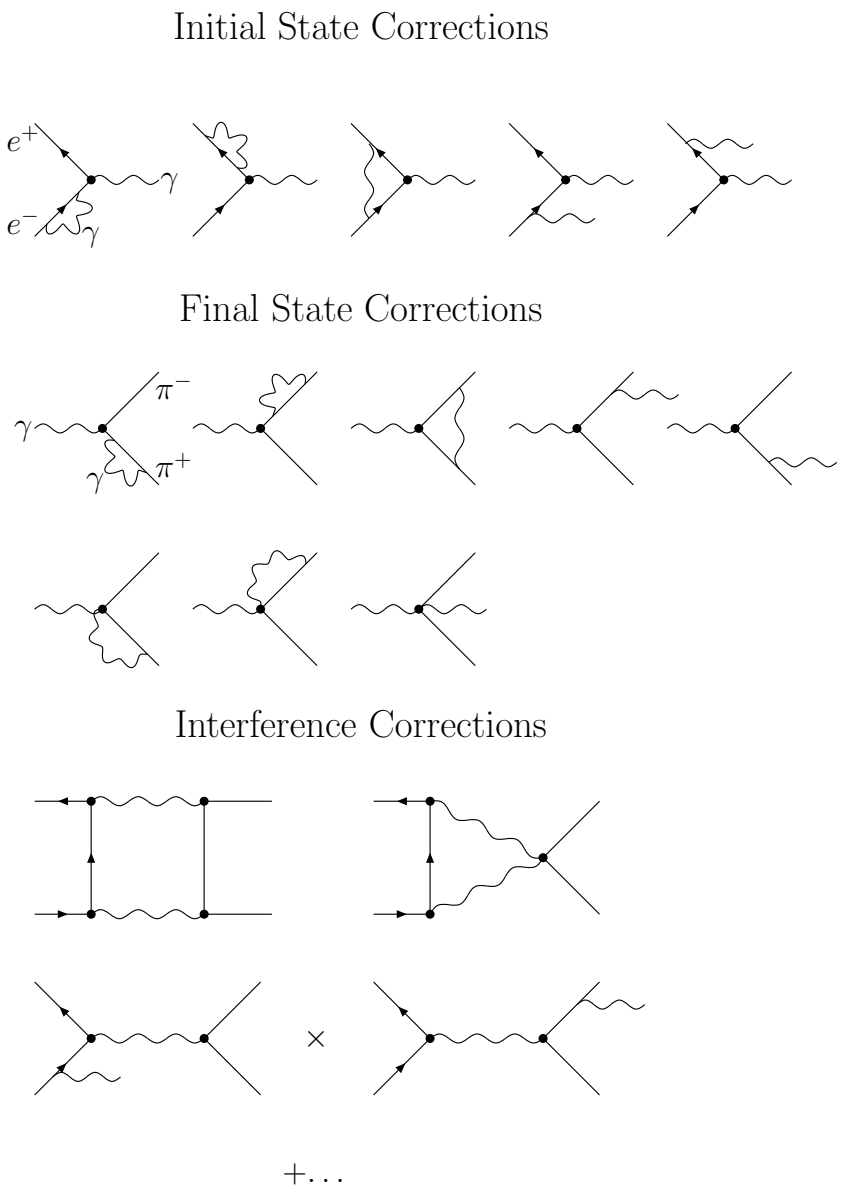


Figure 4.1: Virtual and real $O(\alpha)$ QED corrections to the process $e^+e^- \to \pi^+\pi^-$. The dots stand for the remaining real photon initial-final state interference diagrams.
[1]

In Fig. 4.1 the Feynman diagrams corresponding to the real and virtual $O(\alpha)$ QED corrections are given. If the pions were point-like scalar particles one could calculate the radiative corrections in a more or less straightforward way by using the above Feynman rules. To take into account the non-perturbative QCD effects we use the pion form factor $F_\pi$. A typical parameterization for $F_\pi$ is the Gounaris Sakurai parameterization [90] (for other parameterizations see e.g. [91, 92]). In fact the pion form factor can be "parametrized" in a more model independent way by exploiting analyticity, unitarity and constraints from chiral perturbation theory together with

information from $\pi\pi$ scattering data and by combining $|F_\pi(s)|^2$ data in both the space–like and the time–like region [93, 94, 95, 96, 30].

It is the aim to extract $F_\pi$ from experimental data by undressing the experimentally observed cross sections from radiative corrections. Using the usual procedure of unfolding the QED corrections leads to a model dependence for the results which can be estimated by a comparison of different form factor parameterizations. Later it will be shown that for the radiative return measurement of the pion pair invariant mass distribution $d\sigma/ds'$ one can avoid the choice of a specific form factor parameterization. In fact $F_\pi(s')$ can be evaluated directly from the experimental data.

Why is the above form factor ansatz a reasonable one to parametrize the extended structure of the strongly interacting bound state pion? First of all it leads to the right long range behavior if $F_\pi(0) = 1$ which corresponds to pure scalar QED. It also allows for a consistent treatment of radiative corrections under the condition that one should *not* think of a form factor as being related to a pion vertex but to the Born amplitude (factorization)[2]:

$$\mathcal{M}_0(s)[e^+e^- \to \pi^+\pi^-] \;=\; \mathcal{M}_0^{point}(s) \times F_\pi(s)\;. \tag{4.5}$$

$\mathcal{M}_0^{point}$ is the Born amplitude for point-like pions, obtained from scalar QED. For higher order virtual plus soft photon corrections the amplitudes can then be written as

$$\mathcal{M}_{v+s}(s) \;=\; \delta_{v+s} \times \mathcal{M}_0^{point}(s) \times F_\pi(s) + \left(\text{terms} \to \frac{m_e^2}{s}\right)\;. \tag{4.6}$$

The factor $\delta_{v+s}$ is again calculated in scalar QED. "terms$\to m_e^2/s$" stands for terms which lead to extra contributions to the observables which are of $O(m_e^2/s)$. These can safely be neglected. Clearly the renormalization procedure of scalar QED can then be applied and the cancellation of infrared divergences is also achieved.

## 4.1 The Born Cross Section

Recall the Born amplitude for the production of a hadronic final state as given in eq. (3.1):

$$\mathcal{M}_0 \;=\; \bar{v}_{s_2}(p_2)(-\imath e\gamma_\mu)u_{s_1}(p_1)\; H^\mu(q)\;. \tag{4.7}$$

Using the Feynman rules of scalar QED the tensor $H^\mu$ corresponding to the $\pi^+\pi^-$ final state can be determined:

$$H^\mu(q) \;=\; -\frac{eF_\pi(s)}{s}\,(k_1^\mu - k_2^\mu)\;. \tag{4.8}$$

[2]Often the pion form factor is regarded to be related to the $\gamma\pi^+\pi^-$ triple vertex which would modify the Feynman rules in such a way that the triple vertex of scalar QED is multiplied by $F_\pi$. This automatically leads to the right Born amplitude $\mathcal{M}_0$. However, a consistent and non-ambiguous treatment of the radiative corrections would then be difficult. One should therefore think of the pion form factor as being related to the Born amplitude and not to a vertex.

Note that in eq. (4.8) the form factor is defined to be the function that multiplies the tensor corresponding to pointlike scalar particles. Referring to eq. (3.4) the squared matrix element can then be written as the contraction of the Born initial state tensor $E^0_{\mu\nu}$ with the final state tensor $F^{\mu\nu}$ which was defined in eq. (3.6):

$$\overline{|\mathcal{M}_0|}^2 \;=\; E^0_{\mu\nu} F^{\mu\nu}(q)\;, \tag{4.9}$$

where

$$F^{\mu\nu}(q) \;=\; \frac{e^2|F_\pi(s)|^2}{s^2}\,(k_1^\mu - k_2^\mu)\,(k_1^\nu - k_2^\nu)\;. \tag{4.10}$$

The integrated final state tensor $\mathcal{F}^{\mu\nu}$ is then obtained by integrating over the complete $\pi^+\pi^-$ phase space [see eq. (3.7)]. The integration can easily be carried out in the $\pi^+\pi^-$ center of mass system (CMS) which here coincides with the laboratory system. This yields

$$\begin{aligned}
\mathcal{F}^{\mu\nu}(s) \;&=\; \int \frac{d^3k_1}{(2\pi)^3 2E_1}\frac{d^3k_2}{(2\pi)^3 2E_2}\,(2\pi)^2\delta(q-k_1-k_2)\,F^{\mu\nu}(q)\;,\\
&=\; -\frac{e^2|F_\pi(s)|^2}{s(2\pi)^2}\frac{\pi}{6}\beta_\pi^3(s)\,\left(g^{\mu\nu} - \frac{q^\mu q^\nu}{s}\right)\;, \qquad (4.11)\\
\text{where}\quad \beta_\pi(s) \;&=\; \sqrt{1-\frac{4m_\pi^2}{s}}\;. \qquad (4.12)
\end{aligned}$$

By comparing (4.11) with (3.10) and neglecting the electron mass ($s \gg m_e^2$) one can immediately read off the total Born cross section:

$$\sigma_0(s) \;=\; \frac{e^4|F_\pi(s)|^2}{2s(2\pi)^2}\frac{\pi}{6}\beta_\pi^3(s) = \frac{\pi}{3}\frac{\alpha^2\beta_\pi^3(s)}{s}\,|F_\pi(s)|^2\;. \tag{4.13}$$

The total cross section $\sigma_0(s)$ can of course also be obtained by integration of the angular distribution (taken in the CMS),

$$\left(\frac{d\sigma}{d\Omega}\right)_0 \;=\; \frac{\beta_\pi(s)}{16\pi^2 s}\,\overline{|\mathcal{M}_0|}^2_{\rm CMS} \;=\; \frac{\alpha^2\beta_\pi^3(s)}{8s}\,|F_\pi(s)|^2\,\sin^2\Theta\;. \tag{4.14}$$

In eq. (4.14) $\Theta$ is the scattering angle of the pion in respect to the $e^+e^-$ beam axis in the CMS.

## 4.2 Hard Photon Radiation

Consider now the real photon corrections to pion pair production, thus the brems strahlung process $e^-(p_1)e^+(p_2) \to \pi^-(k_1)\pi^+(k_2)\gamma(k)$. Since the pions are electrically charged, in addition to the radiation by the initial state electron or positron also the radiation by the final state pions has to be taken into account. The bremsstrahlung

amplitude therefore is the sum of the initial state radiation amplitude and the final state radiation amplitude:

$$\mathcal{M}_\gamma \;=\; \mathcal{M}_{\gamma_i} + \mathcal{M}_{\gamma_f} \; . \tag{4.15}$$

The initial state radiation amplitude $\mathcal{M}_{\gamma_i}$ is given in eq. (3.11), where for the final state rank 1 tensor one has to put the tensor corresponding to the $\pi^+\pi^-$ final state (with $q' = k_1 + k_2$):

$$H^\mu(q') \;=\; -\frac{eF_\pi(q'^2)}{s'}(k_1^\mu - k_2^\mu) \; . \tag{4.16}$$

A photon which is radiated by the final state pions can either couple via a triple vertex to the positively or the negatively charged pion or it can couple via a quartic vertex to the pion final state [see Fig. (4.1)]. Using the Feynman rules as discussed before, the final state bremsstrahlung amplitude is determined to be (see also [97]):

$$\mathcal{M}_{\gamma_f} = \bar{v}_{s_2}(p_2)(-\imath e\gamma_\mu)u_{s_1}(p_1)\left(-\imath\,\frac{g^{\mu\nu}}{q^2+i\epsilon}\right)\; F_\pi(q^2)\; T^{(\pi)}_{\nu\rho}\; \epsilon^{*\rho}_\lambda \; , \tag{4.17}$$

with the final state radiation tensor

$$\begin{aligned} T^{(\pi)}_{\nu\rho} \;=\; -ie^2 \Bigg\{ & \frac{(k_1-k_2-k)_\nu(-2k_2-k)_\rho}{2k_2k} \\ & + \frac{(k_1-k_2+k)_\nu(2k_1+k)_\rho}{2k_1k} \;-\; 2g_{\nu\rho}\Bigg\} \; . \end{aligned} \tag{4.18}$$

To obtain the observable quantities, one has to take the absolute square of the amplitude given in (4.15):

$$\frac{1}{4}\sum_{s_1,s_2,\lambda}|\mathcal{M}_\gamma|^2 \;\equiv\; \overline{|\mathcal{M}_\gamma|}^2 \;=\; \overline{|\mathcal{M}_{\gamma_i}|}^2 + \overline{\mathcal{M}_{\gamma_i}\mathcal{M}^*_{\gamma_f}} + \overline{\mathcal{M}_{\gamma_f}\mathcal{M}^*_{\gamma_i}} + \overline{|\mathcal{M}_{\gamma_f}|}^2 \; . \tag{4.19}$$

In eq. (4.19) the squared amplitude has been averaged over the initial $e^+e^-$ spins and summed over the real photon helicities. The contributions $\overline{|\mathcal{M}_{\gamma_i}|}^2$, $\overline{|\mathcal{M}_{\gamma_f}|}^2$ and $\overline{\mathcal{M}_{\gamma_i}\mathcal{M}^*_{\gamma_f}} + \overline{\mathcal{M}_{\gamma_f}\mathcal{M}^*_{\gamma_i}}$ correspond to the IS, the FS and the IFS interference $O(\alpha)$ real photon corrections, respectively. Taking the expressions for the IS and FS radiation amplitudes from eq. (3.11) and (4.17) yields

$$\begin{aligned} \overline{|\mathcal{M}_{\gamma_i}|}^2 \;=\; & \frac{1}{4}\frac{e^6}{q'^4}|F_\pi(q'^2)|^2(-g^{\rho\rho'})(k_1^\mu - k_2^\mu)(k_1^{\mu'} - k_2^{\mu'}) \times \\ \Bigg\{ & \mathrm{tr}\left[(\not{p}_2 - m_e)\gamma_\mu\left[\frac{\not{p}_1 - \not{k} + m_e}{-2p_1k}\right]\gamma_\rho(\not{p}_1 + m_e)\gamma_{\rho'}\left[\frac{\not{p}_1 - \not{k} + m_e}{-2p_1k}\right]\gamma_{\mu'}\right] \\ & + \mathrm{tr}\left[(\not{p}_2 - m_e)\gamma_\mu\left[\frac{\not{p}_1 - \not{k} + m_e}{-2p_1k}\right]\gamma_\rho(\not{p}_1 + m_e)\gamma_{\mu'}\left[\frac{-\not{p}_2 + \not{k} + m_e}{-2p_2k}\right]\gamma_{\rho'}\right] \\ & + \mathrm{tr}\left[(\not{p}_2 - m_e)\gamma_\rho\left[\frac{-\not{p}_2 + \not{k} + m_e}{-2p_2k}\right]\gamma_\mu(\not{p}_1 + m_e)\gamma_{\rho'}\left[\frac{\not{p}_1 - \not{k} + m_e}{-2p_1k}\right]\gamma_{\mu'}\right] \\ & + \mathrm{tr}\left[(\not{p}_2 - m_e)\gamma_\rho\left[\frac{-\not{p}_2 + \not{k} + m_e}{-2p_2k}\right]\gamma_\mu(\not{p}_1 + m_e)\gamma_{\mu'}\left[\frac{-\not{p}_2 + \not{k} + m_e}{-2p_2k}\right]\gamma_{\rho'}\right]\Bigg\} \; , \end{aligned} \tag{4.20}$$

$$\overline{\mathcal{M}_{\gamma_i}\mathcal{M}^*_{\gamma_f}} = \frac{1}{4}\frac{e^6}{q'^2q^2}F_\pi(q'^2)F^*_\pi(q^2)(-g^{\rho\rho'})(k_1^\mu - k_2^\mu)\times$$
$$\left\{\frac{(k_1-k_2-k)^{\mu'}(-2k_2-k)_{\rho'}}{2k_2k} + \frac{(k_1-k_2+k)^{\mu'}(2k_1+k)_{\rho'}}{2k_1k} - 2g^{\mu'}_{\rho'}\right\}\times$$
$$\left\{\mathrm{tr}\left[(\not{p}_2 - m_e)\gamma_\mu\left[\frac{\not{p}_1 - \not{k} + m_e}{-2p_1k}\right]\gamma_\rho(\not{p}_1+m_e)\gamma_{\mu'}\right]\right.$$
$$\left.+\mathrm{tr}\left[(\not{p}_2 - m_e)\gamma_\rho\left[\frac{-\not{p}_2 + \not{k} + m_e}{-2p_2k}\right]\gamma_\mu(\not{p}_1+m_e)\gamma_{\mu'}\right]\right\}, \tag{4.21}$$

$$\overline{\mathcal{M}_{\gamma_f}\mathcal{M}^*_{\gamma_i}} = \frac{1}{4}\frac{e^6}{q'^2q^2}F_\pi(q^2)F^*_\pi(q'^2)(-g^{\rho\rho'})(k_1^{\mu'} - k_2^{\mu'})\times$$
$$\left\{\frac{(k_1-k_2-k)^{\mu}(-2k_2-k)_{\rho}}{2k_2k} + \frac{(k_1-k_2+k)^{\mu}(2k_1+k)_{\rho}}{2k_1k} - 2g^{\mu}_{\rho}\right\}\times$$
$$\left\{\mathrm{tr}\left[(\not{p}_2 - m_e)\gamma_\mu(\not{p}_1+m_e)\gamma_{\rho'}\left[\frac{\not{p}_1 - \not{k} + m_e}{-2p_1k}\right]\gamma_{\mu'}\right]\right.$$
$$\left.+\mathrm{tr}\left[(\not{p}_2 - m_e)\gamma_\mu(\not{p}_1+m_e)\gamma_{\mu'}\left[\frac{-\not{p}_2 + \not{k} + m_e}{-2p_2k}\right]\gamma_{\rho'}\right]\right\}, \tag{4.22}$$

$$\overline{|\mathcal{M}_{\gamma_f}|^2} = \frac{1}{4}\frac{e^6}{q^4}|F_\pi(q^2)|^2(-g^{\rho\rho'})$$
$$\left\{\frac{(k_1-k_2-k)^{\mu}(-2k_2-k)_{\rho}}{2k_2k} + \frac{(k_1-k_2+k)^{\mu}(2k_1+k)_{\rho}}{2k_1k} - 2g^{\mu}_{\rho}\right\}\times$$
$$\left\{\frac{(k_1-k_2-k)^{\mu'}(-2k_2-k)_{\rho'}}{2k_2k} + \frac{(k_1-k_2+k)^{\mu'}(2k_1+k)_{\rho'}}{2k_1k} - 2g^{\mu'}_{\rho'}\right\}\times$$
$$\mathrm{tr}\left[(\not{p}_2 - m_e)\gamma_\mu(\not{p}_1+m_e)\gamma_{\mu'}\right]. \tag{4.23}$$

The calculation of the traces has been carried out by the symbolic manipulation program FORM [98]. Analytic results for the total cross section $\sigma$ and the pion pair invariant mass distribution $d\sigma/ds'$ have been obtained by tensor integration (see App. C). For this purpose the matrix element corresponding to the IS, FS and IFS interference corrections is written as a contraction of an initial state tensor $E^x_{\mu\nu\ldots\tau}$ with a final state tensor $F^{\mu\nu\ldots\tau}_x$, ($x$ = ini, fin, int), respectively:

$$\begin{aligned}
\overline{|\mathcal{M}_{\gamma_i}|^2} &= E^{\mathrm{ini}}_{\mu\nu\ldots\tau}(p_1^\mu, p_2^\mu, k^\mu, p_{1,2}k)\; F^{\mu\nu\ldots\tau}_{\mathrm{ini}}(k_1^\mu, k_2^\mu)\,, \\
\overline{2\Re e(\mathcal{M}_{\gamma_i}\mathcal{M}^*_{\gamma_f})} &= E^{\mathrm{int}}_{\mu\nu\ldots\tau}(p_1^\mu, p_2^\mu, k^\mu, p_{1,2}k)\; F^{\mu\nu\ldots\tau}_{\mathrm{int}}(k_1^\mu, k_2^\mu, k_{1,2}k)\,, \\
\overline{|\mathcal{M}_{\gamma_f}|^2} &= E^{\mathrm{fin}}_{\mu\nu\ldots\tau}(p_1^\mu, p_2^\mu, k^\mu)\; F^{\mu\nu\ldots\tau}_{\mathrm{fin}}(k_1^\mu, k_2^\mu, k_{1,2}k)\,.
\end{aligned} \tag{4.24}$$

As shown in App. C the 3-particle phase space integration can then be written as two subsequent 2-particle phase space integrations, followed by an integration over the invariant mass of the pion pair $s'$ [see eq. (C.7)].

The final state tensor $F_x^{\mu\nu\ldots\tau}$ can then be integrated over the pion momenta in the $\pi^+\pi^-$ center of mass system, leading to a tensor $\mathcal{F}_x^{\mu\nu\ldots\tau}(q^\mu, k^\mu)$ which after contraction with the initial state tensor $E^x_{\mu\nu\ldots\tau}$ can easily be integrated over the remaining 2-particle phase space:

$$\left(\frac{d\sigma}{ds'}\right)_x = \frac{1}{2s}\int \frac{d^3k}{(2\pi)^3 2k^0}\frac{d^3q'}{(2\pi)^3 q'^0}\,\delta^4(q-k-q')\,E^x_{\mu\nu\ldots\tau}\mathcal{F}_x^{\mu\nu\ldots\tau}\,, \qquad (4.25)$$

with

$$\mathcal{F}_x^{\mu\nu\ldots\tau}(q^\mu, k^\mu) = \int \frac{d^3k_1}{(2\pi)^3 2k_1^0}\frac{d^3k_2}{(2\pi)^3 2k_2^0}\,\delta^4(q'-k_1-k_2)\,F_x^{\mu\nu\ldots\tau}\,. \qquad (4.26)$$

The calculation of the tensor integrals in (4.26) has again been carried out by a FORM program, where the results of the master integrals which are given in App. C were used. Due to the fact that the electromagnetic interaction is invariant under charge conjugation (Furry's theorem), in pure QED there is no IFS interference contribution to the pion pair invariant mass distribution $d\sigma/ds'$ and the total cross section $\sigma$. Thus the IFS interference is purely antisymmetric and therefore only contributes to the angular distribution $d\sigma/d\Omega$. The invariant mass distribution can therefore be written as the sum of an IS contribution and a FS contribution:

$$\left(\frac{d\sigma}{ds'}\right) = \rho_{\rm ini}(s,s')\,\sigma_0(s') + \rho_{\rm fin}(s,s')\,\sigma_0(s)\,. \qquad (4.27)$$

The initial state radiator function $\rho_{\rm ini}(s,s')$ is defined in eq. (3.26). It does not depend on the final state particles. The final state radiator function $\rho_{\rm fin}(s,s')$ on the other hand does of course depend on the $\pi^+\pi^-$ final state. The calculation leads to a rather compact expression:

$$\rho_{\rm fin}(s,s') = \frac{2\alpha}{\pi}\,\frac{s'\beta_\pi(s')}{s\beta_\pi(s)}\,\frac{1}{s-s'}\left[-1+\frac{s'-2m_\pi^2}{s'\beta_\pi(s')}\,L_\pi(s')+\frac{(s-s')^2}{s's\beta_\pi^2(s)}\right], \qquad (4.28)$$

with

$$L_\pi(s') = \log\left(\frac{1+\beta_\pi(s')}{1-\beta_\pi(s')}\right)\,, \quad \beta_\pi(s^{(\prime)}) = \sqrt{1-\frac{4m_\pi^2}{s^{(\prime)}}}\,. \qquad (4.29)$$

Since the integration over $s'$ yields an IR divergent result, as before in eq. (3.20) the real photon correction is split into an IR finite hard photon part and a soft photon part which is IR divergent in 4 dimensions but can be regularized by switching to $n = 4+\varepsilon_{IR}$ dimensions. Then the regularized total cross section for the production of a charged pion pair plus an additional real photon reads

$$\begin{aligned}\sigma_\gamma(s) &= \sigma_0(s)\,\left[\delta^S_{\rm ini}(s,\Lambda)+\delta^S_{\rm fin}(s,\Lambda)\right] \\ &+ \int_{4m_\pi^2}^{s-2\sqrt{s}\Lambda} ds'\,\left[\rho_{\rm ini}(s,s')\sigma_0(s')+\rho_{\rm fin}(s,s')\sigma_0(s)\right]. \qquad (4.30)\end{aligned}$$

What still remains to be calculated is therefore the soft photon final state correction factor $\delta^S_{\rm fin}(s,\Lambda)$.

## 4.3 Soft Photon Final State Radiation

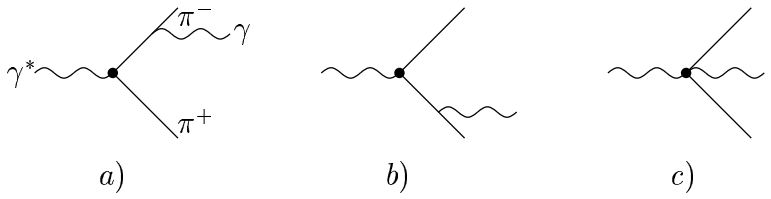


To determine the final state soft photon correction factor $\delta^S_{\rm fin}(s,\Lambda)$ the contributions of $\overline{|\mathcal{M}_{\gamma_f}|}^2$ becoming IR divergent when integrating over the phase space in four spacetime dimensions, have to be extracted. These are the terms with two powers of the photon momentum $k$ in the denominator:

$$\overline{|\mathcal{M}_{\gamma_f}|}^2_{IR} \;=\; \overline{|\mathcal{M}_0|}^2 \left[\frac{s-2m_\pi^2}{(k_1k)(k_2k)} - \frac{m_\pi^2}{(k_1k)^2} - \frac{m_\pi^2}{(k_2k)^2}\right] . \tag{4.31}$$

Thus the final state soft photon correction factor is obtained by integrating over the soft photon phase space. The integral is regularized in $n = 4 + \varepsilon_{IR}$ dimensions:

$$\delta^S_{\rm fin}(s,\Lambda) \;=\; e^2\mu_{IR}^{4-n}\int_{soft}\frac{d^{n-1}k}{2|\vec{k}|(2\pi)^{n-1}}\left[\frac{s-2m_\pi^2}{(k_1k)(k_2k)} - \frac{m_\pi^2}{(k_1k)^2} - \frac{m_\pi^2}{(k_2k)^2}\right] . \tag{4.32}$$

The index "$soft$" indicates that the integral is taken in the soft photon region ($0 \le E_\gamma \le \Lambda$). So the only difference to the initial state soft photon bremsstrahlung is the replacement of the electron mass by the pion mass:

$$\begin{aligned}\delta^S_{\rm fin}(s,\Lambda) \;=\;& \frac{\alpha}{\pi}\left\{\left[-1+\frac{1+\beta_\pi^2}{2\beta_\pi}\,\log\left(\frac{1+\beta_\pi}{1-\beta_\pi}\right)\right]\right. \\ \times\;& \left[\frac{2}{\varepsilon_{IR}} + \log\left(\frac{\Lambda^2}{4\pi\mu_{IR}^2}\right) + \gamma_E + 2\log 2\right] + \frac{1}{\beta_\pi}\,\log\left(\frac{1+\beta_\pi}{1-\beta_\pi}\right) \\ & \left. -\frac{1+\beta_\pi^2}{4\beta_\pi}\,\log^2\left(\frac{1+\beta_\pi}{1-\beta_\pi}\right) - \frac{1+\beta_\pi^2}{\beta_\pi}\,{\rm Li}_2\left(\frac{2\beta_\pi}{1+\beta_\pi}\right)\right\} .\end{aligned} \tag{4.33}$$

Analogous to the IS case the FS soft photon factor in eq. (4.33) is the same for the angular distribution ($d\sigma/d\Omega$) since we are dealing with a neutral current process for which the IS and FS corrections decouple. The IS and FS corrections therefore do not depend on the pion scattering angle.

## 4.4 Soft Photon Initial-Final State Interference

As for the cases of IS and FS radiation we can obtain the IFS interference soft photon contribution by extracting the terms with two powers of the photon momentum $k$

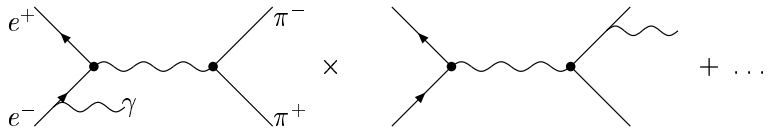


in the denominator of the corresponding expressions in eq. (4.21) and (4.22):

$$\left(\overline{\mathcal{M}_{\gamma_i}\mathcal{M}^*_{\gamma_f}}\right)_{\rm soft} = +e^2\,U\,\left[\frac{1}{(p_1k)(k_1k)}+\frac{1}{(p_2k)(k_2k)}\right]\overline{|\mathcal{M}_0|}^2 \tag{4.34}$$

$$\left(\overline{\mathcal{M}_{\gamma_f}\mathcal{M}^*_{\gamma_i}}\right)_{\rm soft} = -e^2\,T\,\left[\frac{1}{(p_1k)(k_2k)}+\frac{1}{(p_2k)(k_1k)}\right]\overline{|\mathcal{M}_0|}^2 \tag{4.35}$$

with

$$U = -u+m_e^2+m_\pi^2 \equiv 2p_1k_1 = 2p_2k_2\,, \tag{4.36}$$

$$T = -t+m_e^2+m_\pi^2 \equiv 2p_1k_2 = 2p_2k_1\,, \tag{4.37}$$

$$s+t+u = 2m_e^2+2m_\pi^2\,. \tag{4.38}$$

Also the interference correction can be written as a regularized ($n = 4+\varepsilon_{IR}$) correction factor $\delta^S_{\rm int}(t,u,\Lambda)$ which multiplies the Born angular distribution. $\delta^S_{\rm int}$ is antisymmetric which is a consequence of charge conjugation invariance. As noted before the IFS interference correction therefore does not contribute to the soft photon correction of the total cross section and the pion pair invariant mass distributions but only to the angular distribution ($d\sigma/d\Omega$):

$$\int d\Omega\;\delta^S_{\rm int}(t,u,\Lambda)\;\left(\frac{d\sigma}{d\Omega}\right)_0 = 0\,. \tag{4.39}$$

From eq. (4.34) and (4.35) one can immediately read off the soft photon correction factor in the form of a regularized integral over the photon momentum $k$:

$$\delta^S_{\rm int}(t,u,\Lambda) = e^2\mu^{4-n}\int_{soft}\frac{d^{n-1}k}{2|\vec{k}|(2\pi)^{n-1}}\left\{U\left[\frac{1}{(p_1k)(kk_1)}+\frac{1}{(p_2k)(kk_2)}\right]-T\left[\frac{1}{(p_1k)(kk_2)}+\frac{1}{(p_2k)(kk_1)}\right]\right\}. \tag{4.40}$$

In eq. (4.40) again the index "$soft$" indicates that the integral is taken in the soft photon region $0 \le E_\gamma \le \Lambda$. The calculation of the soft photon integral is presented

in App. B and leads to the following result:

$$\begin{aligned}
\delta^S_{\rm int}(t,u,\Lambda) &= \frac{\alpha}{\pi}\Bigg\{\frac{U}{\sqrt{\lambda(u,m_e^2,m_\pi^2)}}\log\left[\frac{U+\sqrt{\lambda(u,m_e^2,m_\pi^2)}}{U-\sqrt{\lambda(u,m_e^2,m_\pi^2)}}\right] \\
&\quad\times\left[\frac{2}{\varepsilon_{IR}}+\gamma_E+\log\left(\frac{\Lambda^2}{4\pi\mu_{IR}^2}\right)+2\log 2\right]-F(u)\Bigg\} \\
&\quad-\{u,U\to t,T\} \\
&\simeq \frac{\alpha}{\pi}\,\sigma_0(s)\,\Bigg\{2\log\left(\frac{-u+m_\pi^2}{-t+m_\pi^2}\right)\,\left[\frac{2}{\varepsilon_{IR}}+\gamma_E\right. \\
&\qquad\left.+\log\left(\frac{\Lambda^2}{\pi\mu_{IR}^2}\right)\right]-\;F(u)+F(t)\;\Bigg\}, \qquad (4.41)
\end{aligned}$$

with $(x=u,t)$

$$\begin{aligned}
F(x) &= \Big[f_1^x(\kappa_1)-f_1^x(\kappa_2)-f_1^x(\kappa_4)+f_2^x(\kappa_3)-f_3^x(\kappa_1,\kappa_2)-f_3^x(\kappa_4,\kappa_1) \\
&+ f_3^x(\kappa_4,\kappa_2)+f_4^x(\kappa_2,\kappa_1)+f_4^x(\kappa_1,\kappa_4)+f_4^x(\kappa_2,\kappa_4)-f_5^x(\kappa_3,\kappa_1) \\
&+ f_5^x(\kappa_3,\kappa_2)-f_5^x(\kappa_3,\kappa_4)-f_6^x(\kappa_1,\kappa_3)-f_6^x(\kappa_2,\kappa_3)+f_6^x(\kappa_4,\kappa_3)\Big]\,, \qquad (4.42)
\end{aligned}$$

where $f_i^x$ $(i=1\ldots6)$ are combinations of logarithms and dilogarithms:

$$\begin{aligned}
f_1^x(\eta) &= \frac{1}{2}\log^2[b_x-\eta]-\frac{1}{2}\log^2[a-\eta]\,, \qquad (4.43)\\
f_2^x(\eta) &= \frac{1}{2}\log^2[\eta-a]-\frac{1}{2}\log^2[\eta-b_x]\,, \qquad (4.44)\\
f_3^x(\eta_1,\eta_2) &= -{\rm Li}_2\left[\frac{(b_x-a)(\eta_1-\eta_2)}{(b_x-\eta_1)(a-\eta_2)}\right]+{\rm Li}_2\left(-\frac{b_x-a}{a-\eta_2}\right) \\
&+ {\rm Li}_2\left(\frac{b_x-a}{b_x-\eta_1}\right)+\log(b_x-\eta_1)\log\left(\frac{b_x-\eta_2}{a-\eta_2}\right)\,, \qquad (4.45)\\
f_4^x(\eta_1,\eta_2) &= {\rm Li}_2\left[\frac{(b_x-a)(\eta_2-\eta_1)}{(b_x-\eta_2)(a-\eta_1)}\right]-{\rm Li}_2\left(-\frac{b_x-a}{a-\eta_1}\right) \\
&- {\rm Li}_2\left(\frac{b_x-a}{b_x-\eta_2}\right)+\log(a-\eta_1)\log\left(\frac{b_x-\eta_2}{a-\eta_2}\right)\,, \qquad (4.46)\\
f_5^x(\eta_1,\eta_2) &= \log[\eta_1-\eta_2]\log\left(\frac{b_x-\eta_2}{a-\eta_2}\right)+{\rm Li}_2\left(\frac{a-\eta_2}{\eta_1-\eta_2}\right) \\
&- {\rm Li}_2\left(\frac{b_x-\eta_2}{\eta_1-\eta_2}\right)\,, \qquad (4.47)\\
f_6^x(\eta_1,\eta_2) &= \log[\eta_2-\eta_1]\log\left(\frac{\eta_2-b_x}{\eta_2-a}\right)+{\rm Li}_2\left(\frac{\eta_2-a}{\eta_2-\eta_1}\right) \\
&- {\rm Li}_2\left(\frac{\eta_2-b_x}{\eta_2-\eta_1}\right)\,, \qquad (4.48)
\end{aligned}$$

with

$$a = \beta_\pi(s)\,, \quad b_x = \beta_e + 2\sqrt{-\frac{x}{s}}\,, \tag{4.49}$$

$$\kappa_{1,2}(x) = -1 + \frac{1}{\sqrt{-sx}}\left[-x + m_e^2 - m_\pi^2 \pm \sqrt{\lambda(x, m_e^2, m_\pi^2)}\right]\,, \tag{4.50}$$

$$\kappa_{3,4}(x) = 1 + \frac{1}{\sqrt{-sx}}\left[-x + m_e^2 - m_\pi^2 \pm \sqrt{\lambda(x, m_e^2, m_\pi^2)}\right]\,, \tag{4.51}$$

$$\lambda(A, B, C) = A^2 + B^2 + C^2 - 2AB - 2AC - 2BC\,. \tag{4.52}$$

For the second equality in eq. (4.41) the high energy approximation $s \gg m_e^2$ was used.

## 4.5 Final State Vertex Correction

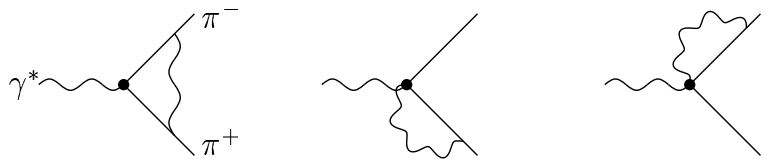


*a)* *b)* *c)*

The amplitude of the final state vertex correction $\mathcal{M}_V^{\pi\pi}$ can be written in a similar form as the initial state vertex correction amplitude in eq. (3.29):

$$\mathcal{M}_V^{\pi\pi} = \bar{v}_2(-ie\gamma_\mu)u_1\left(\frac{-i}{q^2 + i\epsilon}\right) \times \left[-ie\Lambda^\mu_{(\pi)}(q^2)\right]\,, \tag{4.53}$$

$$\text{with} \quad \Lambda^\mu_{(\pi)} = \Lambda^\mu_t + \Lambda^\mu_q\,. \tag{4.54}$$

In (4.54) $\Lambda^\mu_t$ corresponds to the vertex correction diagram *a)* in which the virtual photon couples via two triple photon-pion vertices. $\Lambda^\mu_q$ corresponds to the diagrams *b)* and *c)* in which the virtual photon couples via a triple and a quartic photon-pion vertex. Let's first consider diagram *a)*. Applying the Feynman rules leads to the following 3-point integral ($n = 4 + \varepsilon_{IR}$):

$$\begin{aligned}\Lambda^\mu_t(q^2) &= i(-ie)^2\mu^{4-n} \\ &\times \int \frac{d^n k}{(2\pi)^n} \frac{(k_1^\mu - k_2^\mu + 2k^\mu)(2k_{1\alpha} + k_\alpha)(-2k_2^\alpha + k^\alpha)}{\left[(k_1 + k)^2 - m_\pi^2 + i\epsilon\right]\left[(k_2 - k)^2 - m_\pi^2 + i\epsilon\right]\left[k^2 + i\epsilon\right]} \\ &+ (k_1^\mu - k_2^\mu)(Z_1^{(\pi t)} - 1)^{(1)}\,,\end{aligned} \tag{4.55}$$

which corresponds to the renormalized Lagrangian in eq. (4.4). The 1-loop counter term which is the term $\propto (Z_1^{(\pi t)} - 1)^{(1)}$ cancels the UV divergence of the integral.

As for the case of the initial state vertex correction one can write $\Lambda_t^\mu$ as a sum of an IR divergent, an IR and UV finite and an UV divergent contribution. Compared to to the fermionic case there is an additional contribution, the 2-point function ($\Lambda_{t_{2p}}^\mu$) which seems to be IR finite but UV divergent:

$$\Lambda_t^\mu = \Lambda_{t_{IR}}^\mu + \Lambda_{t_{\rm fin}}^\mu + \Lambda_{t_{UV}}^\mu + \Lambda_{t_{2p}}^\mu \ . \tag{4.56}$$

$\Lambda_{t_{2p}}^\mu$ is a consequence of the cancellation of two powers of $k$ in the numerator of the integrand against the photon propagator $k^2$ in the denominator, leaving just two pion propagators.

The IR divergent contribution to $\Lambda_t^\mu$ can be expressed in the form of the master integral $I_{3S}$ which is given in App. A, eq. (A.50):

$$\Lambda_{t_{IR}}^\mu = -2i(-ie)^2\ (k_1^\mu - k_2^\mu)(s-2m_\pi^2)i(-ie)^2 I_{3S}(k,-k_1,k_2)\ . \tag{4.57}$$

Like for the initial state vertex correction one can express the contributions to $\Lambda_{(\pi)}^\mu$ in terms of electromagnetic form factors. The IR divergent contribution then becomes

$$\Lambda_{t_{IR}}^\mu = F_{1(\pi)}^{IR}(q^2)\ (k_1^\mu - k_2^\mu)\ , \tag{4.58}$$

with the regularized IR form factor

$$\begin{aligned} F_{1(\pi)}^{IR}(q^2) &= \frac{\alpha}{\pi}\,\frac{s-2m_\pi^2}{s\beta_\pi}\left\{\frac{1}{\varepsilon_{IR}}\left\{-\log\left(\frac{1+\beta_\pi}{1-\beta_\pi}\right)+\pi i\right\}\right. \\ &+ \frac{1}{2}\left\{\left[\log\left(\frac{1+\beta_\pi}{1-\beta_\pi}\right)-\pi i\right]\left[\log\left(\frac{4\pi\mu_{IR}^2}{s}\right)-\gamma_E\right]\right. \\ &- \frac{1}{2}\log\left(\frac{1+\beta_\pi}{1-\beta_\pi}\right)\left[\log\left(\frac{1-\beta_\pi^2}{4}\right)+2\log(\beta_\pi)\right] \\ &- \log\left(\frac{1+\beta_\pi}{2\beta_\pi}\right)\log\left(\frac{1-\beta_\pi}{2\beta_\pi}\right)-2{\rm Li}_2\left(-\frac{1-\beta_\pi}{2\beta_\pi}\right) \\ &+ \left.\left.\frac{2}{3}\pi^2+2\pi i\log(\beta_\pi)\right\}\right\}\ . \end{aligned} \tag{4.59}$$

The IR and UV finite contribution to $\Lambda_{(\pi)}^\mu$ in terms of the master integral $I_{3V}^\mu$ reads (see App. A)

$$\begin{aligned} \Lambda_{t_{\rm fin}}^\mu &= -4(s-2m_\pi^2)i(-ie)^2\ I_{3V}^\mu(k,-k_1,k_2) \\ &+ 2(k_1^\mu-k_2^\mu)(k_{1\alpha}-k_{2\alpha})i(-ie)^2\ I_{3V}^\alpha(k,-k_1,k_2)\ . \end{aligned} \tag{4.60}$$

Using the solution of the master integral given in eq. (A.68) also allows us to express $\Lambda_{t_{\rm fin}}^\mu$ in terms of a form factor:

$$\Lambda_{t_{\rm fin}}^\mu = F_{1(\pi)}^{\rm fin}(q^2)\ (k_1^\mu - k_2^\mu)\ , \tag{4.61}$$

where the finite form factor reads

$$F^{\rm fin}_{1(\pi)}(q^2) \;=\; \frac{\alpha}{2\pi}\,\frac{3s-8m_\pi^2}{s\beta_\pi}\,\left[\log\left(\frac{1+\beta_\pi}{1-\beta_\pi}\right)-\pi i\right]\,. \tag{4.62}$$

The UV divergent contribution is the sum of the regularized UV divergent contribution to the integral and the counter term:

$$\begin{aligned}\Lambda^\mu_{t_{UV}} \;&=\; 4(k_1-k_2)_\alpha i(-ie)^2\,\mu_{UV}^{\varepsilon_{UV}}\;I_{3T}^{\alpha\mu}(k,-k_1,k_2)\\ &\quad+\,(k_1^\mu-k_2^\mu)(Z_1^{(\pi t)}-1)^{(1)}\,.\end{aligned} \tag{4.63}$$

Inserting the solution for $I_{3T}^{\alpha\beta}$ [see eq. (A.73)] and choosing as before the $\overline{MS}$ scheme determines the 1-loop renormalization constant:

$$(Z_1^{(\pi t)}-1)^{(1)} \;=\; -\frac{\alpha}{4\pi}\left[\frac{2}{\varepsilon_{UV}}+\log\left(\frac{4\pi\mu_{UV}^2}{\mu^2_{\overline{MS}}}\right)-\gamma_{_E}\right]\,. \tag{4.64}$$

The UV form factor in the $\overline{MS}$ scheme then reads

$$\begin{aligned}F^{UV}_{1(\pi)} \;&=\; \frac{\alpha}{4\pi}\,\left\{\log\left(\frac{\mu^2_{\overline{MS}}}{s}\right)+3-\log\left(\frac{1-\beta_\pi^2}{4}\right)\right.\\ &\quad\left.-\;2\beta_\pi\left[\log\left(\frac{1+\beta_\pi}{1-\beta_\pi}\right)-\pi i\right]\right\}\,.\end{aligned} \tag{4.65}$$

It will now be shown that the 2-point integral contribution

$$\Lambda^\mu_{t_{2p}} \;=\; i(-ie)^2\,\mu^{4-n}\int\frac{d^nk}{(2\pi)^n}\,\frac{k_1^\mu-k_2^\mu+2k^\mu}{[(k_1+k)^2-m_\pi^2+i\epsilon]\,[(k_2-k)^2-m_\pi^2+i\epsilon]} \tag{4.66}$$

vanishes. To see this, substitute $k=P+k_2$:

$$\begin{aligned}\Lambda^\mu_{t_{2p}} \;&=\; i(-ie)^2\,\mu^{4-n}\int\frac{d^nP}{(2\pi)^n}\,\frac{2P^\mu+q^\mu}{[(P+q)^2-m_\pi^2+i\epsilon]\,[P^2-m_\pi^2+i\epsilon]}\\ &=\; i(-ie)^2\,\mu^{4-n}\,\left[\,\mathcal{I}_{1(\pi)}q^\mu\;+\;2\mathcal{I}^\mu_{2(\pi)}\right]\,,\end{aligned} \tag{4.67}$$

where

$$\begin{aligned}\mathcal{I}_{1(\pi)} \;&=\; \int\frac{d^nP}{(2\pi)^n}\,\frac{1}{[(P+q)^2-m_\pi^2+i\epsilon]\,[P^2-m_\pi^2+i\epsilon]}\\ &=\; \frac{i\pi^{n/2}}{(2\pi)^n}\,\Gamma\left(2-\frac{n}{2}\right)\int_0^1 dx\;\left[q^2x(x-1)+m_\pi^2-i\epsilon\right]^{-2+n/2}\,,\end{aligned} \tag{4.68}$$

$$\begin{aligned}\mathcal{I}^\mu_{2(\pi)} \;&=\; \int\frac{d^nP}{(2\pi)^n}\,\frac{P^\mu}{[(P+q)^2-m_\pi^2+i\epsilon]\,[P^2-m_\pi^2+i\epsilon]}\\ &=\; -\frac{i\pi^{n/2}}{(2\pi)^n}\,\Gamma\left(2-\frac{n}{2}\right)\,q^\mu\int_0^1 dx\;x\left[q^2x(x-1)+m_\pi^2-i\epsilon\right]^{-2+n/2}.\end{aligned} \tag{4.69}$$

Here Feynman parameters were used to write $\Lambda^\mu_{t_{2p}}$ in the form of eq. (A.7). Then eq. (A.8) and (A.9) were applied. The UV divergence is regularized in $n = 4 - \varepsilon_{UV}$ dimensions, leading to

$$\begin{aligned}\left[\mathcal{I}_{1(\pi)} q^\mu + 2\mathcal{I}^\mu_{2(\pi)}\right] &= q^\mu \, \frac{i\pi^{2-\varepsilon_{UV}/2}}{(2\pi)^{4-\varepsilon_{UV}}} \, \Gamma\left(\frac{\varepsilon_{UV}}{2}\right) \\ &\quad \times \int_0^1 dx \, (1-2x) \left[q^2 x(x-1) + m_\pi^2 - i\epsilon\right]^{-\varepsilon_{UV}/2} \, . \end{aligned} \tag{4.70}$$

Consider now the integral in (4.70) and substitute $u = x - 1/2$:

$$\begin{aligned}&\int_0^1 dx \, (1-2x) \left[q^2 x(x-1) + m_\pi^2 - i\epsilon\right]^{-\varepsilon_{UV}/2} \\ &= -2 \int_{-1/2}^{1/2} du \, u \left\{q^2 \left[u^2 - \beta_\pi^2\right]\right\}^{-\varepsilon_{UV}/2} = 0 \, . \end{aligned} \tag{4.71}$$

Thus the integral vanishes because the integrand is odd under the interchange $u \leftrightarrow -u$ and the integration interval is symmetric around $u = 0$. Therefore, as already remarked above, the 2-point contribution to the 3-point function also vanishes:

$$\Lambda^\mu_{t_{2p}} = 0 \, . \tag{4.72}$$

This has to be the case since this contribution would have been proportional to $q^\mu$ and therefore would have spoiled gauge invariance. Having calculated all contributions to $\Lambda^\mu_t$, what remains is the calculation of the contributions corresponding to diagram *b*) and *c*) which contain the quartic vertices. The sum of both diagrams in terms of the master integrals $I_{2S}$ and $I^\mu_{2V}$ reads ($n = 4 - \varepsilon_{UV}$)

$$\begin{aligned}\Lambda^\mu_q &= 2ie^2\mu^{4-n} \, [2I_{2S}(-k_1, k)k_1^\mu + I^\mu_{2V}(-k_1, k) - 2I_{2S}(k, -k_2)k_2^\mu \\ &\quad - I^\mu_{2V}(k, -k_2)] \, + \, (k_1^\mu - k_2^\mu)(Z_1^{(\pi q)} - 1)^{(1)} \, . \end{aligned} \tag{4.73}$$

Using the results given in App. A, eq. (A.16) and (A.17) yields

$$I_{2S}(-k_{1(2)}, k) = \frac{i\pi^{n/2}}{(2\pi)^n} \, \Gamma\left(2 - \frac{n}{2}\right) \int_0^1 dx \left[m_\pi^2 x^2 - i\epsilon\right]^{-2+n/2} \, , \tag{4.74}$$

$$I^\mu_{2V}(-k_{1(2)}, k) = -\frac{i\pi^{n/2}}{(2\pi)^n} \, \Gamma\left(2 - \frac{n}{2}\right) k^\mu_{1(2)} \int_0^1 dx \, x \left[m_\pi^2 x^2 - i\epsilon\right]^{-2+n/2} \, . \tag{4.75}$$

Inserting (4.74) and (4.75) into (4.73) and expanding in $\varepsilon_{UV}$ leads to

$$\begin{aligned}\Lambda^\mu_q &= -\frac{3}{4}\frac{\alpha}{\pi} \left\{\frac{2}{\varepsilon_{UV}} - \gamma_E + \log(4\pi\mu^2_{UV}) \right. \\ &\quad \left. -\frac{2}{3}\int_0^1 dx(2-x) \log\left[m_\pi^2 x^2 - i\epsilon\right] + (Z_1^{(\pi q)} - 1)^{(1)}\right\} \, (k_1 - k_2)^\mu \\ &= F^q_{1(\pi)} \, (k_1 - k_2)^\mu \, , \end{aligned} \tag{4.76}$$

where

$$F^q_{1(\pi)} = -\frac{3}{4}\frac{\alpha}{\pi}\left\{\log\left(\frac{\mu^2_{\overline{MS}}}{m^2_\pi}\right)+\frac{7}{3}\right\} \tag{4.77}$$

is the quartic form factor in the $\overline{MS}$ scheme. The corresponding $\overline{MS}$ renormalization constant reads

$$(Z_1^{(\pi q)}-1)^{(1)} = \frac{3}{4}\frac{\alpha}{\pi}\left[\frac{2}{\varepsilon_{UV}}+\log\left(\frac{4\pi\mu^2_{UV}}{\mu^2_{\overline{MS}}}\right)-\gamma_E\right] . \tag{4.78}$$

Adding the contribution of eq. (4.64) then yields

$$\begin{aligned}(Z_1^{(\pi)}-1)^{(1)} &= (Z_1^{(\pi t)}-1)^{(1)}+(Z_1^{(\pi q)}-1)^{(1)} \\ &= \frac{\alpha}{2\pi}\left[\frac{2}{\varepsilon_{UV}}+\log\left(\frac{4\pi\mu^2_{UV}}{\mu^2_{\overline{MS}}}\right)-\gamma_E\right] .\end{aligned} \tag{4.79}$$

## 4.6 Pion Self Energy


The calculation of the pion pair self energy corrections (which are needed for the wave function renormalization of the fields corresponding to the final state pions) is similar to the calculation of the initial state self energy corrections (see the previous chapter). Recalling eq. (3.54), allows us to write the FS self energy amplitude as

$$\mathcal{M}_{S_f} = \mathcal{M}_0\,\Sigma_1^{(\pi)} \quad \text{with} \quad \Sigma_1^{(\pi)} = \left.\frac{\partial\Sigma^{(\pi)}(p^2)}{\partial p^2}\right|_{p^2=m^2_\pi} . \tag{4.80}$$

$\Sigma^{(\pi)}$ is the irreducible 1-loop pion self energy which can be written in terms of the functions $A^{(\pi)}(p^2)$ and $B^{(\pi)}(p^2)$:

$$\begin{aligned}-i\Sigma^{(\pi)}(p^2) &= \mu^{4-n}(-ie)^2\int\frac{d^nk}{(2\pi)^n}\frac{(2p+k)_\mu(2p+k)^\mu}{[(p+k)^2-m^2_\pi+i\epsilon][k^2+i\epsilon]} \\ &\quad +i(Z_0^{(\pi)}-1)^{(1)}m^2_\pi+i(Z_2^{(\pi)}-1)^{(1)}p^2 \\ &= -i\left[A^{(\pi)}(p^2)+B^{(\pi)}(p^2)p^2\right] .\end{aligned} \tag{4.81}$$

with

$$A^{(\pi)}(p^2) = -ie^2I_{1S}(m^2_\pi)-(Z_0^{(\pi)}-1)m^2_\pi , \tag{4.82}$$

$$B^{(\pi)}(p^2) = -4ie^2\left[I_{2S}(p,k)+\frac{p_\alpha I^\alpha_{2V}(p,k)}{p^2}\right]-(Z_2^{(\pi)}-1)^{(1)} . \tag{4.83}$$

The integrals $I_{1S}$, $I_{2S}$ and $I^{\alpha}_{2V}$ are again given in App A [eq. (A.12), (A.18), (A.19)]. In the $\overline{MS}$ scheme the counter terms that cancel the UV divergences read

$$(Z_0^{(\pi)}-1)^{(1)} = \frac{\alpha}{4\pi}\left\{\frac{2}{\varepsilon_{UV}} - \gamma_E + \log\left(4\pi\mu^2\right) - \log\left(\mu^2_{\overline{MS}}\right)\right\}, \tag{4.84}$$

$$(Z_2^{(\pi)}-1)^{(1)} = \frac{\alpha}{2\pi}\left\{\frac{2}{\varepsilon_{UV}} - \gamma_E + \log\left(4\pi\mu^2\right) - \log\left(\mu^2_{\overline{MS}}\right)\right\}. \tag{4.85}$$

This leaves the following UV finite expressions:

$$A^{(\pi)}(p^2) = \frac{\alpha}{4\pi}\left[1+\log\left(\frac{\mu^2_{\overline{MS}}}{m_\pi^2}\right)\right] m_\pi^2\,, \tag{4.86}$$

$$B^{(\pi)}(p^2) = -\frac{\alpha}{\pi}\int_0^1 dx\,(1-x)\,\log\left[\frac{p^2x^2 - x\left(p^2-m_\pi^2\right) - i\epsilon}{\mu^2_{\overline{MS}}}\right]. \tag{4.87}$$

Since $A^{(\pi)}$ does not depend on the momentum $p$, only $B^{(\pi)}$ contributes to the external leg self energy correction:

$$\Sigma_1^{(\pi)} = B^{(\pi)}(m_\pi^2) + \left.\frac{\partial B^{(\pi)}(p^2)}{\partial p^2}\right|_{p^2=m_\pi^2} m_\pi^2\,. \tag{4.88}$$

$\Sigma_1^{(\pi)}$ is UV finite but IR divergent. It is regularized in $n = 4+\varepsilon_{IR}$ dimensions. Here eq. (A.23) and (A.24) of App. A are used. This yields

$$\left.\frac{\partial B^{(\pi)}(p^2)}{\partial p^2}\right|_{p^2=m_\pi^2} = -4ie^2\left[\frac{\partial I_{2S}(p,k)}{\partial p^2} + \frac{\partial}{\partial p^2}\left(\frac{p_\alpha I^{\alpha}_{2V}(p,k)}{p^2}\right)\right]$$

$$= \frac{\alpha}{\pi}\frac{1}{m_\pi^2}\left\{\frac{1}{\varepsilon_{IR}} - \frac{1}{2}\left[-\gamma_E + \log\left(\frac{4\pi\mu^2_{IR}}{m_\pi^2}\right)+3\right]\right\}, \tag{4.89}$$

$$B^{(\pi)}(m_\pi^2) = -\frac{\alpha}{2\pi}\left[\log\left(\frac{m_\pi^2}{\mu^2_{\overline{MS}}}\right) - 3\right]. \tag{4.90}$$

Inserting eq. (4.90) and (4.89) into eq. (4.88) finally yields the pion self energy correction in the $\overline{MS}$ scheme:

$$\Sigma_1^{(\pi)} = \frac{\alpha}{\pi}\left\{\frac{1}{\varepsilon_{IR}} - \frac{1}{2}\left[-\gamma_E + \log\left(\frac{4\pi\mu^2_{IR}}{m_\pi^2}\right) + \log\left(\frac{m_\pi^2}{\mu^2_{\overline{MS}}}\right)\right]\right\}. \tag{4.91}$$

## 4.7 The Box Diagrams

The Feynman diagrams shown above correspond to the 1-loop IFS interference corrections. Let us first consider the diagrams with four vertices, where the initial $e^+e^-$ state is connected to the final $\pi^+\pi^-$ state by the two photons $\gamma(k)$ and $\gamma(l)$, $k$ and $l$ being the 4-momenta of the photons. The convention will be the following:

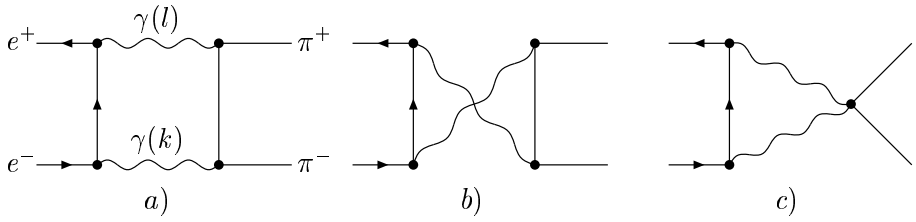


the photon $\gamma(k)$ is connected to the initial state electron $e^-$ and the photon $\gamma(l)$ is connected to the initial state positron $e^+$. For the two different topologies of the box diagrams the labels "$a$)" and "$b$)" will be used, as shown in the figure above. Thus for box $a$) the photon $\gamma(k)$ is connected to the negatively charged pion $\pi^-$ and the photon $\gamma(l)$ is connected to the positively charged pion $\pi^+$. In the case of box $b$) the photon $\gamma(k)$ is connected to $\pi^+$ and the photon $\gamma(l)$ is connected to $\pi^-$. The loop momentum is chosen to flow anti-clockwise. Again the master integrals which are derived in App. A will be used. The following abbreviations for the box propagator terms will be used:

$$\begin{aligned} D_{p_i} &:= (p_i - k)^2 - m_e^2 + i\epsilon \quad , \quad i = 1, 2 \, , && (4.92) \\ D_{k_j} &:= (k_j - k)^2 - m_\pi^2 + i\epsilon \quad , \quad j = 1, 2 \, , && (4.93) \\ D_k &:= k^2 + i\epsilon \quad , \quad D_q := (q - k)^2 + i\epsilon \, . && (4.94) \end{aligned}$$

For the numerators of the box integrals $N_a$ and $N_b$ corresponding to the diagrams $a$) and $b$) we obtain

$$\begin{aligned} N_a &:= \bar{v}_{s_2}(p_2)(\not{k}_1 - \not{k}_2 - \not{k})(\not{p}_1 - \not{k} + m_\pi)(2\not{k}_1 - \not{k})u_{s_1}(p_1) \, , && (4.95) \\ N_b &:= \bar{v}_{s_2}(p_2)(\not{k}_1 - \not{k}_2 + \not{k})(\not{p}_1 - \not{k} + m_\pi)(\not{k} - 2\not{k}_2)u_{s_1}(p_1) \, . && (4.96) \end{aligned}$$

This allows us to write the amplitudes of box $a$) and box $b$) in a compact way:

$$\mathcal{M}_{a(b)} = e^4 \, \mu^{4-n} \int \frac{d^n k}{(2\pi)^n} \, \frac{N_{a(b)}}{D_k D_{p_1} D_q D_{k_{1(2)}}} \, . \qquad (4.97)$$

$N_a$ and $N_b$ can be transformed into a more convenient form by applying the anti-commutation relations of the $\gamma$ matrices and by using the on-shell conditions for the external pions:

$$\begin{aligned} N_a &= j_0 \, (2U + D_{p_1} + D_k) - j_{1\alpha} k^\alpha \, (2U + D_{p_1}) - 2 j^a_{2\alpha} k^\alpha \, , && (4.98) \\ N_b &= -j_0 \, (2T + D_{p_1} + D_k) - j_{1\alpha} k^\alpha \, (2T + D_{p_1}) + 2 j^b_{2\alpha} k^\alpha \, , && (4.99) \end{aligned}$$

where the following definitions have been used:

$$\begin{aligned} j_0 &= \bar{v}_{s_2}(p_2)(\not{k}_1 - \not{k}_2)u_{s_1}(p_1) \, , && (4.100) \\ j_{1\alpha} &= \bar{v}_{s_2}(p_2)\gamma_\alpha u_{s_1}(p_1) \, , && (4.101) \\ j^a_{2\alpha} &= \bar{v}_{s_2}(p_2)(\not{k}_1 - \not{k}_2)\gamma_\alpha \not{k}_1 u_{s_1}(p_1) \, , && (4.102) \\ j^b_{2\alpha} &= \bar{v}_{s_2}(p_2)(\not{k}_1 - \not{k}_2)\gamma_\alpha \not{k}_2 u_{s_1}(p_1) \, , && (4.103) \\ U &= 2p_1k_1 \, , \quad T = 2p_1k_2 \, , \quad u = (p_1 - k_1)^2 \, , \quad t = (p_1 - k_2)^2 \, . && (4.104) \end{aligned}$$

The box amplitudes can now be expressed in terms of the scalar and rank-1-tensor 3-point functions and 4-point functions which are presented in App. A:

$$\begin{aligned}\mathcal{M}_a &= e^4\, F_\pi(s)\, \Big\{ 2U j_0 I_{4S}(k,p_1,q,k_1) - 2\left[U j_{1\alpha} + j^a_{2\alpha}\right] I^\alpha_{4V}(k,p_1,q,k_1) \\ &+ j_0 I_{3S}(k,q,k_1) + j_0 I_{3S}(p_1,q,k_1) - j_{1\alpha} I^\alpha_{3V}(k,q,k_1) \Big\}\,, \qquad (4.105)\\ \mathcal{M}_b &= e^4\, F_\pi(s)\, \Big\{ -2T j_0 I_{4S}(k,p_1,q,k_2) - 2\left[T j_{1\alpha} - j^b_{2\alpha}\right] I^\alpha_{4V}(k,p_1,q,k_2) \\ &- j_0 I_{3S}(k,q,k_2) - j_0 I_{3S}(p_1,q,k_2) - j_{1\alpha} I^\alpha_{3V}(k,q,k_2) \Big\}\,. \qquad (4.106)\end{aligned}$$

Let us now define the $T$ matrix element:

$$T^{box}_{fi} = T^a_{fi} + T^b_{fi} = -i\left(\mathcal{M}_a + \mathcal{M}_a\right)\,, \qquad (4.107)$$

where the indices $i$ and $f$ correspond to the initial $e^+e^-$ state and the final $\pi^+\pi^-$ state, respectively. Then the correction factor $\delta_{box}$ which corresponds to the sum of the diagrams $a$) and $b$) can be related to the $T$ matrix element in the following way:

$$T^0_{fi}\,\delta_{box} = 2\Re e\left[T^a_{fi} + T^b_{fi}\right]\,, \quad \text{with} \quad T^0_{fi} = -i\mathcal{M}_0\,, \qquad (4.108)$$

$\mathcal{M}_0$ being the Born amplitude given in (4.7). The box amplitudes given in (4.105) and (4.106) are IR divergent but UV finite in four dimensions, the IR divergent contribution being proportional to the scalar 4-point integral $I_{4S}$. It is therefore useful to write $\delta_{box}$ as the sum of an IR divergent part which is regularized in $4+\varepsilon_{IR}$ dimensions and a finite part:

$$\delta_{box} = \delta^{IR}_{box} + \delta^{\rm fin}_{box}\,. \qquad (4.109)$$

Then the IR divergent correction factor can be related to the IR divergent contribution of the $T$ matrix elements:

$$\delta^{IR}_{box} = 2\Re e\left[T^{a,IR}_{fi} + T^{b,IR}_{fi}\right]\,, \qquad (4.110)$$

with

$$\begin{aligned}T^{a,IR}_{fi} &= +\,8\pi\alpha\; s\; U\; I_{4S}(k,p_1,q,k_1)\; T^0_{fi}\,, \qquad (4.111)\\ T^{b,IR}_{fi} &= -\,8\pi\alpha\; s\; T\; I_{4S}(k,p_1,q,k_2)\; T^0_{fi}\,. \qquad (4.112)\end{aligned}$$

Using the solution of the real part of the scalar four point integral $I_{4S}$ in App. A, eq. (A.82) then leads to the IR divergent box correction factor:

$$\delta^{IR}_{box} = \frac{2\alpha}{\pi}\,\log\left(\frac{U}{T}\right)\left[-\frac{2}{\varepsilon_{IR}} + \log\left(\frac{4\pi\mu^2_{IR}}{s}\right) - \gamma_E\right]\,. \qquad (4.113)$$

Later, when adding the contribution from the IFS interference correction, the IR pole in eq. (4.113) is going to cancel.

What remains is the evaluation of the finite contribution $\delta_{box}^{\rm fin}$. The rank 1 tensor integrals $I_{3V}^{\alpha}$ and $I_{4V}^{\alpha}$ in eq. (4.105) and (4.106) can be expressed in terms of the scalar integrals by using the method of tensor reduction, as shown in App. C. Then, after some algebra, the amplitudes $\mathcal{M}_a$ and $\mathcal{M}_b$ can be transformed into the following form:

$$\begin{aligned}
\mathcal{M}_a &= e^4\, F_\pi(s)\, j_0 \Big\{ 2U I_{4S}(k,p_1,q,k_1) \\
&- \frac{1}{s\beta_\pi^2}\Big[\frac{s}{2} I_{3S}(k,q,k_1) + I_{2S}(k,q) - I_{2S}(q,k_1)\Big] \\
&+ \frac{1}{U^2 - Us + sm_\pi^2}\Big[U(U-m_\pi^2)[sI_{4S}(k,p_1,q,k_1) - 2I_{3S}(k,p_1,k_1)] \\
&+ (2U^2 - Us + sm_\pi^2) I_{3S}(k,p_1,q) \\
&+ (-U+m_\pi^2)(s-2U) I_{3S}(k,q,k_1)\Big]\Big\}\,, \qquad (4.114) \\
\mathcal{M}_b &= -e^4\, F_\pi(s)\, j_0 \Big\{ 2T I_{4S}(k,p_1,q,k_2) \\
&- \frac{1}{s\beta_\pi^2}\Big[\frac{s}{2} I_{3S}(k,q,k_2) + I_{2S}(k,q) - I_{2S}(q,k_2)\Big] \\
&+ \frac{1}{T^2 - Ts + sm_\pi^2}\Big[T(T-m_\pi^2)[sI_{4S}(k,p_1,q,k_2) - 2I_{3S}(k,p_1,k_2)] \\
&+ (2T^2 - TS + sm_\pi^2) I_{3S}(k,p_1,q) \\
&+ (-T+m_\pi^2)(s-2T) I_{3S}(k,q,k_2)\Big]\Big\}\,. \qquad (4.115)
\end{aligned}$$

The calculation of the master integrals is presented in App. A. Some additional manipulation finally leads to the following box diagram correction factor:

$$\begin{aligned}
\delta_{box} &= \frac{2\alpha}{\pi}\Big\{ \log\left(\frac{u-m_\pi^2}{t-m_\pi^2}\right)\left[-\frac{2}{\varepsilon_{IR}} + \log\left(\frac{4\pi\mu_{IR}^2}{s}\right) - \gamma_E\right] \\
&+ \frac{1}{4}\frac{s^2}{ut-m_\pi^4}\Big\{ \frac{u-t}{s}\Big[c_1(u) + c_1(t) + c_e + c_\pi\Big] \\
&+ \frac{u+t}{s}\Big[c_1(u) - c_1(t)\Big]\Big\}\Big\}\,, \qquad (4.116)
\end{aligned}$$

with $(x = u, t)$

$$
\begin{aligned}
c_1(x) &= \frac{1}{2}\Bigg\{3\log^2\left(\frac{x-m_\pi^2}{x}\right) - \frac{1}{2}\log^2\left(-\frac{m_e^2}{x}\right) - \frac{1}{2}\log^2\left(-\frac{m_\pi^2}{x}\right) \\
&\quad -2\log\left(-\frac{m_\pi^2}{x}\right)\log\left(\frac{x-m_\pi^2}{x}\right) + 2\mathrm{Li}_2\left(-\frac{m_\pi^2}{x-m_\pi^2}\right) - \frac{\pi^2}{3}\Bigg\}, \qquad (4.117) \\
c_\pi &= \frac{1+\beta_\pi^2}{2\beta_\pi}\left[2\mathrm{Li}_2\left(\frac{1+\beta_\pi}{2}\right) - 2\mathrm{Li}_2\left(\frac{1-\beta_\pi}{2}\right) + \mathrm{Li}_2\left(-\frac{1+\beta_\pi}{1-\beta_\pi}\right)\right. \\
&\quad - \left.\mathrm{Li}_2\left(-\frac{1-\beta_\pi}{1+\beta_\pi}\right) + \log\left(\frac{s}{m_\pi^2}\right)\log\left(\frac{1+\beta_\pi}{1-\beta_\pi}\right)\right], \qquad (4.118) \\
c_e &= \frac{1}{2}\log^2\left(\frac{s}{m_e^2}\right) + \frac{\pi^2}{6}\,. \qquad (4.119)
\end{aligned}
$$

Obviously the box correction factor $\delta_{box}$ is an antisymmetric function in the polar angle $\Theta$ in the CMS. Hence, like the real photon IFS interference correction also the box correction drops out due to $C$-symmetry when the differential cross section is integrated over the angles.

Finally let's consider the triangular box diagram shown in Fig. *c*). Using the Feynman rules allows us to write the corresponding amplitude as

$$
\begin{aligned}
\mathcal{M}_c &= -4e^4 \int \frac{d^4k}{(2\pi)^4}\, \frac{\bar{v}_{s_2}(p_2)(\not{k}+m_e)u_{s_1}(p_1)}{[(p_1-k)^2-m_e^2+i\epsilon][k^2+i\epsilon][(q-k)^2+i\epsilon]} \\
&= -4e^4\Big[m_e\ \bar{v}_{s_2}(p_2)u_{s_1}(p_1)\ I_{3S}(k,q,p_1) \\
&\quad + \bar{v}_{s_2}(p_2)\gamma_\mu u_{s_1}(p_1)\ I_{3V}^\mu(k,q,p_1)\Big]\,. \qquad (4.120)
\end{aligned}
$$

The solution for the scalar integral $I_{3S}(k,p_1,q)$ is given in eq. (A.61). The rank 1 tensor integral $I_{3V}^\mu(k,p_1,q)$ can be solved by using the following tensor ansatz:

$$
I_{3V}^\mu(k,p_1,q) = f_q\ q^\mu + f_{p_1}\ p_1^\mu\,. \qquad (4.121)
$$

From gauge invariance it follows that no terms $\propto f_q$ can contribute to $\mathcal{M}_c$. On the other hand the terms $\propto f_{p_1}$ lead to contributions $\propto m_e$ when using the on-shell condition for the initial state electron. Therefore the contributions from the triangular box diagram are $\propto m_e^2/s$. Hence, since $s \gg m_e^2$, the triangular box diagram can be neglected completely.

## 4.8 Results and Discussion

Collecting the results for the real and virtual QED corrections allows us to evaluate precision observables which are relevant for low energy hadronic experiments like at DAΦNE and VEPP-2M. As we will see when adding the soft and virtual contributions the IR poles are going to cancel and the parameters $\mu_{IR}$ and $\mu_{UV}$ are going to

drop out. Adding then the hard photon contribution leads also to a cancellation of the terms containing the soft photon energy cut off $\Lambda$. The NLO total cross section can now be written as the sum of the Born cross section multiplied by a correction factor which contains the IS and FS soft plus virtual corrections $\delta_{\rm ini}$ and $\delta_{\rm fin}$ and the convolution integrals corresponding to the hard IS and FS photons:

$$\begin{aligned}\sigma(s) &= \sigma_0\left[1+\delta_{\rm ini}(\Lambda)+\delta_{\rm fin}(\Lambda)\right] \\ &+ \int_{4m_\pi^2}^{s-2\sqrt{s}\Lambda} ds'\,\sigma_0(s')\rho_{\rm ini}(s,s') + \sigma_0(s)\int_{4m_\pi^2}^{s-2\sqrt{s}\Lambda} ds'\,\rho_{\rm fin}(s,s')\;. \quad (4.122)\end{aligned}$$

The hard photon IS and FS radiator functions $\rho_{\rm ini}$ and $\rho_{\rm fin}$ are given in eq. (3.26) and (4.28). They are written now in a somewhat different way[3] ($z = s'/s$):

$$\rho_{\rm ini}(s,s') = \frac{1}{s}\left[\tilde{\delta}_{\rm ini}^{H(1)}(s,s') + \frac{B_e(s)}{1-z}\right]\;, \quad (4.123)$$

$$\rho_{\rm fin}(s,s') = \frac{1}{s}\left[\tilde{\delta}_{\rm fin}^{H}(s,s') + \frac{B_\pi(s,s')}{1-z}\right]\;, \quad (4.124)$$

with the definitions

$$\tilde{\delta}_{\rm ini}^{H(1)}(s,s') = -\frac{\alpha}{\pi}\,(1+z)\left[\log\left(\frac{s}{m_e^2}\right)-1\right]\;, \quad (4.125)$$

$$\tilde{\delta}_{\rm fin}^{H}(s,s') = \frac{2\alpha}{\pi}(1-z)\frac{\beta_\pi(s')}{\beta_\pi^3(s)}\;, \quad (4.126)$$

$$B_e(s) = \frac{2\alpha}{\pi}\left[\log\left(\frac{s}{m_e^2}\right)-1\right]\;, \quad (4.127)$$

$$B_\pi(s,s') = \frac{2\alpha}{\pi}\frac{s'\beta_\pi(s')}{s\beta_\pi(s)}\left[\frac{1+\beta_\pi^2(s')}{2\beta_\pi(s')}\log\left(\frac{1+\beta_\pi(s')}{1-\beta_\pi(s')}\right)-1\right]\;. \quad (4.128)$$

The IS and FS state soft plus virtual corrections $\delta_{\rm ini}$ and $\delta_{\rm fin}$ are obtained by taking the sum of the self energy-, vertex- and soft photon contributions which were presented in the previous sections. Thus the IS soft plus virtual $O(\alpha)$ correction factor

[3] The conventions are similar to those in [80].

becomes

$$\begin{aligned}
\delta_{\rm ini}(\Lambda) &= 2\Re e\left[F_1^{IR}(s,\varepsilon_{IR})\right] + 2\Re e\left[\Sigma_1(\varepsilon_{IR})\right] + \delta_{\rm ini}^{S}(s,\Lambda,\varepsilon_{IR}) \\
&+ 2\Re e\left[F_1^{\rm fin}(s)\right] + 2\Re e\left[F_1^{UV}(s)\right] \\
&= \frac{\alpha}{\pi}\left\{\left[-1+\frac{1+\beta_e^2}{2\beta_e}\,\log\left(\frac{1+\beta_e}{1-\beta_e}\right)\right]\,\log\left(\frac{4\Lambda^2}{s}\right)\right. \\
&- \frac{3}{2}\,\log\left(\frac{s}{m_e^2}\right) + \frac{5s-8m_e^2}{2s\beta_e}\,\log\left(\frac{1+\beta_e}{1-\beta_e}\right) - \frac{1}{2}\,\log\left(\frac{1-\beta_e^2}{4}\right) \\
&- 2 - \frac{1+\beta_e^2}{2\beta_e}\,\left[\log\left(\frac{1+\beta_e}{1-\beta_e}\right)\left[\log\left(\frac{1+\beta_e}{2}\right)+\log(\beta_e)\right]\right. \\
&+ \log\left(\frac{1+\beta_e}{2\beta_e}\right)\log\left(\frac{1-\beta_e}{2\beta_e}\right) + 2{\rm Li}_2\left(\frac{2\beta_e}{1+\beta_e}\right) \\
&+ \left.\left. 2{\rm Li}_2\left(-\frac{1-\beta_e}{2\beta_e}\right) - \frac{2}{3}\pi^2\right]\right\} \\
&\simeq \log\left(\frac{2\Lambda}{\sqrt{s}}\right)\,B_e(s) + \tilde{\delta}_{\rm ini}^{V+S(1)}(s)\;. \qquad (4.129)
\end{aligned}$$

For the last line in (4.129) the high energy approximation ($s \gg m_e^2$) was taken (which of course is a good approximation for the considered DAΦNE energies), with

$$\tilde{\delta}_{\rm ini}^{V+S(1)}(s) = \frac{\alpha}{\pi}\left[-2+\frac{\pi^2}{3}+\frac{3}{2}\log\left(\frac{s}{m_e^2}\right)\right]\;. \qquad (4.130)$$

The FS soft plus virtual $O(\alpha)$ correction factor is the sum of the FS electromagnetic form factor $F_1$ corresponding to the FS vertex correction, the $\pi^+\pi^-$ external leg self energy corrections and the FS soft photon contribution:

$$\begin{aligned}
\delta_{\rm fin}(\Lambda) &= 2\Re e\left[F_{1(\pi)}^{IR}(s,\varepsilon_{IR})\right] + 2\Re e\left[\Sigma_{1(\pi)}(\varepsilon_{IR})\right] + \delta_{\rm fin}^{S}(s,\Lambda,\varepsilon_{IR}) \\
&+ 2\Re e\left[F_{1(\pi)}^{\rm fin}(s)\right] + 2\Re e\left[F_{1(\pi)}^{UV}(s)\right] + 2\Re e\left[F_{1(\pi)}^{q}(s)\right] \\
&= \log\left(\frac{2\Lambda}{\sqrt{s}}\right)\,B_\pi(s'=s) + \tilde{\delta}_{\rm fin}^{V+S}(s)\;, \qquad (4.131)
\end{aligned}$$

with the definition

$$\begin{aligned}
\tilde{\delta}_{\rm fin}^{V+S}(s) &= \frac{\alpha}{\pi}\left\{\frac{3s-4m_\pi^2}{s\beta_\pi}\,\log\left(\frac{1+\beta_\pi}{1-\beta_\pi}\right) - 2 - \frac{1}{2}\,\log\left(\frac{1-\beta_\pi^2}{4}\right)\right. \\
&-\frac{3}{2}\,\log\left(\frac{s}{m_\pi^2}\right) - \frac{1+\beta_\pi^2}{2\beta_\pi}\,\left[\log\left(\frac{1+\beta_\pi}{1-\beta_\pi}\right)\left[\log\left(\frac{1+\beta_\pi}{2}\right)\right.\right. \\
&+ \left.\log(\beta_\pi)\right] + \log\left(\frac{1+\beta_\pi}{2\beta_\pi}\right)\log\left(\frac{1-\beta_\pi}{2\beta_\pi}\right) \\
&+ \left.\left. 2{\rm Li}_2\left(\frac{2\beta_\pi}{1+\beta_\pi}\right) + 2{\rm Li}_2\left(-\frac{1-\beta_\pi}{2\beta_\pi}\right) - \frac{2}{3}\pi^2\right]\right\}\;. \qquad (4.132)
\end{aligned}$$

| $\sqrt{s}$ [GeV] | $O(\alpha)$ FS contribution |
|---|---|
| 0.3 | 3.6 |
| 0.4 | 1.2 |
| 0.5 | 0.9 |
| 0.6 | 0.9 |
| 0.76 | 0.7 |
| 0.9 | 0.4 |
| 1.02 | 0.3 |

Table 4.1: Contribution of $O(\alpha)$ FS corrections to the total cross section (in%).

To obtain the total cross section $\sigma(s)$ the convolution integrals in eq. (4.122) have to be evaluated. This can be done easily by numerical integration. The next to next to leading order (NNLO) contributions to the total cross section $\sigma$ account for in average less than 3 per mill (at most 1 %, at $\sqrt{s} = 1.02$ the contribution is 2 per mill). The results are plotted in Fig. 4.2. In Table 4.1 the contribution of the $O(\alpha)$ FS corrections for different center of mass energies is shown. Here the pion form factor parameterization by Gounaris and Sakurai [90] was used:

$$F_\pi(s) = \left[ \frac{A_1 - A_2 m_\pi^2}{A_1 + A_2 \frac{s\beta_\pi^2}{4} + f(s)} + A_3 e^{iA_4} \frac{m_\omega^2}{s - m_\omega^2 + i m_\omega \Gamma_\omega} \right] G(s) \,, \quad (4.133)$$

where

$$f(s) = \frac{1}{\pi}\left(m_\pi^2 - \frac{s}{3}\right) + \frac{1}{4\pi}\, s\beta_\pi^3 \, \log\left[\frac{\sqrt{s}}{2m_\pi}\,(1+\beta_\pi)\right] - i\frac{s\beta_\pi^3}{8} \,,$$
$$G(s) = \left(\frac{1}{1 - \frac{s}{M^2} - i\frac{\Gamma}{M}}\right)^n \,.$$

For $\sqrt{s} < m_\pi + m_\omega$ only the real part of $G(s)$ is kept. The second term accounts for the $\rho - \omega$–interference. The factor $G(s)$ incorporates the effect of the $\rho - \omega$ inelastic channels. The parameters are $M = 1.2\,\mathrm{GeV}$, $\Gamma = 0.15\,\mathrm{GeV}$ [99] and $n = 0.22$, $A_1 = 0.29\,\mathrm{GeV}^2$, $A_2 = -2.3$, $A_3 = -0.012$, $A_4 = 1.84$ [17]. Using the form factor given in the paper by Kühn and Santamaria [91] does not change the results substantially. Although it can be hardly recognized directly from Fig. 4.2, the FS contributions are not marginal for energies below the $\rho$ resonance peak which is at 0.76 GeV.

Taking the high energy limit in (4.122) provides a good cross check for the FS correction results. Carrying out the $s'$ integration for $s \to \infty$ and adding this result to the high energy virtual and soft photon FS corrections leads to an expression in which the $s$ dependence drops out. This has to be the case according to the Kinoshita-Lee-Nauenberg theorem [100, 101] which requires the collinear logarithms

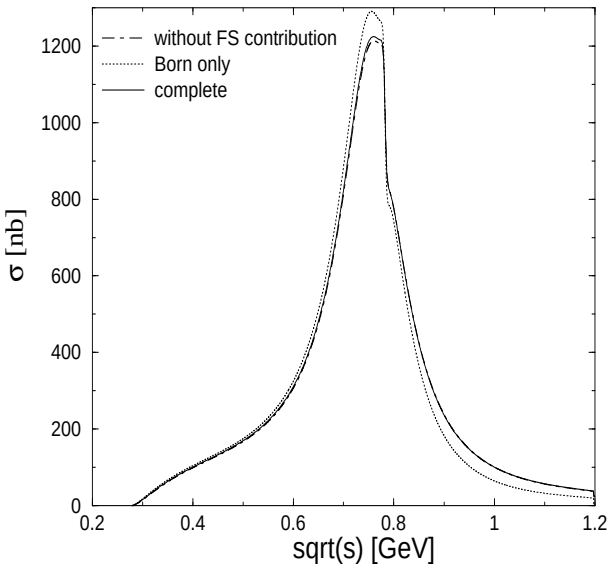


Figure 4.2: Total cross section $\sigma(s)$ as a function of the center of mass energy. The solid line corresponds to $\sigma(s)$ as given in eq. (4.122). The dotted line corresponds to the Born cross section. The dot-dashed line corresponds to the Born cross section with $O(\alpha)$ IS corrections.

to cancel. In addition all terms proportional to $\pi^2$ drop out. Defining

$$\eta(s) \equiv \frac{\pi}{\alpha}\left[\delta_{\rm fin}(\Lambda) + \int_{4m_\pi^2}^{s-2\sqrt{s}\Lambda} ds'\ \rho_{\rm fin}(s,s')\right] , \tag{4.134}$$

one can write the total cross section with only $O(\alpha)$ FS corrections in the following compact way:

$$\sigma_{\rm fin}(s) = \left[1+\eta(s)\frac{\alpha}{\pi}\right]\sigma_0(s) . \tag{4.135}$$

The function $\eta(s)$ is given by [102, 103, 34]

$$\begin{aligned}
\eta(s) &= \frac{1+\beta_\pi^2}{\beta_\pi}\Bigg\{4{\rm Li}_2\left(\frac{1-\beta_\pi}{1+\beta_\pi}\right) + 2{\rm Li}_2\left(-\frac{1-\beta_\pi}{1+\beta_\pi}\right) \\
&- 3\log\left(\frac{2}{1+\beta_\pi}\right)\log\left(\frac{1+\beta_\pi}{1-\beta_\pi}\right) - 2\log(\beta_\pi)\log\left(\frac{1+\beta_\pi}{1-\beta_\pi}\right)\Bigg\} \\
&- 3\log\left(\frac{4}{1-\beta_\pi^2}\right) - 4\log(\beta_\pi) \\
&+ \frac{1}{\beta_\pi^3}\left[\frac{5}{4}(1+\beta_\pi^2)^2 - 2\right]\log\left(\frac{1+\beta_\pi}{1-\beta_\pi}\right) + \frac{3}{2}\frac{1+\beta_\pi^2}{\beta_\pi^2}
\end{aligned} \tag{4.136}$$

and provides a good measure for the dependence of the observables on the pion mass. Neglecting the pion mass is obviously equivalent to taking the high energy limit. In this limit we observe:

$$\eta(s \to \infty) \;=\; 3\,. \tag{4.137}$$

Our result in (4.137) agrees with the result obtained by Schwinger [102] but disagrees with that in [97] for which in this limit the terms $\propto \pi^2$ do not drop out. In Fig. 4.3 $\eta(s)$ is plotted as a function of the center of mass energy. It can be realized that for energies below 1 GeV the pion mass leads to a considerable enhancement of the FS corrections. Regarding the desired precision, ignoring the pion mass would therefore lead to wrong results.

Close to threshold for pion pair production ($s \simeq 4m_\pi^2$) the Coulomb forces between the two final state pions play an important role. In this limit the factor $\eta(s)$ becomes singular [$\eta(s) \to \pi^2/2\beta_\pi$] which means that the $O(\alpha)$ result for the FS correction cannot be trusted anymore. Since these singularities are known to all orders of perturbation theory one can resum these contribution, which leads to an exponentiation [102]:

$$\begin{aligned}\sigma_{\rm fin}(s) \;&=\; \sigma_0 \left(1+\eta(s)\frac{\alpha}{\pi}-\frac{\pi\alpha}{2\beta_\pi}\right)\frac{\pi\alpha}{\beta_\pi} \\ &\quad\times\left[1-\exp\left(-\frac{\pi\alpha}{\beta_\pi}\right)\right]^{-1}\quad .\end{aligned} \tag{4.138}$$

Above a center of mass energy of $\sqrt{s} = 0.3$ GeV the exponentiated correction to the Born cross section deviates from the non-exponentiated correction less than 1 %.

At the DAΦNE collider not the total cross section but the pion pair invariant mass distribution $d\sigma/ds'$ is measured. As we will see, to reach the desired precision also the IS $O(\alpha^2)$ [80] and the leading log $O(\alpha^3)$ [104] photonic corrections as well as the contributions from initial state fermion pair production [80, 105, 106, 107] (see Fig. 17) have to be taken into account. Among the latter only $e^+e^-$ pair production is numerically relevant. The FS corrections are given to $O(\alpha)$ where the pion masses are kept everywhere. Yennie-Frautschi-Suura resummation [82, 83] was applied to the IS and FS soft photon contributions. We then obtain ($z = s'/s$):

$$\frac{d\sigma}{ds'} \;=\; \left(\frac{d\sigma}{ds'}\right)_{\rm ini} + \left(\frac{d\sigma}{ds'}\right)_{\rm fin}\,, \tag{4.139}$$

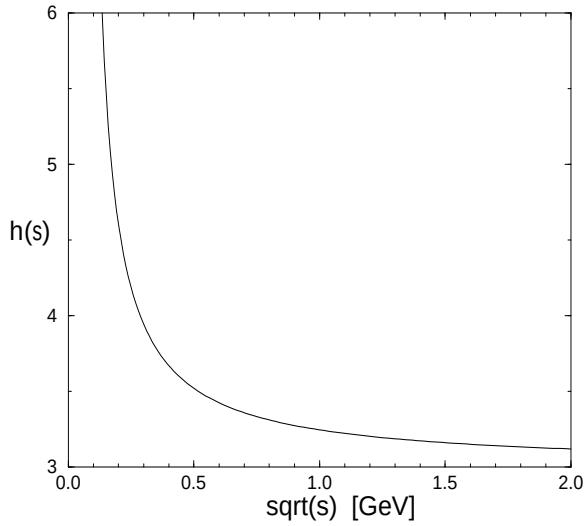


Figure 4.3: The FS correction factor $\eta(s)$ as a function of the squared center of mass energy $s$ [see (4.134-4.137)].

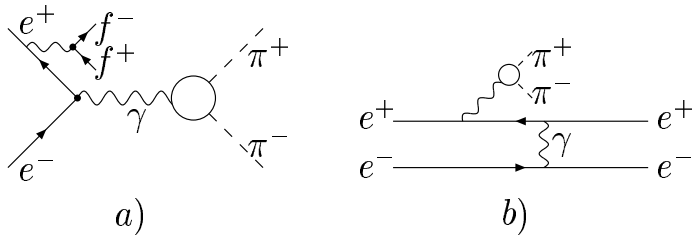


Figure 4.4: Initial state fermion pair production. Diagram $a$) shows an example of a non-singlet contribution, $f^+f^-$ being a fermion pair which is radiated off the initial state electron or positron. For $f = e$ also singlet contributions like diagram $b$) have to be taken into account.

$$\left(\frac{d\sigma}{ds'}\right)_{\rm ini} = \frac{\sigma_0(s')}{s}\left\{\left[1+\tilde{\delta}^{V+S}_{\rm ini}(s)\right] \times B_e(s)\left[1-z\right]^{B_e(s)-1} + \tilde{\delta}^{H}_{\rm ini}(s,s')\right\}, \tag{4.140}$$

$$\left(\frac{d\sigma}{ds'}\right)_{\rm fin} = \frac{\sigma_0(s)}{s}\left\{\left[1+\tilde{\delta}^{V+S}_{\rm fin}(s)\right] \times B_\pi(s,s')\left[1-z\right]^{B_\pi(s,s')-1} + \tilde{\delta}^{H}_{\rm fin}(s,s')\right\}, \tag{4.141}$$

having used the definitions in eq. (4.125), (4.126), (4.127), (4.128), (4.130) (4.131)

and

$$\tilde{\delta}_{\rm ini}^{V+S}(s) = \tilde{\delta}_{\rm ini}^{V+S(1)}(s) + \tilde{\delta}_{\rm ini}^{V+S(2)}(s) + \tilde{\delta}_{\rm ini}^{V+S(3)}(s), \tag{4.142}$$

$$\tilde{\delta}_{\rm ini}^{V+S(2)}(s) = \left(\frac{\alpha}{\pi}\right)^2 \left[L_e^2\left(\frac{9}{8}-\frac{\pi^2}{3}\right) + L_e\left(-\frac{45}{16}+\frac{11}{12}\pi^2+3\zeta(3)\right)\right] + \ldots, \tag{4.143}$$

$$\tilde{\delta}_{\rm ini}^{V+S(3)} = \left(\frac{\alpha}{\pi}\right)^3 (L_e-1)^3\left[\frac{9}{16}-\frac{\pi^2}{2}+\frac{8}{3}\zeta(3)\right], \tag{4.144}$$

$$\tilde{\delta}_{\rm ini}^{H}(s,s') = \tilde{\delta}_{\rm ini}^{H(1)}(s,s') + \tilde{\delta}_{\rm ini}^{H(2)}(s,s') + \tilde{\delta}_{\rm ini}^{H(3)}(s,s') + \tilde{\delta}_{\rm ini}^{pp(2)}(s,s') + \tilde{\delta}_{\rm ini}^{pp(3)}(s,s')\ , \tag{4.145}$$

$$\begin{aligned}\tilde{\delta}_{\rm ini}^{H(2)}(s,s') &= \left(\frac{\alpha}{\pi}\right)^2 \left\{L_e^2\left[-\frac{1+z^2}{1-z}\log z\ (1+z)\left(-2\log(1-z)+\frac{\log z}{2}\right)\right.\right. \\ &- \left.\left.\frac{5}{2}-\frac{z}{2}\right] + L_e\left[\frac{1+z^2}{1-z}\left(\mathrm{Li}_2(1-z)+\log z\log(1-z)\right.\right. \\ &+ \left.\left.\frac{7}{2}\log z-\frac{1}{2}\log^2 z\right)+(1+z)\right. \\ &\times \left.\left(\frac{1}{4}\log^2 z+4\log(1-z)-\frac{\pi^2}{3}\right)\log z+7+\frac{z}{2}\right]\right\}+\ldots\ ,\end{aligned} \tag{4.146}$$

$$\begin{aligned}\tilde{\delta}_{\rm ini}^{H(3)}(s,s') &= \left(\frac{\alpha}{\pi}\right)^3 (L_e-1)^3\ \frac{1}{6}\left\{-\frac{27}{2}+\frac{15}{4}(1-z)+2(1+z)\Big[\pi^2\right. \\ &- \left.6\log^2(1-z)+3\mathrm{Li}_2(1-z)\Big]+3\log z\left(\frac{11}{2}-\frac{6}{1-z}+\frac{3}{2}z\right)\right. \\ &+ \left.\log^2 z\left(-\frac{7}{2}+\frac{4}{1-z}-\frac{7}{2}z\right)-6\log(1-z)(5+z)\right. \\ &+ \left.6\log z\log(1-z)\ \left(3-\frac{4}{1-z}+3z\right)\right\},\end{aligned} \tag{4.147}$$

$$\tilde{\delta}_{\rm ini}^{pp(2)} = \theta(s-s'-4\ m_e\sqrt{s})\left[\ \tilde{\delta}_{\rm ini}^{NSin(2)}+\tilde{\delta}_{\rm ini}^{Sin(2)}+\tilde{\delta}_{\rm ini}^{Int(2)}\right]\ , \tag{4.148}$$

$$
\begin{aligned}
\tilde{\delta}_{\rm ini}^{NSin(2)} &= \left(\frac{\alpha}{\pi}\right)^2 \frac{1}{3}\Bigg\{ \frac{1+z^2}{2(1-z)} L_e^2 + \Bigg[\frac{1+z^2}{1-z}\left(\log\frac{(1-z)^2}{z} - \frac{5}{3}\right) \\
&- 2(1-z)\Bigg] L_e + \frac{1+z^2}{1-z}\left[\frac{1}{2}\log^2\frac{(1-z)^2}{z} - \frac{5}{3}\log\frac{1-z}{z}\right. \\
&- \left.\frac{\pi^2}{3} + \frac{28}{9}\right] - (1-z)\left[2\log\frac{(1-z)^2}{z} - \frac{19}{3}\right] - \frac{z^2}{1-z} \\
&\times \left[\frac{1}{2}\log^2 z + {\rm Li}_2(1-z)\right] - \log z\Bigg\}\,, \qquad (4.149) \\
\tilde{\delta}_{\rm ini}^{Sin(2)} &= \left(\frac{\alpha}{\pi}\right)^2 \Bigg\{ \left[\frac{1}{2}(1+z)\log z + \frac{1}{3z} + \frac{1}{4} - \frac{1}{4}z - \frac{1}{3}z^2\right] L_e^2 \\
&+ \Bigg[(1+z)\Big(2\log z\log(1-z) - \log^2 z + 2{\rm Li}_2(1-z)\Big) \\
&+ \left(\frac{4}{3z} + 1 - z - \frac{4}{3}z^2\right)\log(1-z) - \left(\frac{2}{3z} + 1 - \frac{1}{2}z - \frac{4}{3}z^2\right) \\
&\times \log z - \frac{8}{9z} - \frac{8}{3} + \frac{8}{3}z + \frac{8}{9}z^2\Bigg] L_e\Bigg\} + \dots\,, \qquad (4.150) \\
\tilde{\delta}_{\rm ini}^{Int(2)} &= \left(\frac{\alpha}{\pi}\right)^2 \Bigg\{ \frac{1+z^2}{1-z}\left[-{\rm Li}_2(1-z) - \frac{1}{2}\log^2 z - \frac{3}{4}\log z\right] \\
&- \left.\frac{7}{4}(1+z)\log z - 4 + \frac{7}{2}z\right\}\, L_e + \dots\,, \qquad (4.151) \\
\tilde{\delta}_{\rm ini}^{pp(3)} &= \theta(s - s' - 4\, m_e\sqrt{s})\left[\tilde{\delta}_{\rm ini}^{NSin(3)} + \tilde{\delta}_{\rm ini}^{Sin(3)} + \tilde{\delta}_{\rm ini}^{Int(3)}\right]\,, \qquad (4.152) \\
\tilde{\delta}_{\rm ini}^{NSin(3)} &= \left(\frac{\alpha}{\pi}\right)^3 L_e\Bigg[\frac{1+z^2}{1-z}\, L_e^2\left(\frac{2}{3}\log(1-z) - \frac{1}{3}\log z + \frac{1}{2}\right) \\
&+ L_e^2\left(\frac{1+z}{6}\log z - \frac{1-z}{3}\right) + \frac{1+z^2}{1-z}\, L_e\Bigg(2\log^2(1-z) \\
&- \frac{11}{9}\log(1-z) - \frac{9}{4} - \frac{2}{9}\pi^2 - 2\log z\log(1-z) \\
&+ \frac{1}{3}\log^2 z + \frac{11}{18}\log z\Bigg) + L_e\Bigg(-\frac{8}{3}(1-z)\log(1-z) \\
&+ \frac{2}{3}(1+z)\log z\log(1-z) - \frac{1}{6}(1+z)\log^2 z \\
&+ \frac{4}{9}(1-5z)\log z + \frac{2}{3}(1+z){\rm Li}_2(1-z) + \frac{19}{9}(1-z)\Bigg) \\
&+ \frac{1+z^2}{1-z}\Bigg(\frac{16}{9}\log^3(1-z) - \frac{7}{3}\log^2(1-z) + \frac{67}{27}\log(1-z) \\
&- \frac{8}{9}\pi^2\log(1-z) - \frac{8}{3}\log z\log^2(1-z) + \frac{7}{3}\log z\log(1-z) \\
&+ \frac{5}{6}\log^2 z\log(1-z) - \frac{1}{3}{\rm Li}_2(1-z)\log(1-z) - \frac{1}{18}\log^3 z
\end{aligned}
$$

$$
\begin{aligned}
&- \frac{31}{72}\log^2 z - \frac{67}{54}\log z - \frac{2}{3}\mathrm{Li}_2(1-z)\log z + \frac{4}{9}\pi^2\log z \\
&- \frac{1}{4}\mathrm{Li}_2(1-z) - \frac{5}{3}\mathrm{S}_{1,2}(1-z) - \frac{2}{9}\pi^2 + 4\zeta(3) + \frac{1073}{162}\Bigg)\Bigg] , \quad (4.153)
\end{aligned}
$$

$$
\begin{aligned}
\tilde{\delta}_{\rm ini}^{Sin(3)} &= -\left(\frac{\alpha}{\pi}\right)^3 \frac{1}{36}\left(L_e - 1\right)^3 \left[\frac{1-z}{3z}(4 + 7z + 4z^2)\right. \\
&+ \left. 2(1+z)\log z\right] , \quad (4.154)
\end{aligned}
$$

$$
\begin{aligned}
\tilde{\delta}_{\rm ini}^{Int(3)} &= \left(\frac{\alpha}{\pi}\right)^3 \frac{5}{24}\left(L_e - 1\right)^3 \left[\left(\frac{3}{2} + 2\log(1-z)\right)\right. \\
&\times \left(\frac{1-z}{3z}(4 + 7z + 4z^2)\right) + 2(1+z)\log z\Bigg) \\
&+ (1+z)\Big(-\log^2 z + 4\mathrm{Li}_2(1-z)\Big) \\
&+ \left.\frac{1}{3}\left(-9 - 3z + 8z^2\right)\log z + \frac{2}{3}\left(-\frac{3}{z} - 8 + 8z + 3z^2\right)\right] , \quad (4.155)
\end{aligned}
$$

$$
\mathrm{S}_{1,2}(x) = \frac{1}{2}\int_0^x \frac{\mathrm{d}y}{y}\log^2(1-y) , \; L_e = \log\left(\frac{s}{m_e^2}\right) .
$$

The $O(\alpha^3)$ corrections (4.144), (4.147) and (4.152) are taken from [104] and [106, 107] respectively. The dots in (4.144), (4.146), (4.150) and (4.151) correspond to $O(\alpha^2)$ contributions which do not contain any $\log(s/m_e^2)$ terms and can be neglected safely.

Fig. 4.5 shows the pion pair invariant mass distributions $d\sigma/ds'$ with radiative corrections normalized to $d\sigma/ds'$ with only $O(\alpha)$ IS corrections ($\sqrt{s} = 1.02$ GeV). In Table 4.2 the contribution from IS $O(\alpha^2)$ and FS $O(\alpha)$ photonic corrections are shown for different center of mass energies.

The following points can be recognized:

1. The FS corrections (dotted line) are quite large, especially in the region of soft photons as well as for very hard photons;

2. The $O(\alpha^2)$ IS effects are considerable;

3. The FS and IS contributions compensate each other significantly for large $s'$.

Fig. 4.6 shows $d\sigma/ds'$ for different center of mass energies $\sqrt{s}$. Going to smaller center of mass energies the $O(\alpha^2)$ IS corrections become smaller and smaller. On the other hand the FS contributions remain considerably large. Interestingly, for the $\phi$ resonance energy ($\sqrt{s} = 1.02$ GeV) both the $O(\alpha^2)$ IS and the $O(\alpha)$ FS contributions are large. Quantitatively this is shown in Table 4.2. The resummation of the $O(\alpha^2)$ IS soft photon logarithms [see (4.140)] gives a contribution smaller than 5 per mill for $s'$ below the $\rho$ resonance peak and smaller than 3 per mill above it. The resummation

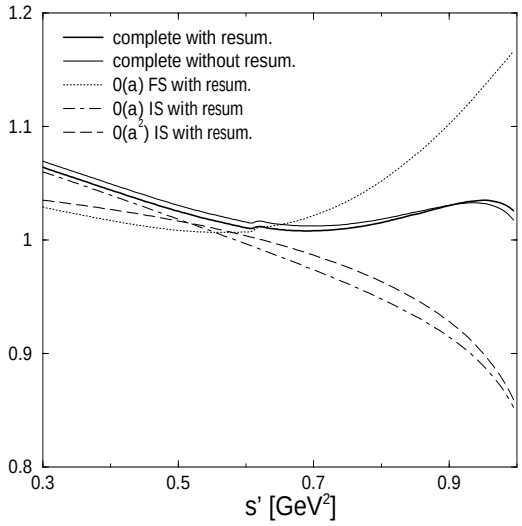


Figure 4.5: Pion pair invariant mass distributions ($d\sigma/ds'$) with radiative corrections, normalized to $d\sigma/ds'$ with only $O(\alpha)$ IS corrections. The thick line shows the case when up to $O(\alpha^2)$ IS and $O(\alpha)$ FS contributions (excluding IS pair production) are taken into account and appropriately resummed [see (4.139-4.141)]. The thin solid line shows the same but this time without resummation. The dotted line corresponds to the $O(\alpha)$ FS corrections (together with $O(\alpha)$ IS corrections). For the long-dashed and the dot-dashed lines only the resummed IS $O(\alpha^2)$ and the resummed IS $O(\alpha)$ radiative corrections are taken into account, respectively.

of FS soft photon logarithms [see (4.141)] changes the complete results only slightly (less than 0.5 per mill). To reduce the theoretical error to a few per mill one also has to include the contributions from initial state $e^+e^-$ pair production [80, 105, 106, 107], given in (4.148) and (4.152). In Table 4.3 and 4.4 the $O(\alpha^2)$ and leading $O(\alpha^3)$ pair production contributions to $d\sigma/ds'$ for different hadronic energies are presented. What is remarkable is the very large singlet contribution [see Fig. 17b)] in the region of low hadronic energies which amounts about 8 per cent for $\sqrt{s'} = 0.3$ GeV. Since these effects are related to $e^+e^-$ pairs which are mainly emitted collinearly to the beam axis they escape detection and therefore have to be included into the data analysis. Hence when unfolding the data from radiative corrections also these effects have to be subtracted. The leading contribution from $O(\alpha^3)$ pair production appears to be less than 1 per mill which gives us a good estimate about the precision we can expect. Also the leading log $O(\alpha^3)$ IS photon correction [104], which is given in (4.144) and (4.147) is taken into account. The contribution can be of the order of 4 per mill for hadronic energies below the $\rho$ resonance peak, as shown in Table 4.5.

The total cross section $\sigma(s)$ can be obtained by integrating $d\sigma/ds'$ in eq. (4.139) over $s'$ numerically. The perturbative precision is now better than of per mill level which is more accurate than the $O(\alpha)$ result in eq. (4.122).

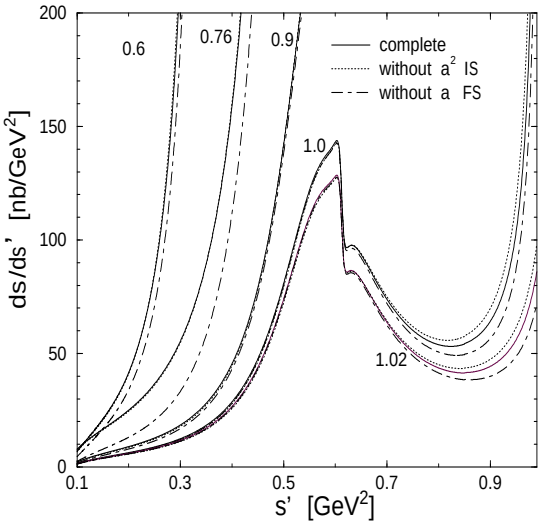


Figure 4.6: Pion pair invariant mass distributions ($d\sigma/ds'$) for different center of mass energies $\sqrt{s} = 0.6, 0.76, 0.9, 1.0, 1.02$ GeV. The solid lines stands for the "complete" cross section, including $O(\alpha^2)$ IS and $O(\alpha)$ FS corrections [see eq. (4.139-4.141)]. The dotted lines give the results when the $O(\alpha^2)$ IS corrections are neglected. The dot-dashed lines correspond to the case when the $O(\alpha)$ FS contribution is neglected.

| $\sqrt{s'}$ [GeV] | $O(\alpha^2)$ IS contribution | $O(\alpha)$ FS contribution |
|---|---|---|
| 0.3 | 4.3 | 11.5 |
| 0.4 | 4.4 | 4.3 |
| 0.5 | 4.0 | 3.2 |
| 0.6 | 3.4 | 2.0 |
| 0.7 | 2.2 | 0.9 |
| 0.76 | 1.2 | 0.7 |
| 0.8 | 0.2 | 1.2 |
| 0.9 | − 3.6 | 5.5 |
| 0.95 | − 6.9 | 10.1 |
| 1.0 | − 15.3 | 16.6 |

Table 4.2: Contribution of $O(\alpha^2)$ IS and $O(\alpha)$ FS corrections to $d\sigma/ds'$ (in %), $\sqrt{s} = 1.02$ GeV.

We now consider the IFS interference corrections (see Fig. 4.1) which modify the

| $\sqrt{s'}$ [GeV] | $O(\alpha^2)$ IS pp contribution | Singlet contribution |
|---|---|---|
| 0.3 | 79.1 | 74.9 |
| 0.4 | 36.3 | 31.9 |
| 0.5 | 16.6 | 12.2 |
| 0.6 | 8.3 | 4.0 |
| 0.7 | 4.8 | 0.76 |
| 0.76 | 3.9 | − 0.01 |
| 0.8 | 3.4 | − 0.24 |
| 0.9 | 2.7 | − 0.27 |
| 1.0 | 1.2 | 0.06 |

Table 4.3: $O(\alpha^2)$ contribution from IS pair production to $d\sigma/ds'$ (in per mill). In the second column only the singlet contribution (including singlet-non-singlet interference) is shown.

| $\sqrt{s'}$ [GeV] | $O(\alpha^3)$ IS pp contribution | Singlet contribution |
|---|---|---|
| 0.3 | − 0.87 | − 1.27 |
| 0.4 | − 0.45 | − 0.82 |
| 0.5 | − 0.18 | − 0.48 |
| 0.6 | − 0.07 | − 0.27 |
| 0.7 | − 0.09 | − 0.15 |
| 0.76 | − 0.15 | − 0.10 |
| 0.8 | − 0.21 | − 0.07 |
| 0.9 | − 0.43 | − 0.03 |
| 1.0 | − 0.72 | − 0.001 |

Table 4.4: $O(\alpha^3)$ IS pair production contribution to $d\sigma/ds'$ (in per mill).

angular distribution. To $O(\alpha)$ we can write:

$$\left(\frac{d\sigma}{d\Omega}\right) \;=\; \left(\frac{d\sigma_0}{d\Omega}\right)\,\Big[1+\delta(\Lambda)\Big] + \left(\frac{d\sigma_h}{d\Omega}\right)(\Lambda)\;,$$

where the correction factor $\delta$ is the sum of the virtual plus soft photon IS, FS and IFS interference correction factors:

$$\delta(\Lambda) \;=\; \delta_{\rm ini}(\Lambda)+\delta_{\rm fin}(\Lambda)+\delta_{\rm int}(\Lambda)\;. \tag{4.156}$$

$d\sigma_h/d\Omega$ is the hard photon contribution which is calculated numerically. $\delta_{\rm ini}(\Lambda)$ and $\delta_{\rm fin}(\Lambda)$ are given in (4.129) and (4.131). $\delta_{\rm int}(\Lambda)$ is obtained by summing the box

| $\sqrt{s'}$ [GeV] | $O(\alpha^3)$ IS contribution |
|---|---|
| 0.3 | 3.9 |
| 0.4 | 4.3 |
| 0.5 | 4.2 |
| 0.6 | 3.8 |
| 0.7 | 3.0 |
| 0.76 | 2.4 |
| 0.8 | 1.8 |
| 0.9 | 0.3 |
| 1.0 | 0.6 |

Table 4.5: $O(\alpha^3)$ leading log IS photon contribution to $d\sigma/ds'$ (in per mill).

contribution given in eq. (4.116) to the IFS interference soft photon contribution given in eq. (4.41). It can be written in the following, compact way:

$$\begin{aligned}
\delta_{\rm int} &= \frac{2\alpha}{\pi}\Bigg\{\log\left(\frac{-u+m_\pi^2}{-t+m_\pi^2}\right)\log\left(\frac{4\Lambda^2}{s}\right) \\
&+ \frac{1}{4}\frac{s^2}{ut-m_\pi^4}\Bigg\{\frac{u-t}{s}\Big[c_1(u)+c_1(t)+c_e+c_\pi\Big] \\
&+ \frac{u+t}{s}\Big[c_1(u)-c_1(t)\Big]\Bigg\} - \frac{F(u)}{2}+\frac{F(t)}{2}\Bigg\}, \qquad (4.157)
\end{aligned}$$

with ($\kappa_i=\kappa_i(x)$, $x=u,t$)

$$\begin{aligned}
c_1(x) &= \frac{1}{2}\Bigg\{3\log^2\left(\frac{x-m_\pi^2}{x}\right)-\frac{1}{2}\log^2\left(-\frac{m_e^2}{x}\right) \\
&- \frac{1}{2}\log^2\left(-\frac{m_\pi^2}{x}\right)-2\log\left(-\frac{m_\pi^2}{x}\right)\log\left(\frac{x-m_\pi^2}{x}\right) \\
&+ 2{\rm Li}_2\left(-\frac{m_\pi^2}{x-m_\pi^2}\right)-\frac{\pi^2}{3}\Bigg\}, \\
c_\pi &= \frac{1+\beta_\pi^2}{2\beta_\pi}\Bigg[2{\rm Li}_2\left(\frac{1+\beta_\pi}{2}\right)-2{\rm Li}_2\left(\frac{1-\beta_\pi}{2}\right) \\
&\quad +{\rm Li}_2\left(-\frac{1+\beta_\pi}{1-\beta_\pi}\right)-{\rm Li}_2\left(-\frac{1-\beta_\pi}{1+\beta_\pi}\right) \\
&\quad +\log\left(\frac{s}{m_\pi^2}\right)\log\left(\frac{1+\beta_\pi}{1-\beta_\pi}\right)\Bigg], \\
c_e &= \frac{1}{2}\log^2\left(\frac{s}{m_e^2}\right)+\frac{\pi^2}{6},
\end{aligned}$$

$$
\begin{aligned}
F(x) &= [f_1^x(\kappa_1) - f_1^x(\kappa_2) - f_1^x(\kappa_4) + f_2^x(\kappa_3) \\
&- f_3^x(\kappa_1,\kappa_2) - f_3^x(\kappa_4,\kappa_1) + f_3^x(\kappa_4,\kappa_2) \\
&+ f_4^x(\kappa_2,\kappa_1) + f_4^x(\kappa_1,\kappa_4) + f_4^x(\kappa_2,\kappa_4) \\
&- f_5^x(\kappa_3,\kappa_1) + f_5^x(\kappa_3,\kappa_2) - f_5^x(\kappa_3,\kappa_4) \\
&- f_6^x(\kappa_1,\kappa_3) - f_6^x(\kappa_2,\kappa_3) + f_6^x(\kappa_4,\kappa_3)] \,,
\end{aligned}
$$

$$
\begin{aligned}
f_1^x(\eta) &= \frac{1}{2}\log^2[b_x - \eta] - \frac{1}{2}\log^2[a - \eta], \\
f_2^x(\eta) &= \frac{1}{2}\log^2[\eta - a] - \frac{1}{2}\log^2[\eta - b_x], \\
f_3^x(\eta_1,\eta_2) &= -\mathrm{Li}_2\left[\frac{(b_x - a)(\eta_1 - \eta_2)}{(b_x - \eta_1)(a - \eta_2)}\right] \\
&+ \mathrm{Li}_2\left(-\frac{b_x - a}{a - \eta_2}\right) + \mathrm{Li}_2\left(\frac{b_x - a}{b_x - \eta_1}\right) \\
&+ \log(b_x - \eta_1)\log\left(\frac{b_x - \eta_2}{a - \eta_2}\right), \\
f_4^x(\eta_1,\eta_2) &= \mathrm{Li}_2\left[\frac{(b_x - a)(\eta_2 - \eta_1)}{(b_x - \eta_2)(a - \eta_1)}\right], \\
&- \mathrm{Li}_2\left(-\frac{b_x - a}{a - \eta_1}\right) - \mathrm{Li}_2\left(\frac{b_x - a}{b_x - \eta_2}\right) \\
&+ \log(a - \eta_1)\log\left(\frac{b_x - \eta_2}{a - \eta_2}\right), \\
f_5^x(\eta_1,\eta_2) &= \log[\eta_1 - \eta_2]\log\left(\frac{b_x - \eta_2}{a - \eta_2}\right) \\
&+ \mathrm{Li}_2\left(\frac{a - \eta_2}{\eta_1 - \eta_2}\right) - \mathrm{Li}_2\left(\frac{b_x - \eta_2}{\eta_1 - \eta_2}\right), \\
f_6^x(\eta_1,\eta_2) &= \log[\eta_2 - \eta_1]\log\left(\frac{\eta_2 - b_x}{\eta_2 - a}\right) \\
&+ \mathrm{Li}_2\left(\frac{\eta_2 - a}{\eta_2 - \eta_1}\right) - \mathrm{Li}_2\left(\frac{\eta_2 - b_x}{\eta_2 - \eta_1}\right),
\end{aligned}
$$

$$
a = \beta_\pi(s) \,, \quad b_x = \beta_e(s) + 2\sqrt{-\frac{x}{s}},
$$

$$
\begin{aligned}
\kappa_{1,2} \equiv \kappa_{1,2}(x) &= -1 + \frac{1}{\sqrt{-sx}}\Big[-x + m_e^2 - m_\pi^2 \\
&\pm \sqrt{\lambda(x, m_e^2, m_\pi^2)}\Big], \\
\kappa_{3,4} \equiv \kappa_{3,4}(x) &= 1 + \frac{1}{\sqrt{-sx}}\Big[-x + m_e^2 - m_\pi^2 \\
&\pm \sqrt{\lambda(x, m_e^2, m_\pi^2)}\Big], \\
\lambda(x, y, z) &= z^2 + y^2 + z^2 - 2xy - 2xz - 2yz.
\end{aligned}
$$

From (4.157) it can be seen immediately that $\delta_{\rm int}$ is antisymmetric, thus it changes sign under the exchange $t \leftrightarrow u$ $[t(u) = (p_1 - k_{2(1)})^2]$. This is actually required by charge conjugation invariance.

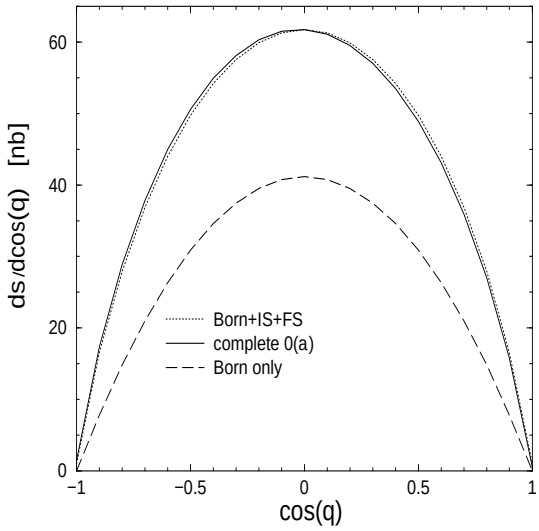


Figure 4.7: $\pi^-$ angular distribution for $\sqrt{s} = 1.02$ GeV. The solid line, corresponding to the complete $O(\alpha)$ corrections, is not symmetric as a consequence of the IFS interference corrections. Both the tree level distribution and the distribution with only IS and FS corrections are symmetric.

Table 4.6 shows the IFS interference contribution to the pion angular distribution (Fig. 4.7). One can recognize, that with an angular cut between the pion momentum and the beam axis of $20^o \leq \Theta \leq 160^o$ this is not bigger than 5.6 %. The importance of the interference contribution can be enhanced by tagging the photon and imposing a strong cut on the angle between the photon momentum and the beam axis [76] (see Fig. 4.9 and 4.8). By such a strong cut scenario the IS brems strahlung contribution which is dominated by photons emitted collinearly to the beam axis is reduced dramatically. This seems to be the only way to tackle the imaginary part of the pion form factor.

| $\cos\Theta$ | $\frac{d\sigma_{B+IS+FS}}{d\cos\Theta}/\frac{d\sigma_{tot}}{d\cos\Theta}$ | IFS interference |
|---|---|---|
| $-1.0$ | 0.99/ 1.46 | 47.5 |
| $-0.99$ | 2.95/3.33 | 12.9 |
| $-0.94$ | 11.12/11.74 | 5.6 |
| $-0.6$ | 44.03/44.97 | 2.1 |
| $-0.2$ | 59.91/60.3 | 0.6 |
| 0. | 61.76/ 61.76 | 0.0 |
| 0.2 | 59.91/ 59.53 | $-0.6$ |
| 0.6 | 44.03/43.09 | $-2.1$ |
| 0.94 | 11.12/10.49 | $-5.6$ |
| 0.99 | 2.95/2.56 | $-13.2$ |
| 1.0 | 0.99/ 0.52 | $-47.5$ |

Table 4.6: Contribution of the interference terms (in %) to the differential cross section (corresponding to the solid and dotted line in Fig. 4.7).

The results presented so far have been obtained by the dedicated Fortran program A$\phi\rho\omega$DITE . It generates cross sections with the option of kinematical cuts as needed by experiment. As shown before, the $O(\alpha^2)$ IS (photonic and IS pair production) contributions to $d\sigma/ds'$ are considerable and even $O(\alpha^3)$ leading log contributions should be included. Analytical formulae for the full $O(\alpha^2)$ IS corrections with cuts have not been calculated so far. At this stage we therefore rely on the complete results without cuts $d\sigma^{(compl)}/ds'$ as given in (4.139) with the following approximation[4]:

$$\left(\frac{d\sigma^{(\mathrm{compl})}}{ds'}\right)_{\mathrm{cuts}} \simeq \frac{\left(\frac{d\sigma^{(\mathrm{compl})}}{ds'}\right)_{\text{no cuts}}}{\left(\frac{d\sigma^{(\alpha)}}{ds'}\right)_{\text{no cuts}}} \left(\frac{d\sigma^{(\alpha)}}{ds'}\right)_{\mathrm{cuts}} . \tag{4.158}$$

$d\sigma^{(\alpha)}/ds'$ is the differential cross section to $O(\alpha)$. See Fig. 4.10 for an example. In the limit $s' \to s$ the above approximation is exact since then the radiated photons are soft. In principle we can expect that away from this limit the situation is different since the contribution from a second hard photon could distort the angular distribution of the pions. The distortion however remains below 1 per mill for $s' \geq 0.3$ GeV$^2$ and an angular cut between the pion momenta and the beam axis of less than 30 degrees[5].

In the case of a tagged photon the FS corrections can be reduced by applying strong cuts between the photon and the final state particles. See Fig. 4.11 for such a

[4]For an exact treatment we would need the analytic expression for the angular distribution at $O(\alpha^2)$.

[5]We thank S. Jadach for help in checking this with a dedicated MC program based on [108].

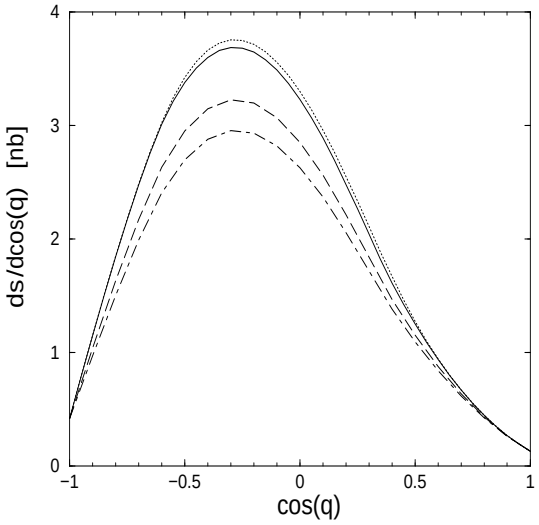


Figure 4.8: Lowest order $\pi^-$ angular distribution for the case of a tagged photon. The angular cut between the photon momentum and the beam axis is chosen such that only photons in the angular range $60^o \leq \Theta_\gamma \leq 120^o$ are detected. The difference between the solid and dotted line is due to an additional cut between the tagged photon and the pions $7^o \leq \Theta_{\gamma\pi} \leq 173^o$ (solid line). This cut was also applied to the remaining dashed and dot-dashed line. The curves correspond to different values for the minimal photon energy $\Lambda$. The solid and the dotted line correspond to $\Lambda = 0.01$ GeV, the dashed line to $\Lambda = 0.02$ GeV and the dot-dashed line to $\Lambda = 0.03$ GeV.

| s' | Set A | | Set B | | set A − set B | |
|---|---|---|---|---|---|---|
| | all | no FS | all | no FS | all | no FS |
| 0.8 | 11.994 | 9.981 | 18.231 | 16.121 | 6.237 | 6.140 |
| 0.85 | 12.252 | 9.494 | 18.201 | 15.313 | 5.949 | 5.819 |
| 0.9 | 14.212 | 10.168 | 20.615 | 16.384 | 6.403 | 6.216 |

Table 4.7: $d\sigma/ds'$ in $[nb/\mathrm{GeV}^2]$, for some values of $s'$. The FS contribution for a strong cut scenario (SetA-SetB) is shown. It is 1.6 %, 2.2 %, 2.9 % for $s' =$ 0.8, 0.85, 0.9 $\mathrm{GeV}^2$, respectively.

strong cut scenario at the $\phi$ peak. It can be seen that the strong cuts reduce the FS contribution considerably. However, as shown in Table 4.7, the FS contribution still amounts up to a few per cent. Although the presented results are based on an $O(\alpha)$ calculation (a similar approximation as the one given in (4.158) is not possible) it is highly unprobable that the situation will improve if $O(\alpha^2)$ corrections are included.

Finally a few remarks about the A$\phi\rho\omega$DITE program. To check the numerical accuracy, the four dimensional phase space integration has been carried out numer-

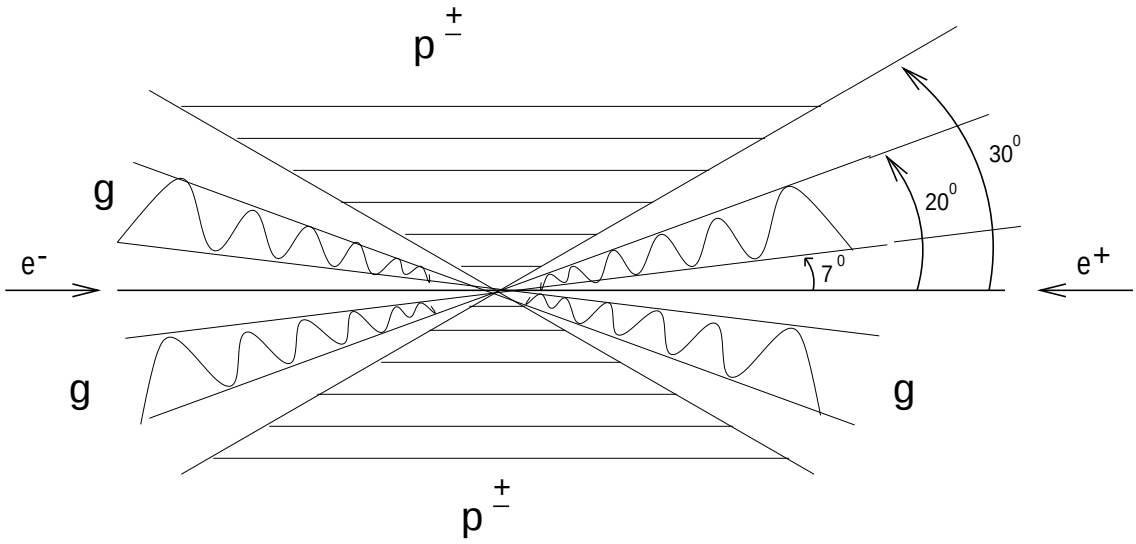


Figure 4.9: An example of event selection by photon tagging at DAΦNE . In the blind zone ($|\Theta| \leq 7^o$) all particles escape detection. The angular range $7^o \leq |\Theta| \leq 20^o$ is covered by the QCAL electromagnetic calorimeter which can detect photons at low angles. To suppress the contribution from FS radiation the pions with a scattering angle $|\Theta| \leq 30^o$ are excluded from the analysis.

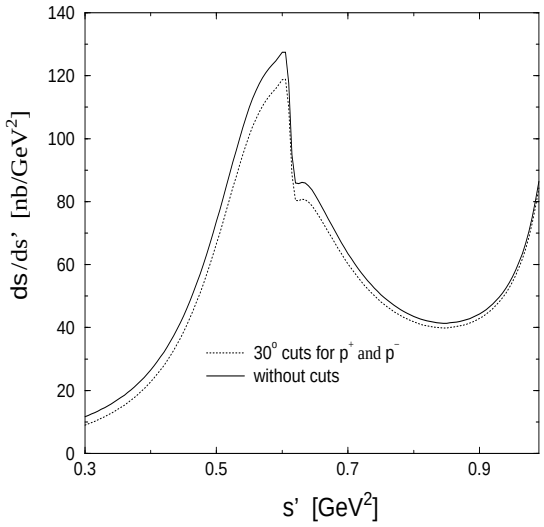


Figure 4.10: Pion pair invariant mass distribution with an angular cut $30^o \leq \Theta \leq 150^o$ between the $\pi^{\pm}$ momenta and the beam axis, $\sqrt{s} = 1.02$ GeV.

ically to obtain the total cross section without cuts (see Table 4.8). This is then compared to the total cross section obtained from (4.122) by one-dimensional integration (Table 4.9). We observe excellent agreement. Table 4.9 and Table 4.8 in

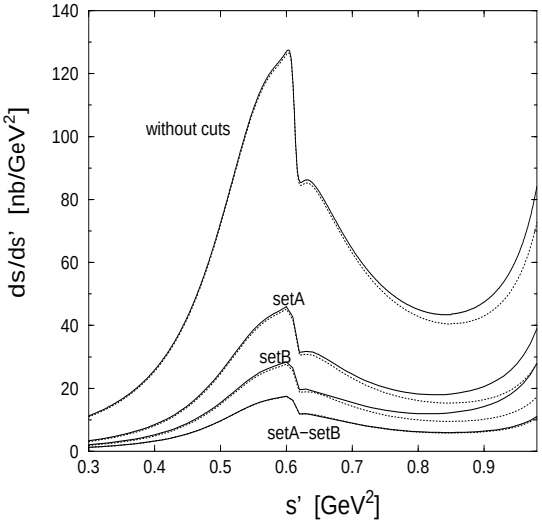


Figure 4.11: Pion pair invariant mass distribution $d\sigma/ds'$ for the case of a tagged photon. Set A corresponds to a $7^o$ angular cut between the photon momentum and the beam axis and a $30^o$ cut between the $\pi^{\pm}$ momenta and the beam axis. For set B the pion cuts are the same but the photon cut is now $20^o$. Taking the difference (SetA-SetB) the photon is restricted to a region well separated from the pion momenta. The solid lines correspond to the complete cross section (Born plus IS and FS bremsstrahlung), for the dotted lines FS bremsstrahlung is neglected.

| $\Lambda$ [GeV] | $\sigma$ [nb] | $\delta\sigma$ [nb] |
|---|---|---|
| 0.1 | **9**4.907 | 0.0095 |
| 0.01 | **99**.123 | 0.0104 |
| 0.001 | **99**.394 | 0.0129 |
| 0.0001 | **99.42**0 | 0.0157 |
| $10^{-5}$ | **99.42**2 | 0.0210 |
| $10^{-6}$ | **99.42**2 | 0.0255 |
| $10^{-7}$ | **99.42**2 | 0.0303 |
| $10^{-8}$ | **99.42**1 | 0.0357 |
| $10^{-9}$ | **99.42**2 | 0.0418 |
| $10^{-10}$ | **99.42**1 | 0.0493 |

Table 4.8: Cut-off dependence of the total cross section $\sigma$ obtained from 4-dimensional numerical integration, $\sqrt{s} = 1.02$ GeV. $\delta\sigma$ is the absolute numerical error to $\sigma$.

addition show the total cross section as a function of the soft photon energy cut-off $\Lambda$. For values of $\Lambda < 10^{-4}$ GeV we get stable cut-off-independent results.

| $\Lambda$ [GeV] | $\sigma$ [nb] | $\delta\sigma$ [nb] |
|---|---|---|
| 0.1 | **9**4.909344406421 | $2{\cdot}10^{-9}$ |
| 0.01 | **99**.126309344279 | $2 \cdot 10^{-11}$ |
| 0.001 | **99**.396403660854 | $2 \cdot 10^{-9}$ |
| 0.0001 | **99.42**2466900996 | $3 \cdot 10^{-9}$ |
| $10^{-5}$ | **99.425**064117054 | $6 \cdot 10^{-9}$ |
| $10^{-6}$ | **99.4253**23747942 | $7 \cdot 10^{-9}$ |
| $10^{-7}$ | **99.4253**49708976 | $7 \cdot 10^{-9}$ |
| $10^{-8}$ | **99.425352**318987 | $1 \cdot 10^{-8}$ |
| $10^{-9}$ | **99.425352**327085 | $1 \cdot 10^{-8}$ |
| $10^{-10}$ | **99.425352**168781 | $1 \cdot 10^{-8}$ |

Table 4.9: Cut-off dependence of the total cross section $\sigma$ obtained from 1-dimensional numerical integration, $\sqrt{s} = 1.02$ GeV. $\delta\sigma$ is the absolute error to $\sigma$

.

# Chapter 5

# The Unfolding Procedure

As explained before the goal of measuring hadronic cross sections is to extract the undressed cross section ratio $R(s)$ [see eq. (1.10)] from the experimental data which is needed for the dispersion integrals (1.7) and (1.9). Concerning pion pair production this means that we have to subtract the vacuum polarization effects according to eq. (4.2) which yields the undressed form factor $F_\pi^{(0)}$; graphically:

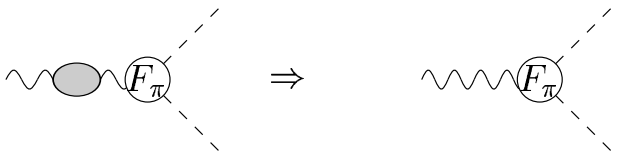


However, before we can do this we have to subtract the IS and FS QED corrections from the observed cross section to determine the dressed pion form factor $F_\pi$. At the DAΦNE collider the $\pi^+\pi^-$ invariant mass distribution is measured which may be written in the form

$$\frac{d\sigma}{ds'} = \left(\frac{d\sigma}{ds'}\right)_{\rm ini} + \left(\frac{d\sigma}{ds'}\right)_{\rm int} + \left(\frac{d\sigma}{ds'}\right)_{\rm fin} , \tag{5.1}$$

with

$$\begin{aligned}
\left(\frac{d\sigma}{ds'}\right)_{\rm ini} &= N_{\rm ini}(s,s')\,|F_\pi(s')|^2\ \times \\
&\int_{\rm cuts} d\cos\Theta_\gamma\, d\cos\Theta_{\pi^-}\, d\phi_{\pi^-} \sum_\lambda |\mathcal{M}_{\rm ini}^{\rm point}|^2 , \\
\left(\frac{d\sigma}{ds'}\right)_{\rm int} &= N_{\rm int}(s,s')\,2{\rm Re}\left[F_\pi(s')F_\pi^*(s)\ \times \right. \\
&\left. \int_{\rm cuts} d\cos\Theta_\gamma\, d\cos\Theta_{\pi^-}\, d\phi_{\pi^-} \sum_\lambda \mathcal{M}_{\rm ini}^{\rm point}\mathcal{M}_{\rm fin}^{*\ \rm point}\right] ,
\end{aligned}$$

$$\left(\frac{d\sigma}{ds'}\right)_{\rm fin} = N_{\rm fin}(s,s')\,|F_\pi(s)|^2\,\times \int_{\rm cuts} d\cos\Theta_\gamma\; d\cos\Theta_{\pi^-}\; d\phi_{\pi^-} \sum_\lambda |\mathcal{M}^{\rm point}_{\rm fin}|^2\;,$$

where the $N_i(s,s')$'s are appropriate normalization factors. $\Theta_{\pi^-}$ is the $\pi^-$ production angle and $\Theta_\gamma$ the angle between the emitted photon and the $\pi^-$ in the center of mass system of the $\pi^+\pi^-$ pair. Cuts in the laboratory system may be implemented easiest by first performing a boost from the center of mass system of the pion pair to the laboratory system. If the integration over $\Theta_{\pi^-}$ is performed with symmetric cuts in the acceptance angles $\Theta_{\pi^\pm}$ in the laboratory frame, the interference term drops out due to $C$–invariance and we are left with the IS and FS terms only. Photons are assumed to be treated fully inclusively, i.e., we integrate over the complete photon phase space and thus obtain:

$$\begin{aligned}\left(\frac{d\sigma}{ds'}\right)_{\rm sym-cut} &= |F_\pi(s')|^2\,\left(\frac{d\sigma}{ds'}\right)^{\rm point}_{\rm ini,\,sym-cut} \\ &+ |F_\pi(s)|^2\,\left(\frac{d\sigma}{ds'}\right)^{\rm point}_{\rm fin,\,sym-cut}\end{aligned} \tag{5.2}$$

and hence we may resolve for the pion form factor as

$$\begin{aligned}|F_\pi(s')|^2 &= \frac{1}{\left(\frac{d\sigma}{ds'}\right)^{\rm point}_{\rm ini,\,sym-cut}}\left\{\left(\frac{d\sigma}{ds'}\right)_{\rm sym-cut}\right. \\ &\left. -|F_\pi(s)|^2\,\left(\frac{d\sigma}{ds'}\right)^{\rm point}_{\rm fin,\,sym-cut}\right\}.\end{aligned} \tag{5.3}$$

This is a remarkable equation since it tells us that the inclusive pion pair invariant mass spectrum allows us to get the pion form factor unfolded from photon radiation directly as for fixed $s$ and a given $s'$ the photon energy is determined. The point cross sections are assumed to be given by theory (scalar QED) and $d\sigma/ds'$ is the observed experimental pion-pair spectral function. In spite of the fact that both terms on the r.h.s. of (5.3) are of $O(\alpha)$ the second one can be treated as a correction because the IS radiation dominates in comparison to the FS radiation. We observe that in the determination of $|F_\pi(s')|^2$ via the radiative return mechanism the to be subtracted FS radiation only depends on $|F_\pi(s)|^2$ at the fixed energy $s = M_\phi^2$. Note that we also benefit from the fact that $|F_\pi(M_\phi^2)|^2$ is small in comparison to $|F_\pi(s')|^2$ in the most relevant region around the $\rho$ peak. Below about 600 MeV, however, $|F_\pi(s')|^2$ drops below $|F_\pi(M_\phi^2)|^2$ and a precise and model independent determination of $F_\pi$ becomes more difficult. Note that because of the $1/s^2$ enhancement in the dispersion integral (1.9) the low energy tail is not unimportant as a contribution to $a_\mu^{\rm had}$.

Having extracted $F_\pi(s)$ by eq. (5.3) from the data we can evaluate $R(s)$ via eq. (4.2) and (1.10) which gives us the leading hadronic photon self energy contribution to the running fine structure constant $\alpha(s)$ and to the muon anomaly $a_\mu$ by eq. (1.7) and (1.9). However we can do better. The above procedure only yields the hadronic contributions corresponding to the irreducible hadronic vacuum polarization. Aiming at increasing precision we would like to include photonic corrections to the hadronic 1-particle-irreducible blob: This can be achieved by adding the inclu-


sive FS photonic contribution to the undressed form factor, leading to the modified form factor

$$|F_\pi^{(\gamma)}(s)|^2 = |F_\pi^{(0)}(s)|^2 \left(1 + \eta(s)\frac{\alpha}{\pi}\right) , \tag{5.4}$$

$\eta(s)$ being the correction factor given in eq. (4.134). The corresponding $O(\alpha)$ contribution to the anomalous magnetic moment of the muon (1.7) is $\delta^\gamma a_\mu^{\rm had} = (38.6 \pm 1.0) \times 10^{-11}$ [81], which compares to $(46.0 \pm 0.5 \pm 9.0) \times 10^{-11}$ estimated in [30] (see also [34]).

Note that adding the inclusive FS photonic contribution at the end obviously does not mean that we do not have to consider FS radiation at all since on an event basis it is not possible to distinguish between photons which are radiated off the initial state from final state photons. As we have seen the FS corrections can contribute more than 10 % to the pion spectral function $d\sigma/ds'$ whereas the integrated FS correction contribution stays below 1 %.

The following procedure is advocated: Try to measure the pion pair invariant mass spectrum $d\sigma/ds'$ in a fully inclusive manner, counting all events $\pi^+\pi^-$, $\pi^+\pi^-\gamma$, $\pi^+\pi^-\gamma\gamma$, $\pi^+\pi^-e^+e^-$, $\pi^+\pi^-e^+e^-\gamma$ ... as much as possible, imposing $C$-symmetric angular cuts on the production angles of the charged pions. Determine the bare pion form factor $F_\pi^{(0)}$ via eq. (4.139), (4.158), (5.3) and (4.2). Finally add the inclusive FS corrections as shown in eq. (5.4).

This allows us to obtain the improved cross section ratio being analogous to eq. (4.3):

$$R_{\pi\pi}^{(\gamma)}(s) = \frac{\beta_\pi^3}{4}|F_\pi^{(\gamma)}(s)|^2 , \tag{5.5}$$

This is the quantity which can be inserted into the dispersion integrals (1.7) and (1.9). In contrast to the radiative return scenario for a measurement of the total cross section $\sigma$ the only way to extract the pion form factor from the data appears to be by iteration from a comparison of the observed spectrum to the radiatively corrected theoretical prediction in terms of the bare pion form factor.

Recall that in eq. (5.3) the IS and FS spectral function for point-like scalar particles with $C$-symmetric cuts are needed which have to be supplied by theory. This can be achieved by the A$\phi\rho\omega$DITE program. A$\phi\rho\omega$DITE carries out the 3-particle phase space integration corresponding to the process $e^+e^- \to \pi^+\pi^-\gamma$ numerically. Here the central object is the 4-fold differential cross section (see App. C)

$$\frac{d\sigma}{ds' d\cos\theta_\gamma d\cos\theta_{\pi^-} d\phi_{\pi^-}} \,, \tag{5.6}$$

$\theta_\gamma$ and $\theta_{\pi^-}$ being now the polar angle of the photon- and the $\pi^-$-momentum in respect to the beam axis respectively and $\phi_{\pi^-}$ being the $\pi^-$ azimuthal angle. All angles can be chosen in the laboratory system which leads to a non-trivial phase space volume[1]. Since the A$\phi\rho\omega$DITE program carries out the integrations numerically it is possible to integrate over any sub space of the 4-dimensional phase space volume. This allows us to apply any kind of kinematical cuts. In the A$\phi\rho\omega$DITE program this option is realized by a convolution with dedicated Heavyside $\Theta$-functions. More generally the 4-fold differential cross section in eq. (5.6) can be convoluted with arbitrary functions $f(s', \theta_\gamma, \theta_{\pi^-}, \phi_{\pi^-})$ corresponding e.g. to the detector acceptance.

Following our inclusive strategy the photon angle $\theta_\gamma$ is integrated out. Integrating the remaining angles while applying $C$-symmetric cuts on the pion momenta leads to the desired point-like spectral functions that are needed in eq. (5.3). As discussed in the last chapter by including higher order effects using eq. (4.158) the theoretical uncertainty can be reduced to per mill level.

To summarize we can state that we have all ingredients to extract $R^{(\gamma)}_{\pi\pi}(s)$ with per mill precision from the experimental data. Here the A$\phi\rho\omega$DITE program can be a very useful tool.

[1] Note that the 4-momenta of the five particles participating in the scattering process can all be expressed in terms of the five kinematical variables $s$, $s'$, $\theta_\gamma$, $\theta_{\pi^-}$ and $\phi_{\pi^-}$.

# Chapter 6

# Final Remarks and Outlook

Experimental data on pion pair production in low energy $e^+e^-$ collisions of percent level accuracy will be available soon from Frascati and from Novosibirsk. That is why theoretical calculations of at least an accuracy of the same order are needed. Analytic and numerical results have been presented which should allow us to reach the desired accuracy for the appropriate observables. It appears to be recommendable to look at the $\pi^+\pi^-$ invariant mass spectrum in an inclusive way for what concerns the accompanying photon radiation and $e^+e^-$ pairs. We observed that $O(\alpha)$ massive FS corrections as well as $O(\alpha^2)$ IS photonic and $e^+e^-$ pair production corrections have to be taken into account. Also the resummation of higher order soft photon logarithms and leading $O(\alpha^3)$ IS photonic and pair production contributions may be necessary.

Under the condition that pion-pair acceptance cuts are applied in a $C$–symmetric way and hence the IFS correction drops out, the inclusive pion–pair distribution $d\sigma/ds'$ is of the form (4.139)

$$\frac{d\sigma}{ds'} = \sigma_0(s')\,\rho_{ini}(s,s') + \sigma_0(s)\,\rho_{fin}(s,s')\;, \tag{6.1}$$

which we may solve for $\sigma_0(s')$ [alternative form of (5.3)]:

$$\sigma_0(s') = \frac{1}{\rho_{ini}(s,s')}\left\{\frac{d\sigma}{ds'} - \sigma_0(s)\,\rho_{fin}(s,s')\right\}\quad . \tag{6.2}$$

At DAΦNE $s$ is fixed at $s = M_\phi^2$ and hence the FS radiation factor multiplies the fixed pion–pair cross–section $\sigma_0(s = M_\phi^2)$ at the $\phi$. The FS subtraction term in (6.2) is an at most 10% correction of the first and leading term for $0.3\,\mathrm{GeV} < \sqrt{s'} < 0.95\,\mathrm{GeV}$ (in the $\rho$ resonance region the contribution is of the order of 1%), although both terms are formally of the same order $O(\alpha)$.

Such a measurement should be complementary to the photon tagging method[1], which is not yet as well under control as the inclusive pion mass spectrum. Since

[1] For recent progress see [109].

the process $e^+e^- \to \mu^+\mu^-$ is theoretically very well under control but the separation of $\pi^+\pi^-$ and $\mu^+\mu^-$ states is quite non-trivial, experimentally one actually should perform an inclusive measurement also with respect to muon pair production and then subtract the theoretical $\mu^+\mu^-$ cross section. At least this could provide an important cross check for the particle identification procedure.

Apart from the fact that it might be desirable to have available a full $O(\alpha^2)$ calculation for the differential cross section, the main limitation of our approach lies in applying scalar QED to the pions generalized to an arbitrary pion form factor.

There are strong indications that the treatment of point-like pions together with its generalization to extended pions modeled by a form factor provides a reliable framework for extracting the pion form factor from the data. The sensitivity to the quark structure is minimized for the relevant observables by the fact that the QED radiative corrections are ultraviolet finite and hence no large renormalization group log's show up. Furthermore, the region $s' \lesssim s$ exhibiting large FS corrections corresponds to the soft photon regime where our generalized scalar QED treatment of the photonic corrections is reliable. However, the fact that the corrections which could be sensitive to the hadronic compositeness are small in the region where hard photons are involved does not mean that uncertainties are small at low $s'$. The reason is that for small $s'$ the emitted photons are hard and therefore can probe the substructure of the pions. One therefore can question the applicability of scalar QED when treating FS radiation in this region. At the same time it is the region where $|F_\pi(s')|^2$ drops below $|F_\pi(M_\phi^2)|^2$ which enhances the FS contribution in (5.3). The uncertainty in the FS correction term carries over to the extracted form factor.

It should be mentioned that the fact that we have to include FS corrections according to (5.4) does not reduce the sensitivity to the details of the emission of photons by hadrons, because the FS correction one has to subtract [see (5.3)] is different from what one has to add at the end. The first reflects the photon spectrum locally the second is an integral over the photon phase space.

As a crude estimate of the uncertainty related to the pion substructure we replace the pions by fermions of the same charge and mass [2]. Hence in (6.2) in stead of $\rho_{fin}$ we take the fermion final state radiator function

$$\begin{aligned}\rho^f_{\rm fin}(s,s') &= \frac{\alpha}{\pi}\,\frac{1+\frac{s'^2}{s^2}}{s-s'}\,\frac{\beta_\pi(s')}{\beta_\pi(s)}\,\frac{s}{s+2m_\pi^2}\left\{\frac{1}{\beta_\pi(s')}\right.\\ &\times \log\left(\frac{1+\beta_\pi(s')}{1-\beta_\pi(s')}\right)\left[1-4m_\pi^2\frac{s-s'+2m_\pi^2}{s^2+s'^2}\right]\\ &- \left.1-\frac{4s'm_\pi^2}{s^2+s'^2}\right\}. \end{aligned} \tag{6.3}$$

In the soft photon region we have $\rho^f_{fin}(s' \lesssim s) \simeq \rho_{fin}(s' \lesssim s)$ which reflects the correct long range behavior. For the extraction of the pion form factor we observe

[2] We cannot just replace the pions by the quarks produced in first place because the wrong net charge would not allow to match the proper long distance limit.

deviations of the fermionic from the scalar approach of less than 0.1 % for energies above 560 MeV. For $\sqrt{s'} > 420$ MeV the deviation is less than 1 %. At lower energies the difference between both approaches becomes larger since the radiated photons become harder: at $\sqrt{s'} = 360$ MeV we observe a deviation of 2 %, at $\sqrt{s'} = 300$ MeV of 6.5 % which is of the same order as the complete FS contribution in this region. Concerning the determination of $a_\mu^{\rm had}$ we obtain a difference between the fermionic and the scalar approach of about 2(7) per mill if we restrict the analysis to a region where $\sqrt{s'} > 420$ (300) MeV. The guesstimate looks reasonable because the such obtained uncertainty goes to zero in the classical limit ($s' \to s$) and becomes of the order of the FS radiation itself in the hard photon limit. Note that the increasing uncertainty for low energies $\sqrt{s'}$ here is a consequence of the radiative return method since in this region the emitted photons are necessarily hard.

The error due to the missing FS $O(\alpha^2)$ and IS $O(\alpha^3)$ corrections (including IS pair production contributions) is estimated to be not more than 1 per mill, respectively. Concerning the QED corrections we therefore estimate the accuracy to be at the 2 per mill level. On top of the perturbative uncertainty we have to take into account the hadronic uncertainty discussed in the previous paragraph. Altogether the precision of the theoretical prediction matches the requirements of low energy $e^+e^-$ experiments like the ones going on at DA$\Phi$NE or VEPP-2M.

# Appendix A

# Loop Integrals

The calculation of the relevant 1-loop integrals in dimensional regularization will be presented. The following notation for the scalar ($S$), rank 1 tensor ($V$) and rank 2 tensor ($T$) $r$-point integrals in $n$ dimensions is used:

$$I_{rS}(a_1, a_2 \ldots a_r) = \mu^{4-n} \int \frac{d^n k}{(2\pi)^n} \frac{1}{D_{a_1} D_{a_2} \ldots D_{a_r}} , \tag{A.1}$$

$$I^{\alpha}_{rV}(a_1, a_2 \ldots a_r) = \mu^{4-n} \int \frac{d^n k}{(2\pi)^n} \frac{k^{\alpha}}{D_{a_1} D_{a_2} \ldots D_{a_r}} , \tag{A.2}$$

$$I^{\alpha\beta}_{rT}(a_1, a_2 \ldots a_r) = \mu^{4-n} \int \frac{d^n k}{(2\pi)^n} \frac{k^{\alpha} k^{\beta}}{D_{a_1} D_{a_2} \ldots D_{a_r}} , \tag{A.3}$$

where the inverse propagators are defined as

$$D_{p_i} = (p_i - k)^2 - m_e^2 + i\epsilon \quad , \quad i = 1, 2 , \tag{A.4}$$

$$D_{k_j} = (k_j - k)^2 - m_\pi^2 + i\epsilon \quad , \quad j = 1, 2 , \tag{A.5}$$

$$D_k = k^2 + i\epsilon \quad , \quad D_q = (q - k)^2 + i\epsilon . \tag{A.6}$$

They correspond to the internal electron-, pion- and photon lines respectively. The parameter $\mu$ is the usual mass parameter in dimensional regularization. For the subsequent calculation the solutions of the following kind of integrals are needed:

$$[\mathcal{I}_S, \mathcal{I}^{\mu}_V, \mathcal{I}^{\mu\nu}_T] = \int \frac{d^n k}{(2\pi)^n} \frac{[1, k^{\mu}, k^{\mu} k^{\nu}]}{(k^2 + 2kK - m^2 + i\epsilon)^{\alpha}} , \tag{A.7}$$

which can be calculated in Euclidean space for the relevant cases. A straight forward calculation yields

$$\mathcal{I}_S(K, m^2, \alpha) = \frac{i}{(-1)^{\alpha}} \frac{\pi^{n/2}}{(2\pi)^n} (m^2 + K^2 - i\epsilon)^{-\alpha + n/2} \frac{\Gamma\left(\alpha - \frac{n}{2}\right)}{\Gamma(\alpha)} , \tag{A.8}$$

$$\mathcal{I}^{\mu}_V(K, m^2, \alpha) = -K^{\mu} \, I_S(K, m^2, \alpha) , \tag{A.9}$$

$$\mathcal{I}^{\mu\nu}_T(K, m^2, \alpha) = \mathcal{I}_S(K, m^2, \alpha) \left[ K^{\mu} K^{\nu} - \frac{1}{2} \, g^{\mu\nu} \, \frac{m^2 + K^2 - i\epsilon}{\alpha - \frac{n+2}{2}} \right] . \tag{A.10}$$

See e.g. [84, 110].

## A.1 The Integral with 1 Propagator

The most simple 1-loop integral only contains one propagator:

$$I_{1S}(m_A^2) \;=\; \mu^{4-n}\int \frac{d^nk}{(2\pi)^n}\,\frac{1}{(P_A+k)^2-m_A^2+i\epsilon}\,. \tag{A.11}$$

It can immediately be solved by applying eq. (A.8). The UV divergence is regularized in $n=4-\varepsilon_{UV}$ dimensions ($\mu=\mu_{UV}$). An expansion in $\varepsilon_{UV}$ then yields

$$I_{1S}(m_A^2) \;=\; \frac{i}{16\pi^2}\left[\frac{2}{\varepsilon_{UV}}-\gamma_E+\log\left(\frac{4\pi\mu_{UV}^2}{m_A^2}\right)+1\right]m_A^2\,. \tag{A.12}$$

## A.2 Integrals with 2 Propagators

Consider the 2-point integrals that are needed for the external leg self energy corrections:

$$I_{2S}(P_A,k) \;=\; \mu^{4-n}\int \frac{d^nk}{(2\pi)^n}\frac{1}{D_{P_A}D_k}\,, \tag{A.13}$$

$$I_{2V}^{\alpha}(P_A,k) \;=\; \mu^{4-n}\int \frac{d^nk}{(2\pi)^n}\frac{k^{\alpha}}{D_{P_A}D_k}\,, \tag{A.14}$$

where the inverse propagators are defined as:

$$D_{P_A}=(P_A+k)^2-m_A^2+i\epsilon\,. \tag{A.15}$$

By using Feynman parameters the integrals in eq. (A.13) and (A.14) can be brought into the standard form of (A.7). Applying eq. (A.8) and (A.9) yields

$$\begin{aligned} I_{2S}(P_A,k) \;&=\; \mu^{4-n}\int_0^1 dx\;\mathcal{I}_S(xP_A,x(P_A^2-m_A^2),2) \;=\; \mu^{4-n}\,\frac{i\pi^{n/2}}{(2\pi)^n} \\ &\times\; \Gamma\left(2-\frac{n}{2}\right)\int_0^1 dx\left[x^2P_A^2-x\left(P_A^2-m_e^2\right)-i\epsilon\right]^{-2+n/2}\,, \end{aligned} \tag{A.16}$$

$$\begin{aligned} I_{2V}^{\alpha}(P_A,k) \;&=\; \int_0^1 dx\;\mathcal{I}_V^{\alpha}(xP_A,x(P_A^2-m_A^2),2) \;=\; -\mu^{4-n}\frac{i\pi^{n/2}}{(2\pi)^n} \\ &\times\; \Gamma\left(2-\frac{n}{2}\right)P_A^{\mu}\int_0^1 dx\;x\left[x^2P_A^2-x\left(P_A^2-m_A^2\right)-i\epsilon\right]^{-2+n/2}\,. \end{aligned} \tag{A.17}$$

The 2-point functions in eq. (A.16) and (A.17) are UV divergent in 4 dimensions. Taking $n=4-\varepsilon_{UV}$ ($\mu=\mu_{UV}$) and expanding the factors in front of the integral in

the parameter $\varepsilon_{UV}$ leads to the following expressions:

$$I_{2S}(P_A,k) = \frac{i}{16\pi^2}\left[\frac{2}{\varepsilon_{UV}} - \gamma_E + \log(4\pi\mu_{UV}^2)\right] , \times \int_0^1 dx \, \left[x^2P_A^2 - x(P_A^2 - m_A^2) - i\epsilon\right]^{-\varepsilon_{UV}/2} , \quad \text{(A.18)}$$

$$I_{2V}^{\alpha}(P_A,k) = -\frac{i}{16\pi^2}\left[\frac{2}{\varepsilon_{UV}} - \gamma_E + \log(4\pi\mu_{UV}^2)\right] \times \int_0^1 dx \, x \left[x^2P_A^2 - x(P_A^2 - m_A^2) - i\epsilon\right]^{-\varepsilon_{UV}/2} . \quad \text{(A.19)}$$

For the calculation of the external leg corrections the on-shell derivatives of the 2-point integrals with respect to $P_A^2$ are needed ($m_A$ being the physical mass). They are UV finite but include IR divergent contributions which are regularized in $n = 4+\varepsilon_{IR}$ dimensions. Hence, with $\varepsilon_{UV} \to -\varepsilon_{IR}$, $\mu_{UV} \to \mu_{IR}$ we obtain

$$\left.\frac{\partial I_{2S}(P_A,k)}{\partial P_A^2}\right|_{P_A^2=m_A^2} = \frac{i}{16\pi^2}\left\{-1 + \frac{\varepsilon_{IR}}{2}\left[-\gamma_E + \log(4\pi\mu_{IR}^2)\right]\right\} \times m_A^{-2+\varepsilon_{IR}} \int_0^1 dx \, \left(x^{\varepsilon_{IR}} - x^{-1+\varepsilon_{IR}}\right) , \quad \text{(A.20)}$$

$$\left.\frac{\partial}{\partial P_A^2}\left(\frac{P_{A\alpha} I_{2V}^{\alpha}}{P_A^2}\right)\right|_{P_A^2=m_A^2} = -\frac{i}{16\pi^2}\left\{-1 + \frac{\varepsilon_{IR}}{2}\left[-\gamma_E + \log(4\pi\mu_{IR}^2)\right]\right\} \times m_A^{-2+\varepsilon_{IR}} \int_0^1 dx \, \left(x^{1+\varepsilon_{IR}} - x^{\varepsilon_{IR}}\right) . \quad \text{(A.21)}$$

The integrals in eq. (A.20) and (A.21) just have the form of the Euler beta function, which is defined as

$$B(m,n) = \int_0^1 dx \, x^{m-1}(1-x)^{n-1} = \frac{\Gamma(m)\Gamma(n)}{\Gamma(m+n)} , \quad \text{(A.22)}$$

$\Gamma(x)$ being the gamma function. Applying eq. (A.22), expanding (A.20) and (A.21) in $\varepsilon_{IR}$ and neglecting terms of $O(\varepsilon_{IR})$, yields

$$\left.\frac{\partial I_{2S}(P_A,k)}{\partial P_A^2}\right|_{P_A^2=m_A^2} = \frac{1}{m_A^2}\frac{i}{16\pi^2} \times \left\{\frac{1}{\varepsilon_{IR}} - \frac{1}{2}\left[-\gamma_E + \log\left(\frac{4\pi\mu_{IR}^2}{m_A^2}\right) + 2\right]\right\} , \quad \text{(A.23)}$$

$$\left.\frac{\partial}{\partial P_A^2}\left(\frac{P_{A\alpha} I_{2V}^{\alpha}}{P_A^2}\right)\right|_{P_A^2=m_A^2} = -\frac{1}{m_A^2}\frac{i}{32\pi^2} . \quad \text{(A.24)}$$

## A.3 Integrals with 3 Propagators

For the vertex correction diagrams and the box diagrams the following 3-point integrals have to be calculated:

$$\begin{aligned} &I_{3S}(k,-p_1,p_2)\ ,\ I^{\alpha}_{3V}(k,-p_1,p_2)\ ,\ I^{\alpha\beta}_{3T}(k,-p_1,p_2)\ ,\\ &I_{3S}(k,p_1,q)\ ,\ I_{3S}(p_1,q,k_{1,2})\ ,\ I_{3S}(k,q,k_{1,2})\ ,\ I^{\alpha}_{3V}(k,q,k_{1,2})\ . \end{aligned} \tag{A.25}$$

Taking into account that $I_{3S}(p_1,q,k_{1,2}) = I_{3S}(p_2,k,k_{2,1})$ only leaves the five master integrals $I_{3S}(k,P_A,P_B)$, $I_{3S}(k,P_A,q)$, $I^{\alpha}_{3V}(k,P_A,q)$, $I^{\alpha}_{3V}(k,-p_1,p_2)$ and $I^{\alpha\beta}_{3T}(k,-p_1,p_2)$ .

### A.3.1 The Integral $I_{3S}(k,P_A,P_B)$

The following scalar integral will now be calculated:

$$I_{3S}(k,P_A,P_B) = \mu^{4-n}\int\frac{d^nk}{(2\pi)^n}\,\frac{1}{D_kD_{P_A}D_{P_B}}\ , \tag{A.26}$$

$$\text{with}\quad D_{P_{A,B}} = (P_{A,B}-k)^2 - m^2_{A,B} + i\epsilon\ ,$$

$$P^2_{A,B} = m^2_{A,B}\ . \tag{A.27}$$

Using again Feynman parameters allows to write $I_{3S}(k,P_A,P_B)$ in the standard form of eq. (A.7):

$$I_{3S}(k,P_A,P_B) = \mu^{4-n}\int_0^1 dx\int_0^1 dy\int\frac{d^nk}{(2\pi)^n}\,\frac{2y}{\Delta^3} \tag{A.28}$$

$$\begin{aligned}\text{with}\qquad \Delta &= xyD_A + y(1-x)D_B + (1-y)D_k\\ &= k^2 + 2y[x(P_B-P_A)-P_B]k + i\epsilon\ . \end{aligned} \tag{A.29}$$

Applying eq. (A.8) then leads to

$$\int\frac{d^nk}{(2\pi)^n}\,\frac{1}{\Delta^3} = -i\frac{\pi^{n/2}}{(2\pi)^n}\,(K^2)^{-3+n/2}\,\frac{\Gamma\left(3-\frac{n}{2}\right)}{\Gamma(3)}\ , \tag{A.30}$$

$$\text{with}\qquad K^2 = y^2[x^2t_{AB} - x(t_{AB}+m^2_B-m^2_A)+m^2_B] - i\epsilon\ , \tag{A.31}$$

$$t_{AB} = (P_A-P_B)^2\ ,\quad t_{AB} = \Re e(t_{AB}) + i\epsilon\ . \tag{A.32}$$

The scalar integral $I_{3S}(k,P_A,P_B)$ is IR divergent in four dimensions. It therefore has to be regularized by switching to $n = 4+\varepsilon_{IR}$ dimensions. Hence inserting (A.30) into (A.28) yields

$$\begin{aligned} I_{3S}(k,P_A,P_B) &= \mu^{-\varepsilon_{IR}}\frac{-i\pi^{2+\varepsilon_{IR}/2}}{(2\pi)^{4+\varepsilon_{IR}}}\,\Gamma\left(1-\frac{\varepsilon_{IR}}{2}\right)\int_0^1 dy\ y^{-1+\varepsilon_{IR}}\\ &\times\int_0^1 dx\ \left[m^2_B - x(t_{AB}+m^2_B-m^2_A)+x^2t_{AB}-i\epsilon\right]^{-1+\varepsilon_{IR}/2}\ . \end{aligned} \tag{A.33}$$

Using again the Euler beta function,

$$\int_0^1 dy\; y^{-1+\varepsilon_{IR}} \;=\; B(1,\varepsilon_{IR}) = \frac{\Gamma(1)\Gamma(\varepsilon_{IR})}{\Gamma(1+\varepsilon_{IR})} = \frac{1}{\varepsilon_{IR}} + O(\varepsilon_{IR})\;, \tag{A.34}$$

and expanding the IR divergent integral in $\varepsilon_{IR}$ leads to

$$\begin{aligned} & -\frac{i\pi^{2+\varepsilon_{IR}/2}\mu^{-\varepsilon_{IR}}}{(2\pi)^{4+\varepsilon_{IR}}}\,\Gamma\left(1-\frac{\varepsilon_{IR}}{2}\right)\,\int_0^1 dy\; y^{-1+\varepsilon_{IR}} \\ & \quad = \;\frac{i}{32\pi^2}\left[-\frac{2}{\varepsilon_{IR}} + \log(4\pi\mu_{IR}^2) - \gamma_E\right] + O(\varepsilon_{IR})\;. \end{aligned} \tag{A.35}$$

The $x$-integral remains to be calculated. Since it is IR finite it can safely be expanded in $\varepsilon_{IR}$:

$$I_x \;\equiv\; \int_0^1 dx\;\left[m_B^2 - x(t_{AB}+m_B^2-m_A^2) + x^2 t_{AB} - i\epsilon\right]^{-1+\varepsilon_{IR}/2} \tag{A.36}$$

$$\;=\; \frac{1}{t_{AB}}\left\{\int_0^1 dx\;\frac{1+\frac{\varepsilon_{IR}}{2}\log(t_{AB})}{P(x)} \;+\; \frac{\varepsilon_{IR}}{2}\int_0^1 dx\;\frac{\log[P(x)]}{P(x)}\right\} \tag{A.37}$$

$$\text{with}\quad P(x) \;=\; x^2 - x\;\frac{t_{AB}+m_B^2-m_A^2}{t_{AB}} + \frac{m_B^2}{t_{AB}} - \frac{i\epsilon}{t_{AB}}\;. \tag{A.38}$$

Let us now factorize the polynomial $P(x)$:

$$P(x) \;=\; (x-x_1)(x-x_2) \quad\text{with}\quad x_{1,2} \;=\; \frac{1}{2}\left(c_{AB} \pm \beta_{AB}\right)\;, \tag{A.39}$$

$$c_{AB} \;=\; \frac{t_{AB}+m_B^2-m_A^2}{t_{AB}}\;,\quad \beta_{AB} \;=\; \frac{\sqrt{\lambda(t_{AB},m_A^2,m_B^2)}}{t_{AB}}(\pm)i\epsilon\;. \tag{A.40}$$

Here one has to be careful with the $\pm i\epsilon$ terms. The equation $P(x)=0$ does not have a solution for the values $0<x<1$ if $t_{AB}$ is taken to be the $u$ or $t$ channel variable since then $t_{AB}=t(u)<0$. On the other hand $t_{AB}=\Re e(t_{AB})+i\epsilon$ of course holds for positive as well as for negative values of $\Re e(t_{AB})$. Therefore we have to take $\beta_{AB}+i\epsilon$ for the $s$-channel integral ($t_{AB}=s$) and $\beta_{AB}-i\epsilon$ for the $u$- and $t$-channel integral [$t_{AB}=t(u)$]. These two distinct cases are denoted by "$\pm$". One can now rewrite the $x$-integral as:

$$\begin{aligned} I_x \;=\; & \frac{1}{t_{AB}(x_1-x_2)}\left\{\left[1+\frac{\varepsilon_{IR}}{2}\log(t_{AB})\right]\int_0^1 dx\;\left[\frac{1}{x-x_1}-\frac{1}{x-x_2}\right]\right. \\ & \left. +\;\frac{\varepsilon_{IR}}{2}\int_0^1 dx\;\left[\frac{\log(x-x_1)}{x-x_1}+\frac{\log(x-x_2)}{x-x_1}-\frac{\log(x-x_1)}{x-x_2}-\frac{\log(x-x_2)}{x-x_2}\right]\right\}. \end{aligned} \tag{A.41}$$

Let us define

$$c_{BA} \;=\; \frac{t_{AB}+m_A^2-m_B^2}{t_{AB}}\;,\quad \text{which implies}\quad \frac{1}{2}\left(c_{AB}+c_{BA}\right) \;=\; 1\;. \tag{A.42}$$

This allows us to write the integrals in a compact form. We find the following solutions:

$$\int_0^1 dx\ \left[\frac{1}{x-x_1}-\frac{1}{x-x_2}\right] = -\left[\log\left(\frac{c_{AB}+\beta_{AB}}{c_{BA}-\beta_{AB}}\right)+\log\left(\frac{c_{BA}+\beta_{AB}}{c_{AB}-\beta_{AB}}\right)\right] \pm 2\pi i\ , \tag{A.43}$$

$$\int_0^1 dx\ \frac{\log(x-x_1)}{x-x_1} = \frac{1}{2}\log^2\left(\frac{c_{BA}-\beta_{AB}}{2}\right)-\frac{1}{2}\log^2\left(\frac{c_{AB}+\beta_{AB}}{2}\right) \pm \pi i\log\left(\frac{c_{AB}+\beta_{AB}}{2}\right)+\frac{\pi^2}{2}\ , \tag{A.44}$$

$$\int_0^1 dx\ \frac{\log(x-x_2)}{x-x_2} = \frac{1}{2}\log^2\left(\frac{c_{BA}+\beta_{AB}}{2}\right)-\frac{1}{2}\log^2\left(\frac{c_{AB}-\beta_{AB}}{2}\right) \mp \pi i\log\left(\frac{c_{AB}-\beta_{AB}}{2}\right)+\frac{\pi^2}{2}\ , \tag{A.45}$$

$$\begin{aligned}\int_0^1 dx\ \frac{\log(x-x_1)}{x-x_2} &= \log\left(\frac{c_{BA}-\beta_{AB}}{2}\right)\log\left(\frac{c_{BA}+\beta_{AB}}{2\beta_{AB}}\right)\\ &-\log(\beta_{AB})\log\left(\frac{c_{AB}-\beta_{AB}}{2\beta_{AB}}\right)+\mathrm{Li}_2\left(-\frac{c_{AB}-\beta_{AB}}{2\beta_{AB}}\right)\\ &+\mathrm{Li}_2\left(-\frac{c_{BA}-\beta_{AB}}{2\beta_{AB}}\right)-\frac{7}{6}\pi^2\pm i\pi\log\left(\frac{c_{AB}-\beta_{AB}}{2\beta_{AB}^2}\right)\ ,\end{aligned} \tag{A.46}$$

$$\begin{aligned}\int_0^1 dx\ \frac{\log(x-x_2)}{x-x_1} &= -\log\left(\frac{c_{AB}-\beta_{AB}}{2}\right)\log\left(\frac{c_{AB}+\beta_{AB}}{2\beta_{AB}}\right)\\ &+\log(\beta_{AB})\log\left(\frac{c_{BA}-\beta_{AB}}{2\beta_{AB}}\right)-\mathrm{Li}_2\left(-\frac{c_{AB}-\beta_{AB}}{2\beta_{AB}}\right)\\ &-\mathrm{Li}_2\left(-\frac{c_{BA}-\beta_{AB}}{2\beta_{AB}}\right)+\frac{\pi^2}{6}\mp i\pi\log\left(\frac{c_{AB}+\beta_{AB}}{2\beta_{AB}^2}\right)\ ,\end{aligned} \tag{A.47}$$

A straight forward calculation then yields

$$\begin{aligned}&\int_0^1 dx\ \left[\frac{\log(x-x_1)}{x-x_1}+\frac{\log(x-x_2)}{x-x_1}-\frac{\log(x-x_1)}{x-x_2}-\frac{\log(x-x_2)}{x-x_2}\right]\\ &=\frac{1}{2}\left\{-\log\left(\frac{c_{AB}+\beta_{AB}}{c_{AB}-\beta_{AB}}\right)\left[\log\left(\frac{c_{AB}^2-\beta_{AB}^2}{4}\right)+2\log(\beta_{AB})\right]\right.\\ &-2\log\left(\frac{c_{AB}+\beta_{AB}}{2\beta_{AB}}\right)\log\left(\frac{c_{AB}-\beta_{AB}}{2\beta_{AB}}\right)\\ &\left.-4\mathrm{Li}_2\left(-\frac{c_{AB}-\beta_{AB}}{2\beta_{AB}}\right)+\frac{4}{3}\pi^2\pm 4\pi i\log(\beta_{AB})\right\}+(c_{AB}\leftrightarrow c_{BA})\ .\end{aligned} \tag{A.48}$$

This finally leads to the general solution of the scalar 3-point function:

$$\begin{aligned} I_{3S}(k,P_A,P_B) &= -\frac{i}{16\pi^2}\frac{1}{t_{AB}\beta_{AB}}\left\{\frac{1}{\varepsilon_{IR}}\left[-\log\left(\frac{c_{AB}+\beta_{AB}}{c_{AB}-\beta_{AB}}\right)\pm\pi i\right]\right. \\ &+\frac{1}{2}\left\{\left[\log\left(\frac{c_{AB}+\beta_{AB}}{c_{AB}-\beta_{AB}}\right)\mp\pi i\right]\left[\log\left(\frac{4\pi\mu_{IR}^2}{t_{AB}}\right)-\gamma_E\right]\right. \\ &-\frac{1}{2}\log\left(\frac{c_{AB}+\beta_{AB}}{c_{AB}-\beta_{AB}}\right)\left[\log\left(\frac{c_{AB}^2-\beta_{AB}^2}{4}\right)+2\log(\beta_{AB})\right] \\ &-\log\left(\frac{c_{AB}+\beta_{AB}}{2\beta_{AB}}\right)\log\left(\frac{c_{AB}-\beta_{AB}}{2\beta_{AB}}\right) \\ &\left.\left.-2\mathrm{Li}_2\left(-\frac{c_{AB}-\beta_{AB}}{2\beta_{AB}}\right)+\frac{2}{3}\pi^2\pm 2\pi i\log(\beta_{AB})\right\}\right\}+(c_{AB}\to c_{BA})\,. \end{aligned} \tag{A.49}$$

The scalar 3-point integral corresponding to the initial state vertex correction can be obtained from eq. (A.49) by making the replacements $P_A = -p_1$, $P_B = p_2$, $m_B = m_A = m_e$. This leads to ($t_{AB} = s$, $\beta_{AB} = \beta_e$, $c_{AB} = c_{BA} = 1$):

$$\begin{aligned} I_{3S}(k,-p_1,p_2) &= -\frac{i}{8\pi^2}\frac{1}{s\beta_e}\left\{\frac{1}{\varepsilon_{IR}}\left[-\log\left(\frac{1+\beta_e}{1-\beta_e}\right)+\pi i\right]\right. \\ &+\frac{1}{2}\left\{\left[\log\left(\frac{1+\beta_e}{1-\beta_e}\right)-\pi i\right]\left[\log\left(\frac{4\pi}{s}\right)-\gamma_E\right]\right. \\ &-\frac{1}{2}\log\left(\frac{1+\beta_e}{1-\beta_e}\right)\left[\log\left(\frac{1-\beta_e^2}{4}\right)+2\log(\beta_e)\right] \\ &-\log\left(\frac{1+\beta_e}{2\beta_e}\right)\log\left(\frac{1-\beta_e}{2\beta_e}\right) \\ &\left.\left.-2\mathrm{Li}_2\left(-\frac{1-\beta_e}{2\beta_e}\right)+\frac{2}{3}\pi^2+2\pi i\log(\beta_e)\right\}\right\}+O(\varepsilon_{IR})\,. \end{aligned} \tag{A.50}$$

The scalar 3-point integral $I_{3S}(k,-k_1,k_2)$ corresponding to the pion vertex correction can be obtained from eq. (A.50) simply by replacing $\beta_e$ by $\beta_\pi$.

Also the integrals $I_{3S}(k,p_1,k_{1,2})$ and $I_{3S}(p_1,q,k_{1,2})$ can now easily be obtained from eq. (A.49). Consider first $I_{3S}(k,p_1,k_1)$. Then we have

$$\begin{aligned} p_A &= p_1\,, \quad p_B = k_1\,, \quad m_A = m_e\,, \\ t_{AB} &= u+i\epsilon\,, \quad m_B = m_\pi\,, \\ c_{AB} &= \frac{u+m_e^2-m_\pi^2}{u}\,, \quad c_{BA} = \frac{u-m_e^2+m_\pi^2}{u}\,, \\ \beta_{AB} &= -\frac{u-m_\pi^2}{u}+\frac{u+m_\pi^2}{u-m_\pi^2}\,\frac{m_e^2}{u}-i\epsilon\,, \end{aligned} \tag{A.51}$$

Neglecting the electron mass where possible then leads to the following solution:

$$\begin{aligned} I_{3S}(k,p_1,k_1) &= \frac{i}{16\pi^2}\frac{1}{U}\Bigg\{\left[-\frac{2}{\varepsilon_{IR}}+\log\left(-\frac{4\pi\mu_{IR}^2}{u}\right)-\gamma_E\right]\log\left(\frac{U}{m_e m_\pi}\right) \\ &\quad -\frac{1}{2}\Bigg\{3\log^2\left(\frac{u-m_\pi^2}{u}\right)-\frac{1}{2}\log^2\left(-\frac{m_e^2}{u}\right)-\frac{1}{2}\log^2\left(-\frac{m_\pi^2}{u}\right) \\ &\quad -2\log\left(-\frac{m_\pi^2}{u}\right)\log\left(\frac{u-m_\pi^2}{u}\right)+2\mathrm{Li}_2\left(-\frac{m_\pi^2}{u-m_\pi^2}\right)-\frac{\pi^2}{3}\Bigg\}\Bigg\}\,. \end{aligned} \tag{A.52}$$

The integral $I_{3S}(k,p_1,k_2)$ can be obtained by replacing in eq. (A.52) $u$ by $t$ and $U$ by $T$. Making in $I_{3S}(k,p_1,k_1)$ and $I_{3S}(k,p_1,k_2)$ the combined replacements $p_1 \to p_2$, $k_1 \to k_2$ does not change these integrals. Since in addition $I_{3S}(p_1,q,k_{1,2}) = I_{3S}(p_2,k,k_{2,1})$, the only remaining scalar master integral to be calculated is the integral $I_{3S}(k,q,P)$.

### A.3.2 The Integral $I_{3S}(k,q,P)$ and $I_{3V}^{\alpha}(k,q,P)$

Let us finally consider the scalar 3-point integral:

$$\begin{aligned} I_{3S}(k,q,P) &= \int\frac{d^4k}{(2\pi)^4}\frac{1}{[(P-k)^2-m^2+i\epsilon][k^2+i\epsilon][(q-k)^2+i\epsilon]}\,, \\ \text{with}\quad & P_1+P_2=q\,,\ q^2=s\,,\ P_1^2=P_2^2=m^2\,, \\ & \beta = \sqrt{1-4m^2/s}\,. \end{aligned} \tag{A.53}$$

As before, by using Feynman parameters one can transform the integral into the form of eq. (A.8). Hence, with

$$\Delta = k^2+2y(xP_2-q)k+y(1-x)s+i\epsilon \tag{A.54}$$

the scalar integral can be written as

$$\begin{aligned} I_{3S}(k,q,P) &= \int_0^1 dx\int_0^1 dy\;2y\int\frac{d^4k}{(2\pi)^4}\,\frac{1}{\Delta^3} \\ &= -\frac{i\pi^2}{(2\pi)^4}\int_0^1 dx\,\frac{\log\left[\frac{x^2m^2}{(1-x)s}\right]+i\pi}{s(1-x)+x^2m^2}\,. \end{aligned} \tag{A.55}$$

Now only the $x$-integration remains to be carried out. Using

$$\begin{aligned}
\int_0^1 dx\ \frac{\log x^2}{s(1-x)+x^2m^2} &= \frac{2}{s\beta}\left[\mathrm{Li}_2\left(\frac{1-\beta}{2}\right)-\mathrm{Li}_2\left(\frac{1+\beta}{2}\right)\right] \\
&\simeq -\frac{1}{s}\,\frac{\pi^2}{3}\,, \qquad \text{(A.56)} \\
\int_0^1 dx\ \frac{\log(1-x)}{s(1-x)+x^2m^2} &= \frac{1}{s\beta}\left[\mathrm{Li}_2\left(-\frac{1+\beta}{1-\beta}\right)-\mathrm{Li}_2\left(-\frac{1-\beta}{1+\beta}\right)\right] \\
&\simeq \frac{1}{s}\,\log\left(\frac{s}{m^2}\right)\,, \qquad \text{(A.57)} \\
\int_0^1 dx\ \frac{1}{s(1-x)+x^2m^2} &= \frac{1}{s\beta}\log\left(\frac{1+\beta}{1-\beta}\right) \simeq \frac{1}{s}\,\log\left(\frac{s}{m^2}\right)\,, \qquad \text{(A.58)}
\end{aligned}$$

finally yields

$$\begin{aligned}
I_{3S}(k,q,P) &= \frac{-i\pi^2}{(2\pi)^4}\frac{1}{s\beta}\left[2\mathrm{Li}_2\left(\frac{1-\beta}{2}\right)-2\mathrm{Li}_2\left(\frac{1+\beta}{2}\right)\right. \\
&\quad -\mathrm{Li}_2\left(-\frac{1+\beta}{1-\beta}\right)+\mathrm{Li}_2\left(-\frac{1-\beta}{1+\beta}\right) \\
&\quad \left.-\log\left(\frac{s}{m^2}\right)\log\left(\frac{1+\beta}{1-\beta}\right)+i\pi\log\left(\frac{1+\beta}{1-\beta}\right)\right] \\
&\simeq \frac{i\pi^2}{(2\pi)^4}\frac{1}{s}\left[\frac{1}{2}\log^2\left(\frac{s}{m^2}\right)+\frac{\pi^2}{6}-i\pi\log\left(\frac{s}{m^2}\right)\right]\,. \qquad \text{(A.59)}
\end{aligned}$$

"$\simeq$" here corresponds to the case that $s \gg m^2$, which is true if $m = m_e$ for the considered cases. If on the other hand pions are considered the pion mass has to be kept. Hence

$$\begin{aligned}
I_{3S}(k,q,k_{1,2}) &= \frac{-i\pi^2}{(2\pi)^4}\frac{1}{s\beta_\pi}\left[2\mathrm{Li}_2\left(\frac{1-\beta_\pi}{2}\right)-2\mathrm{Li}_2\left(\frac{1+\beta_\pi}{2}\right)\right. \\
&\quad -\mathrm{Li}_2\left(-\frac{1+\beta_\pi}{1-\beta_\pi}\right)+\mathrm{Li}_2\left(-\frac{1-\beta_\pi}{1+\beta_\pi}\right) \\
&\quad \left.-\log\left(\frac{s}{m_\pi^2}\right)\log\left(\frac{1+\beta_\pi}{1-\beta_\pi}\right)+i\pi\log\left(\frac{1+\beta_\pi}{1-\beta_\pi}\right)\right]\,, \qquad \text{(A.60)} \\
I_{3S}(k,q,p_{1,2}) &\simeq \frac{i\pi^2}{(2\pi)^4}\frac{1}{s}\left[\frac{1}{2}\log^2\left(\frac{s}{m_e^2}\right)+\frac{\pi^2}{6}-i\pi\log\left(\frac{s}{m_e^2}\right)\right]\,. \qquad \text{(A.61)}
\end{aligned}$$

The rank-1 tensor integral can be obtained using tensor reduction, by making the following general tensor ansatz:

$$I_{3V}^{\alpha}(k,q,P) = C_q\,q^\alpha + C_P\,P^\alpha\,. \qquad \text{(A.62)}$$

By contracting eq. (A.62) successively with $q_\alpha$ and $P_\alpha$ one can detetermine the constants as functions of scalar 3-point and 2-point integrals:

$$C_q = -\frac{2m_\pi^2\, I_{3S}(k,q,P) + I_{2S}(k,q) - I_{2S}(q,P)}{s\beta^2}\,, \tag{A.63}$$

$$C_P = \frac{2I_{2S}(k,q) - 2I_{2S}(q,P) + sI_{3S}(k,q,P)}{s\beta^2}\,. \tag{A.64}$$

### A.3.3 The integrals $I^\alpha_{3V}(-p_1,p_2,k)$ and $I^{\alpha\beta}_{3T}(-p_1,p_2,k)$

For the initial state vertex correction the (in four dimensions) IR and UV finite rank-1 tensor integral and the UV divergent rank-2 tensor integral have to be calculated. Feynman parameters are again used to write the integrals in the form of eq. (A.9) and (A.10). Although these integrals can also be solved by using tensor reduction it appears to be more convenient to solve them directly. Using the expression in eq. (A.29) with $P_A = -p_1$ and $P_A = p_2$ we obtain

$$\Delta = k^2 + 2y(xq - p_2)k + i\epsilon\,. \tag{A.65}$$

Since the integral $I^\alpha_{3V}(-p_1,p_2,k)$ is IR and UV finite no IR or UV regulator has to be introduced. The calculation can be carried out in four dimensions ($n = 4$):

$$\begin{aligned}
I^\alpha_{3V}(-p_1,p_2,k) &= \int_0^1 dx \int_0^1 dy\, 2y \int \frac{d^4k}{(2\pi)^4}\,\frac{k^\alpha}{\Delta^3} \\
&= \frac{i\pi^2}{(2\pi)^4}\int_0^1 dx \int_0^1 dy\, \frac{xq^\alpha - p_2^\alpha}{m_e^2 - x(1-x)s - i\epsilon} \\
&= \frac{i\pi^2}{(2\pi)^4}\,\frac{1}{s}\int_0^1 dx\, \frac{xq^\alpha - p_2^\alpha}{x^2 - x + \frac{m_e^2}{s} - i\epsilon} \\
&= \frac{i\pi^2}{(2\pi)^4}\,\frac{1}{s}\,\frac{1}{x_1 - x_2}\left[q^\alpha \int_0^1 dx\, \left(\frac{x}{x-x_1} - \frac{x}{x-x_2}\right)\right. \\
&\qquad \left. - p_2^\alpha \int_0^1 dx\, \left(\frac{1}{x-x_1} - \frac{1}{x-x_2}\right)\right]\,,
\end{aligned} \tag{A.66}$$

where the variables $x_1$ and $x_2$ in eq (A.39) ($c_{AB} = c_{BA} = 1$) have been used:

$$x_1 = \frac{1}{2}\left[1 + (\beta_e + i\epsilon)\right]\,, \quad x_2 = \frac{1}{2}\left[1 - (\beta_e + i\epsilon)\right] \quad . \tag{A.67}$$

Carrying out the simple integrations in eq. (A.66) yields

$$I^\alpha_{3V}(-p_1,p_2,k) = \frac{-i\pi^2}{(2\pi)^4}\,\frac{1}{s\beta_e}\,\left[p_1^\alpha - p_2^\alpha\right]\left[\log\left(\frac{1+\beta_e}{1-\beta_e}\right) - \pi i\right]\,. \tag{A.68}$$

For the UV divergent integral $I_{3T}^{\alpha\beta}(-p_1,p_2,k)$ an UV-regulator has to be introduced which is done by dimensional regularization ($n=4-\varepsilon_{UV}$). The integral can be written in a similar way as $I_{3V}^{\alpha}(-p_1,p_2,k)$ in (A.66):

$$\begin{aligned}
I_{3T}^{\alpha\beta}(-p_1,p_2,k) &= \int_0^1 dx \int_0^1 dy\; 2y \int \frac{d^nk}{(2\pi)^n}\,\frac{k^\alpha k^\beta}{\Delta^3} \\
&= \frac{-i\pi^{n/2}}{(2\pi)^n}\,\frac{\Gamma\left(3-\frac{n}{2}\right)}{\Gamma(3)} \int_0^1 dx \int_0^1 dy\; 2y\; \left[y^2\left(xq-p_2\right)^2-i\epsilon\right]^{-3+n/2} \\
&\times \left[y^2\left(xq^\alpha-p_2^\alpha\right)\left(xq^\beta-p_2^\beta\right)-\frac{1}{2}\,g^{\alpha\beta}\,\frac{y^2\left(xq-p_2\right)^2-i\epsilon}{2-\frac{n}{2}}\right] \\
&= \frac{-i\pi^{2-\varepsilon_{UV}/2}}{(2\pi)^{4-\varepsilon_{UV}}}\,\Gamma\left(1+\frac{\varepsilon_{UV}}{2}\right)\int_0^1 dy\; y^{1-\varepsilon_{UV}} \\
&\times \int_0^1 dx\;\left\{\frac{\left(xq^\alpha-p_2^\alpha\right)\left(xq^\beta-p_2^\beta\right)}{\left(xq-p_2\right)^2-i\epsilon}-\frac{g^{\alpha\beta}}{\varepsilon_{UV}}\left[\left(xq-p_2\right)^2-i\epsilon\right]^{-\varepsilon_{UV}/2}\right\} \qquad \text{(A.69)} \\
&+ O(\varepsilon_{UV}) \quad .
\end{aligned}$$

The integrations can be carried out easily:

$$\int_0^1 dy\; y^{1-\varepsilon_{UV}} = \frac{1}{2-\varepsilon_{UV}}\,1^{2-\varepsilon_{UV}} = \frac{1}{2-\varepsilon_{UV}}\;, \qquad \text{(A.70)}$$

$$\begin{aligned}
\int_0^1 dx\;\frac{\left(xq^\alpha-p_2^\alpha\right)\left(xq^\beta-p_2^\beta\right)}{\left(xq-p_2\right)^2-i\epsilon} &= \frac{q^\alpha q^\beta}{s}\Bigg\{1-\frac{1+\beta_e^2}{2\beta_e} \\
&\quad\times\left[\log\left(\frac{1+\beta_e}{1-\beta_e}\right)-\pi i\right]\Bigg\} \\
&\quad+\frac{p_1^\alpha p_2^\beta+p_2^\alpha p_1^\beta}{s\beta_e}\left[\log\left(\frac{1+\beta_e}{1-\beta_e}\right)-\pi i\right]\;. \qquad \text{(A.71)}
\end{aligned}$$

The remaining integral contains the UV divergent contribution of $I_{3T}^{\alpha\beta}$. Expanding in $\varepsilon_{UV}$ therefore leads to a pole term $\propto 1/\varepsilon_{UV}$:

$$\begin{aligned}
-\frac{g^{\alpha\beta}}{\varepsilon_{UV}}\int_0^1 dx\;\left[\left(xq-p_2\right)^2-i\epsilon\right]^{-\varepsilon_{UV}/2} &= -\frac{g^{\alpha\beta}}{\varepsilon_{UV}}\int_0^1 dx\;\Bigg\{1-\frac{\varepsilon_{UV}}{2}\Big[\log(s) \\
+\log\left(x-x_1\right)+\log\left(x-x_2\right)\Big]\Bigg\} &= -g^{\alpha\beta}\left\{\frac{1}{\varepsilon_{UV}}+\frac{1}{2}\Bigg[-\log(s)+2\right. \\
&\quad\left.-\log\left(\frac{1-\beta_e^2}{4}\right)-\beta_e\left[\log\left(\frac{1+\beta_e}{1-\beta_e}\right)-\pi i\right]\Bigg]\right\}\;. \qquad \text{(A.72)}
\end{aligned}$$

Inserting the results into eq. (A.69) leads to the result:

$$\begin{aligned} I_{3T}^{\alpha\beta}(-p_1,p_2,k)) &= \frac{i\pi^2}{2(2\pi)^4}\Bigg\{ g^{\alpha\beta}\left\{\frac{1}{\varepsilon_{UV}}+\frac{1}{2}\Bigg[\log\left(\frac{4\pi}{s}\right)-\gamma_E+3 \right. \\ &\quad \left. -\log\left(\frac{1-\beta_e^2}{4}\right)-\beta_e\left[\log\left(\frac{1+\beta_e}{1-\beta_e}\right)-\pi i\right]\Bigg]\right\} \\ &\quad -\frac{q^\alpha q^\beta}{s}\left\{1-\frac{1+\beta_e^2}{2\beta_e}\left[\log\left(\frac{1+\beta_e}{1-\beta_e}\right)-\pi i\right]\right\} \\ &\quad -\frac{p_1^\alpha p_2^\beta+p_2^\alpha p_1^\beta}{s\beta_e}\left[\log\left(\frac{1+\beta_e}{1-\beta_e}\right)-\pi i\right]\Bigg\}\,. \end{aligned} \tag{A.73}$$

## A.4 Integrals with 4 Propagators

### A.4.1 The Scalar Box

Cutcosky's rule and the dispersion relation will now be used to solve the scalar 4-point functions $I_{4S}(k,p_1,q,k_{1(2)})$ (see also [111]). The two photon lines are cut, leading to the subprocesses $e^-(p_1)e^+(p_2)\to\gamma_1(k)\gamma_2(l)$ and $\pi^-(k_1)\pi^+(k_2)\to\gamma_1(k)\gamma_2(l)$. They correspond to the amplitudes $T_{ni}^{a(b)}$ and $T_{nf}^{a(b)}$, where $a$ and $b$ are the labels for the two different box diagram topologies as defined in chapter 4 [$iT_{fi}^{a(b)}=\mathcal{M}_{a(b)}$]. Multiplying the amplitude that corresponds to the subprocess $e^+e^-\to\gamma\gamma$ with the complex conjugated amplitude of the process $\pi^+\pi^-\to\gamma\gamma$ yields:

$$\sum_{\lambda_i} T_{ni}^{a(b)}T_{nf}^{a(b)*} = e^4\,\frac{N_{a(b)}}{D_{p_1}D_{k_{1(2)}}}\,. \tag{A.74}$$

The numerators of the box integrals $N_a$ and $N_b$ are given in eq. (4.95) and (4.96). The photon spins $\lambda_i$ have been summed over. Note that the two photon propagators have disappeared now. Cutkosky's rule relates the imaginary part of the box amplitude to the phase-space-integrated expression in eq. (A.74):

$$\Im m T_{fi} = \frac{\mu_{IR}^{4-n}}{2}\int dLips(k,l)\,\sum_{\lambda_i} T_{ni}T_{nf}^*\,, \tag{A.75}$$

$$\text{with}\qquad dLips(k,l) = \frac{d^{n-1}k}{2|\vec{k}|(2\pi)^{n-1}}\frac{d^{n-1}l}{2|\vec{l}|(2\pi)^{n-1}}\,(2\pi)^n\delta^n(q-l-k)\,. \tag{A.76}$$

The momenta $k$ and $l$ are the photon momenta of the subprocess final states. Similarily for the scalar box integrals we can write

$$\begin{aligned} \Im m[-iI_{4S}(k,p_1,q,k_{1(2)})] &= \frac{\mu_{IR}^{4-n}}{2}\int dLips(k,l)\,\frac{1}{D_{p_1}D_{k_{1(2)}}} \\ &= \frac{\mu_{IR}^{4-n}s^{n/2-2}}{8(16\pi)^{n/2-1}\Gamma\left(\frac{n}{2}-1\right)}\,J_{a(b)}\,. \end{aligned} \tag{A.77}$$

For the last equality the integration was carried out in the $e^+e^-$ CMS. The functions $J_{a(b)}$ are defined as

$$J_{a(b)} \;=\; 4\int \frac{d\phi}{2\pi}\int_{-1}^{1} dc\,\frac{(1-c^2)^{n/2-2}}{D_{p_1}D_{k_{1(2)}}} \;=\; \frac{1+\varepsilon_{IR}\log(2)}{s}\,J_1(u(t))\;, \tag{A.78}$$

$$\text{with}\quad J_1(x) \;=\; \frac{8}{\sqrt{\lambda(x,m_e^2,m_\pi^2)}}\log\left[\frac{-x+m_e^2+m_\pi^2+\sqrt{\lambda(x,m_e^2,m_\pi^2)}}{-x+m_e^2+m_\pi^2-\sqrt{\lambda(x,m_e^2,m_\pi^2)}}\right]+\text{rest}\;,$$

$$J_1(u(t)) \;\simeq\; \frac{16}{U(T)}\log\left(\frac{U(T)}{m_e m_\pi}\right)+\text{rest}\;. \tag{A.79}$$

Here 'rest' corresponds to terms that are multiplied by $\varepsilon_{IR}$ and vanish in the limit $\varepsilon_{IR}\to 0$ even after dispersion integration. Hence

$$\begin{aligned}\Im m[-iI_{4S}(k,p_1,q,k_{1(2)})] \;&=\; \frac{s^{-1+\varepsilon_{IR}/2}}{8\pi}\,\frac{1}{U(T)}\log\left(\frac{U(T)}{m_e m_\pi}\right)\\ &\quad\times\left[1-\frac{\varepsilon_{IR}}{2}\left(\log(4\pi\mu_{IR}^2)-\frac{\gamma_E}{2}\right)\right]\;.\end{aligned} \tag{A.80}$$

The real part is obtained by applying the dispersion relation. Only the following integral is needed:

$$\frac{1}{\pi}\int_0^\infty ds'\,\frac{s'^{-1+\varepsilon_{IR}/2}}{s'-s-i\epsilon} \;=\; -\frac{1}{\pi}\frac{1}{s}\left[\frac{2}{\varepsilon_{IR}}+\log(s)-i\pi\right]\;+\;O(\varepsilon_{IR})\;, \tag{A.81}$$

leading to

$$\begin{aligned}\Re e[-iI_{4S}(k,p_1,q,k_{1(2)})] \;&=\; \frac{1}{8\pi^2 s}\,\frac{1}{U(T)}\log\left(\frac{U(T)}{m_e m_\pi}\right)\\ &\quad\times\left[-\frac{2}{\varepsilon_{IR}}+\log\left(\frac{4\pi\mu_{IR}^2}{s}\right)-\gamma_E\right]\;.\end{aligned} \tag{A.82}$$

### A.4.2 The Rank 1 Tensor Box

The rank 1 tensor box will be solved by using tensor reduction. Making the substitution $k=p_1+K$ leads to

$$I_{4V}^\alpha(k,p_1,q,k_1) \;=\; p_1^\alpha I_{4S}(k,p_1,q,k_1)+J_{4V}^\alpha(p_1,k_1)\qquad\text{with} \tag{A.83}$$

$$\begin{aligned}J_{4V}^\alpha(p_1,k_1) \;&:=\; \mu^{4-n}\int\frac{d^nK}{(2\pi)^n}\left\{\frac{K^\alpha}{[(p_1+K)^2+i\epsilon][K^2-m_e^2+i\epsilon]}\right.\\ &\quad\left.\times\;\frac{1}{[(p_2-K)^2+i\epsilon][(p_1-k_1+K)^2-m_\pi^2+i\epsilon]}\right\}\;.\end{aligned}$$

It is now apparent that due to momentum conservation the following symmetries hold:

$$I_{4S}(k,p_1,q,k_1) \;=\; I_{4S}(k,-p_2,q,-k_2)\;, \tag{A.84}$$

$$J_{4V}^\alpha(p_1,k_1) \;=\; J_{4V}^\alpha(-p_2,-k_2)\;. \tag{A.85}$$

Let us choose a set of three linear independent 4 vectors:

$$q = p_1 + p_2 \,, \quad P_p = p_1 - p_2 \,, \quad P_k = k_1 - k_2 \,, \tag{A.86}$$

$$\text{with} \quad qP_p = qP_k = 0 \,, \quad P_pP_k = t - u \,, \tag{A.87}$$

$$q^2 = s \,, \quad P_p^2 = -s + 4m_e^2 \,, \quad P_k^2 = -s + 4m_\pi^2 \,.$$

Note that under the transformation $(p_1, k_1) \leftrightarrow (-p_2, -k_2)$ being equivalent to the combined transformation

$$q \rightarrow -q \quad , \quad P_p \rightarrow P_p \quad , \quad P_k \rightarrow P_k \tag{A.88}$$

all possible scalars that can be formed by contracting two 4-vectors are invariant. As a consequence the integrals $J^\alpha_{4V}(p_1, k_{1(2)})$ cannot have a contribution proportional to $q^\alpha$. One can therefore make the following general ansatz:

$$J^\alpha_{4V}(p_1, k_1) \equiv \int \frac{d^nk}{(2\pi)^n} \frac{-p_1^\alpha + k^\alpha}{D_k D_{p_1} D_q D_{k_1}} = a_{P_p} P_p^\alpha + a_{P_k} P_k^\alpha \,. \tag{A.89}$$

Using the following identities

$$P_{p\alpha}(-p_1 + k)^\alpha = -2m_e^2 - D_{p_1} + \frac{1}{2}D_q + \frac{1}{2}D_k \,, \tag{A.90}$$

$$P_{k\alpha}(-p_1 + k)^\alpha = -\frac{s + t - u}{2} - D_{k_1} + \frac{1}{2}D_q + \frac{1}{2}D_k \,, \tag{A.91}$$

and contracting eq. (A.89) successively with $P_{p\alpha}$ and $P_{k\alpha}$ yields the following two equations for $a_{P_p}$ and $a_{P_k}$:

$$\begin{aligned} a_{P_p}(-s\beta_e^2) + a_{P_k}(t - u) &= -2m_e^2 \, I_{4S}(k_1) - I_{3S}(k, q, k_1) \\ &\quad + I_{3S}(k, p_1, k_1) \,, \end{aligned} \tag{A.92}$$

$$\begin{aligned} a_{P_p}(t - u) + a_{P_k}(-s\beta_\pi^2) &= -\frac{s + t - u}{2} \, I_{4S}(k_1) - I_{3S}(k, p_1, q) \\ &\quad + I_{3S}(k, p_1, k_1) \,, \end{aligned} \tag{A.93}$$

which have the following solution:

$$\begin{aligned} a_{P_p} &= -\frac{1}{2}\frac{1}{(t-u)^2 - s^2\beta_\pi^2} \left[ I_{4S}(k_1)(t-u)(s+t-u) \right. \\ &\quad -2I_{3S}(k, p_1, k_1)(s\beta_\pi^2 + t - u) + 2I_{3S}(k, p_1, q)(t-u) \\ &\quad \left. + 2I_{3S}(k, q, k_1)s\beta_\pi^2 \right] \,, \end{aligned} \tag{A.94}$$

$$\begin{aligned} a_{P_k} &= -\frac{1}{2}\frac{1}{(t-u)^2 - s^2\beta_\pi^2} \left[ I_{4S}(k_1)s(s+t-u) \right. \\ &\quad +2I_{3S}(k, q, k_1)(t-u) - 2I_{3S}(k, p_1, k_1)(s+t-u) \\ &\quad \left. + \; 2I_{3S}(k, p_1, q)s \right] \,. \end{aligned} \tag{A.95}$$

Here the electron mass has been neglected where possible. $I^\alpha_{4V}$ is now expressed in terms of the scalar integrals that have been calculated before. Thus all relevant integrals have been calculated.

# Appendix B

# The Soft Photon Integrals

The IS, FS and IFS soft photon correction factors $\delta^S_{ini}$, $\delta^S_{fin}$ and $\delta^S_{int}$ are going to be calculated in dimensional regularization ($n = 4+\varepsilon_{IR}$). They are IR divergent in the limit $\varepsilon_{IR} \to 0$.

The IS soft photon correction factor reads [see eq. (3.24)]:

$$\delta^S_{ini}(s,\Lambda) \;=\; e^2\,\mu_{IR}^{n-4}\int_{soft}\frac{d^{n-1}k}{2|\vec{k}|(2\pi)^{n-1}}\left[\frac{s-2m_e^2}{(p_1k)(p_2k)}-\frac{m_e^2}{(p_1k)^2}-\frac{m_e^2}{(p_2k)^2}\right]. \quad \text{(B.1)}$$

The soft photon integral in eq. (B.1) is IR divergent for $n = 4$ and is therefore regularized by using dimensional regularization, thus by switching from 4 to $n = 4+\varepsilon_{IR}$ dimensions. We can now write the integral in polar coordinates:

$$\int_{soft}\frac{d^{n-1}k}{2|\vec{k}|(2\pi)^{n-1}}\,\mu_{IR}^{4-n} = \int_0^\Lambda \frac{\mu_{IR}^{4-n}}{2|\vec{k}|(2\pi)^{n-1}}\,d|\vec{k}|\;|\vec{k}|^{n-2}\int d\Omega_{n-1}\,, \quad \text{(B.2)}$$

with the angular contribution

$$\begin{aligned}\int d\Omega_{n-1} &= \int_0^{2\pi}d\phi\int_0^\pi d\theta_1\;\sin\theta_1\int_0^\pi d\theta_2\;\sin^2\theta_2\ldots\int_0^\pi d\theta_{n-3}\;\sin^{n-3}\theta_{n-3}\\ &= \int d\Omega_{n-2}\int_{-1}^{+1}d\cos\theta_{n-3}\;(1-\cos^2\theta_{n-3})^{n/2-2}\,. \quad \text{(B.3)}\end{aligned}$$

In the CMS the integrand is only depending on one polar angle which will be identified with the photon polar angle ($\theta_{n-3} \equiv \theta_\gamma$). The relevant scalar products are

$$p_1k \;=\; |\vec{k}|\frac{\sqrt{s}}{2}(1-\beta_e\cos\theta_\gamma)\,, \quad \text{(B.4)}$$

$$p_2k \;=\; |\vec{k}|\frac{\sqrt{s}}{2}(1+\beta_e\cos\theta_\gamma)\,. \quad \text{(B.5)}$$

The integral over $d\Omega_{n-2}$ has the following solution:

$$\int d\Omega_{n-2} = \frac{2\pi^{n/2-1}}{\Gamma(n/2-1)}\,, \quad \text{(B.6)}$$

which allows us to write the phase space integration as an integration over the absolute of the photon 3-momentum and an integration over one polar angle:

$$\begin{aligned}\int \frac{d^{n-1}k}{2|\vec{k}|(2\pi)^{n-1}} &= \frac{2\pi^{n/2-1}}{\Gamma(n/2-1)} \int \frac{1}{2(2\pi)^{n-1}}\, d|\vec{k}|\ |\vec{k}|^{n-3} \\ &\times \int_{-1}^{+1} d\cos\theta_\gamma\ (1-\cos^2\theta_\gamma)^{n/2-2}\ . \end{aligned} \tag{B.7}$$

Thus in dimensional regularization the soft photon factor becomes

$$\begin{aligned}\delta^S_{ini}(s,\Lambda,\varepsilon_{IR}) &= e^2\, \frac{2\pi^{1+\varepsilon_{IR}/2}}{\Gamma(1+\varepsilon_{IR}/2)} \int_0^\Lambda \frac{\mu_{IR}^{-\varepsilon_{IR}}}{2(2\pi)^{3+\varepsilon_{IR}}}\, d|\vec{k}|\ |\vec{k}|^{1+\varepsilon_{IR}} \\ &\times \int_{-1}^{+1} d\cos\theta_\gamma\ (1-\cos^2\theta_\gamma)^{\varepsilon_{IR}/2}\ \left[\frac{s-2m_e^2}{(p_1k)(p_2k)} - \frac{m_e^2}{(p_1k)^2} - \frac{m_e^2}{(p_2k)^2}\right]\ . \end{aligned} \tag{B.8}$$

First the (IR finite) angular integral will be calculated. For this we expand in $\varepsilon_{IR}$ ($c \equiv \cos\theta_\gamma$):

$$\begin{aligned}(1-c^2)^{\varepsilon_{IR}/2} &= 1 + \frac{\varepsilon_{IR}}{2}\log(1-c^2) + O(\varepsilon_{IR}^2) \\ &= 1 + \frac{\varepsilon_{IR}}{2}\Big[\log(1-c) + \log(1+c)\Big] + O(\varepsilon_{IR}^2)\ . \end{aligned} \tag{B.9}$$

Using the method of Feynman parameters for the first term in the soft photon integral leads to:

$$\frac{s-2m_e^2}{(p_1k)(p_2k)} = \frac{4(s-2m_e^2)}{s|\vec{k}|^2} \int_0^1 dx\ \frac{1}{\left[1+(1-2x)\beta_e c\right]^2}\ , \tag{B.10}$$

$$\frac{m_e^2}{(p_1k)^2} = \frac{4}{|\vec{k}|^2}\frac{m_e^2}{s}\ \frac{1}{\left[1-\beta_e c\right]^2}\ , \tag{B.11}$$

$$\frac{m_e^2}{(p_2k)^2} = \frac{4}{|\vec{k}|^2}\frac{m_e^2}{s}\ \frac{1}{\left[1+\beta_e c\right]^2}\ . \tag{B.12}$$

Therefore the integrations are of the form:

$$\int_{-1}^{+1} dc\ \frac{1}{(1+\eta c)^2} \quad \text{and} \quad \int_{-1}^{+1} dc\ \frac{\log(1\pm c)}{(1+\eta c)^2}\ , \tag{B.13}$$

which have the following the solutions:

$$\int_{-1}^{+1} dc\ \frac{1}{(1+\eta c)^2} = \frac{2}{1-\eta^2}\ , \tag{B.14}$$

$$\int_{-1}^{+1} dc\ \frac{\log(1\pm c)}{(1+\eta c)^2} = \frac{2\log 2}{1-\eta^2} - \frac{1}{\eta}\frac{1}{1\mp\eta}\log\left(\frac{1+\eta}{1-\eta}\right)\ . \tag{B.15}$$

For the first term of the soft photon integral, containing both $p_1$ and $p_2$, we have $\eta = (1-2x)\beta_e$. This yields:

$$\int_{-1}^{1} d\cos\theta_\gamma \, (1-\cos^2\theta_\gamma)^{\varepsilon_{IR}/2} \, \frac{s-2m_e^2}{(p_1k)(p_2k)} \;=\; \frac{2(s-2m_e^2)}{s\beta_e|\vec{k}|^2}$$
$$\times \int_{-\beta_e}^{\beta_e} d\eta \, \left\{ \frac{2}{1-\eta^2} \, [1+\varepsilon_{IR}\log 2] - \varepsilon_{IR} \, \frac{1}{1-\eta^2} \, \frac{1}{\eta} \, \log\left(\frac{1+\eta}{1-\eta}\right) \right\} . \quad \text{(B.16)}$$

The first integral in (B.16) is easy to calculate and yields

$$\int_{-\beta_e}^{+\beta_e} d\eta \, \frac{2}{1-\eta^2} = 2\log\left(\frac{1+\beta_e}{1-\beta_e}\right) . \quad \text{(B.17)}$$

For the second integration it is convenient to make the substitution

$$u = \frac{1+\eta}{1-\eta} \quad \Rightarrow \quad \eta = \frac{u-1}{u+1} , \quad \text{(B.18)}$$

leading to

$$\int_{-\beta_e}^{+\beta_e} d\eta \, \frac{\log\left(\frac{1+\eta}{1-\eta}\right)}{\eta(1-\eta^2)} = \frac{1}{2} \int_{\frac{1-\beta_e}{1+\beta_e}}^{\frac{1+\beta_e}{1-\beta_e}} du \, \frac{u+1}{u-1} \, \frac{\log(u)}{u} = \left( \int_1^{\frac{1-\beta_e}{1+\beta_e}} du \right.$$
$$\left. - \int_1^{\frac{1+\beta_e}{1-\beta_e}} du \right) \, \frac{\log(u)}{1-u} = 2\mathrm{Li}_2\left(\frac{2\beta_e}{1+\beta_e}\right) + \frac{1}{2}\log^2\left(\frac{1+\beta_e}{1-\beta_e}\right) . \quad \text{(B.19)}$$

With these results we arrive at

$$\int_{-1}^{1} d\cos\theta_\gamma \, (1-\cos^2\theta_\gamma)^{\varepsilon_{IR}/2} \, \frac{s-2m_e^2}{(p_1k)(p_2k)} = \frac{4(s-2m_e^2)}{s\beta_e|\vec{k}|^2} \left\{ \log\left(\frac{1+\beta_e}{1-\beta_e}\right) \right.$$
$$\left. + \frac{\varepsilon_{IR}}{2} \left[ 2\log(2)\log\left(\frac{1+\beta_e}{1-\beta_e}\right) - \frac{1}{2}\log^2\left(\frac{1+\beta_e}{1-\beta_e}\right) - 2\mathrm{Li}_2\left(\frac{2\beta_e}{1+\beta_e}\right) \right] \right\} . \quad \text{(B.20)}$$

The remaining angular integrals in eq. (B.16) yield

$$\int_{-1}^{1} d\cos\theta_\gamma \, (1-\cos^2\theta_\gamma)^{\varepsilon_{IR}/2} \, \frac{m_e^2}{(p_{1,2}k)^2}$$
$$= \frac{2}{|\vec{k}|^2} \, \left\{ 1 + \frac{\varepsilon_{IR}}{2} \left[ 2\log 2 - \frac{1}{\beta_e} \log\left(\frac{1+\beta_e}{1-\beta_e}\right) \right] \right\} . \quad \text{(B.21)}$$

Collecting the solutions for all three angular integrations finally leads to

$$\begin{aligned}
&\int_{-1}^{+1} d\cos\theta_\gamma\,(1-\cos^2\theta_\gamma)^{\varepsilon_{IR}/2}\,\left[\frac{s-2m_e^2}{(p_1k)(p_2k)}-\frac{m_e^2}{(p_1k)^2}-\frac{m_e^2}{(p_2k)^2}\right]\\
&=\frac{4}{|\vec{k}|^2}\Bigg\{\left[-1+\frac{s-2m_e^2}{s\beta_e}\,\log\left(\frac{1+\beta_e}{1-\beta_e}\right)\right]\left[1+\frac{\varepsilon_{IR}}{2}\,2\log 2\right]\\
&+\frac{\varepsilon_{IR}}{2}\left[\frac{1}{\beta_e}\,\log\left(\frac{1+\beta_e}{1-\beta_e}\right)-\frac{s-2m_e^2}{s\beta_e}\,\frac{1}{2}\,\log^2\left(\frac{1+\beta_e}{1-\beta_e}\right)\right.\\
&\left.-2\,\frac{s-2m_e^2}{s\beta_e}\,\mathrm{Li}_2\left(\frac{2\beta_e}{1+\beta_e}\right)\right]\Bigg\}\,. \qquad \text{(B.22)}
\end{aligned}$$

What remains is the evaluation of the (in four spacetime dimensions) IR divergent part of the soft photon correction factor being a consequence of the integration over $|\vec{k}|$ in eq. (B.2). It can be solved by using now the definition of the Euler beta function:

$$B(m,n)=\int_0^1 dx\;x^{m-1}(1-x)^{n-1}=\frac{\Gamma(m)\Gamma(n)}{\Gamma(m+n)}\,. \qquad \text{(B.23)}$$

We then find

$$\begin{aligned}
\int_0^\Lambda d|\vec{k}|\;|\vec{k}|^{-1+\varepsilon_{IR}} &= (\Lambda)^{\varepsilon_{IR}}\int_0^1 dx\;x^{-1+\varepsilon_{IR}}\\
&= \left[1+\varepsilon_{IR}\log(\Lambda)+O(\varepsilon_{IR}^2)\right]\,\frac{\Gamma(\varepsilon_{IR})\Gamma(1)}{\Gamma(1+\varepsilon_{IR})}\\
&= \frac{1}{\varepsilon_{IR}}+\log(\Lambda)+O(\varepsilon_{IR})\,. \qquad \text{(B.24)}
\end{aligned}$$

For the last equality in (B.24) the expansion in $\varepsilon_{IR}$ has been carried out. Expanding also the remaining factors in $\varepsilon_{IR}$ and inserting the results into eq. (B.8) finally yields

$$\begin{aligned}
\delta_{ini}^S(s,\Lambda) \;\equiv\; &\frac{\alpha}{\pi}\,\left\{\left[-1+\frac{s-2m_e^2}{s\beta_e}\,\log\left(\frac{1+\beta_e}{1-\beta_e}\right)\right]\right.\\
\times\;&\left[\frac{2}{\varepsilon_{IR}}+\log\left(\frac{\Lambda^2}{4\pi\mu_{IR}^2}\right)+\gamma_E+2\log 2\right]+\frac{1}{\beta_e}\,\log\left(\frac{1+\beta_e}{1-\beta_e}\right) \qquad \text{(B.25)}\\
&\left.-\frac{s-2m_e^2}{s\beta_e}\,\frac{1}{2}\,\log^2\left(\frac{1+\beta_e}{1-\beta_e}\right)-2\,\frac{s-2m_e^2}{s\beta_e}\,\mathrm{Li}_2\left(\frac{2\beta_e}{1+\beta_e}\right)\right\}\quad .
\end{aligned}$$

Since the final state soft photon integral is obtained by replacing $p_1$ and $p_2$ by $k_1$ and $k_2$ respectively, replacing $m_e$ by $m_\pi$ and $\beta_e$ by $\beta_\pi$ immediately yields the final state correction factor:

$$\delta_{fin}^S(s,\Lambda) \;=\; \delta_{ini}^S(s,\Lambda,m_e\to m_\pi,\beta_e\to\beta_\pi)\,. \qquad \text{(B.26)}$$

Consider now the soft photon IFS correction factor [$U = p_1k_1$, $T = p_1k_2$, $u = (p_1 - k_1)^2$, $t = (p_1 - k_2)^2$]:

$$\begin{aligned}
\delta^S_{int} &= e^2\,\mu_{IR}^{4-n}\int_{soft}\frac{d^{n-1}k}{2|\vec{k}|(2\pi)^{n-1}}\left\{U\left[\frac{1}{(p_1k)(k_1k)}+\frac{1}{(p_2k)(k_2k)}\right]\right.\\
&- \left. T\left[\frac{1}{(p_1k)(k_2k)}+\frac{1}{(p_2k)(k_1k)}\right]\right\}\\
&= 2e^2\,\frac{\pi^{n/2-1}\mu_{IR}^{4-n}}{\Gamma(n/2-1)}\int_0^\Lambda\frac{d|\vec{k}||\vec{k}|^{n-3}}{(2\pi)^{n-1}}\int_{-1}^1 d\cos\theta_\gamma\,(1-\cos^2\theta_\gamma)^{n/2-2}\\
&\times \left\{\frac{U}{(p_1k)(k_1k)}-\frac{T}{(p_1k)(k_2k)}\right\}\,. \qquad \text{(B.27)}
\end{aligned}$$

Let us begin with the calculation of the integral containing $p_1$ and $k_2$. It is convenient to rewrite the corresponding integrand in the following way:

$$\frac{1}{(p_1k)(k_2k)} = \int_0^1 da\frac{1}{(P_{12a}k)^2}\,, \quad \text{with} \quad P_{12a} = ap_1 + (1-a)k_2\,, \qquad \text{(B.28)}$$

In the center of mass system ($\vec{p}_1 + \vec{p}_2 = 0$) we get

$$\begin{aligned}
P^0_{12a} &= \frac{\sqrt{s}}{2}\,, \quad P^2_{12a} = a^2m_e^2 + (1-a)^2m_\pi^2 + a(1-a)2p_1k_2\,,\\
\beta^2_{12a} &= \frac{|\vec{P}_{12a}|}{(P^0_{12a})^2} = 1 - \frac{4}{s}\left[a^2m_e^2 + (1-a)^2m_\pi^2 + a(1-a)2p_1k_2\right]\,. \qquad \text{(B.29)}
\end{aligned}$$

Let us choose now $\vec{P}_{12a}$ to point in the $z$-direction and $\vec{k}$ in the $x-z$-plane, forming the angle $\theta_\gamma$ with the $z$-axis ($n = 4 + \varepsilon_{IR}$, $c \equiv \cos\theta_\gamma$). This yields

$$\begin{aligned}
\int_{-1}^1 dc\,\frac{(1-c^2)^{n/2-2}}{(p_1k)(k_2k)} &= \frac{4}{s|\vec{k}|^2}\int_0^1 da\int_{-1}^1 dc\,\frac{(1-c^2)^{n/2-2}}{(1-\beta_{12a}c)^2}\\
&= \frac{4}{s|\vec{k}|^2}\int_0^1 da\int_{-1}^1 dc\,\frac{1+\frac{\varepsilon_{IR}}{2}\log(1-c^2)}{(1-\beta_{12a}c)^2}\,, \qquad \text{(B.30)}\\
\int_{-1}^1 dc\,\frac{1}{(1-\beta_{12a}c)^2} &= \frac{2}{1-\beta^2_{12a}}\,, \qquad \text{(B.31)}\\
\int_{-1}^1 dc\,\frac{\log(1-c^2)}{(1-\beta_{12a}c)^2} &= \frac{4\log(2)}{1-\beta^2_{12a}} - \frac{1}{\beta_{12a}}\frac{2}{1-\beta^2_{12a}}\log\left(\frac{1+\beta_{12a}}{1-\beta_{12a}}\right)\,. \qquad \text{(B.32)}
\end{aligned}$$

With the definition

$$a_{1,2} = \frac{t - m_e^2 + m_\pi^2}{2t} \pm \frac{\sqrt{\lambda(t, m_e^2, m_\pi^2)}}{2t}\,, \qquad \text{(B.33)}$$

we can write

$$1 - \beta^2_{12a} = \frac{4t}{s}(a - a_1)(a - a_2)\,. \qquad \text{(B.34)}$$

This allows us to solve the first of the two integrals in (B.31) and (B.32). With

$$\begin{aligned}\frac{1}{1-\beta_{12a}^2} &= \frac{s}{4t}\,\frac{1}{a_1-a_2}\left(\frac{1}{a-a_1}-\frac{1}{a-a_2}\right)\\ &= \frac{s}{4\sqrt{\lambda(t,m_e^2,m_\pi^2)}}\left(\frac{1}{a-a_1}-\frac{1}{a-a_2}\right)\,,\end{aligned}\tag{B.35}$$

a simple integration yields

$$\int_0^1 da\,\frac{1}{1-\beta_{12a}^2} = \frac{s}{4\sqrt{\lambda(t,m_e^2,m_\pi^2)}}\log\left[\frac{-t+m_e^2+m_\pi^2+\sqrt{\lambda(t,m_e^2,m_\pi^2)}}{-t+m_e^2+m_\pi^2-\sqrt{\lambda(t,m_e^2,m_\pi^2)}}\right]\,.\tag{B.36}$$

Before evaluating the second integration over $a$ let us calculate the remaining angular-independent integral in (B.27) ($n=4+\varepsilon_{IR}$):

$$\frac{\pi^{n/2-1}\mu_{IR}^{4-n}}{\Gamma(n/2-1)}\int_0^\Lambda \frac{d|\vec{k}||\vec{k}|^{n-5}}{(2\pi)^{n-1}} = \frac{1}{16\pi^2}\left[\frac{2}{\varepsilon_{IR}}+\gamma_E+\log\frac{\Lambda^2}{4\pi\mu_{IR}^2}\right]\,.\tag{B.37}$$

Note that the calculation of the second integral in (B.27) (with $p_1$ and $k_1$ in the denominator of the integrand) is analogous to the previous calculation. Collecting the results finally leads to the IFS correction factor:

$$\begin{aligned}\delta_{int}^S &= \frac{\alpha}{\pi}\left[\frac{2}{\varepsilon_{IR}}+\gamma_E+\log\left(\frac{\Lambda^2}{4\pi\mu_{IR}^2}\right)\right]\left\{\frac{U}{\sqrt{\lambda(u,m_e^2,m_\pi^2)}}\right.\\ &\quad\times\log\left[\frac{-u+m_e^2+m_\pi^2+\sqrt{\lambda(u,m_e^2,m_\pi^2)}}{-u+m_e^2+m_\pi^2-\sqrt{\lambda(u,m_e^2,m_\pi^2)}}\right]\Big[1+\varepsilon_{IR}\log(2)\Big]\\ &\quad\left.-\frac{\varepsilon_{IR}}{2}F(u)\right\}\;-\;(u,U\to t,T)\\ &\simeq \frac{\alpha}{\pi}\left\{2\log\left(\frac{-u+m_\pi^2}{-t+m_\pi^2}\right)\left[\frac{2}{\varepsilon_{IR}}+\gamma_E+\log\left(\frac{\Lambda^2}{\pi\mu_{IR}^2}\right)\right]\right.\\ &\qquad\left.-F(u)+F(t)\right\}\,,\end{aligned}\tag{B.38}$$

where the function $F(x)$ ($x=u,t$) is the IR finite expression

$$F(x) = \frac{2U}{s}\int_0^1 da\,\frac{1}{\beta_{12a}(x)}\frac{2}{1-\beta_{12a}^2(x)}\log\left[\frac{1+\beta_{12a}(x)}{1-\beta_{12a}(x)}\right]\,.\tag{B.39}$$

To solve this integral let us define:

$$A = -\frac{4x}{s}+i\epsilon\quad,\quad B = -\frac{4(x-m_e^2+m_\pi^2)}{s}+i\epsilon\quad,\quad C = \beta_\pi^2\,.\tag{B.40}$$

We can then make the following substitutions:

$$\begin{aligned} \beta_{12a}(x) \;=\; \sqrt{Aa^2 - Ba + C} \;&=\; -\sqrt{A}\,a + z \\ \Longrightarrow \quad a \;=\; \frac{z^2 - C}{2\sqrt{A}\,z - B} \quad &, \quad \beta_{12a}(x) \;=\; \frac{\sqrt{A}\,z^2 - B\,z + \sqrt{A}\,C}{2\sqrt{A}\,z - B}\,. \end{aligned} \tag{B.41}$$

Defining further

$$\begin{aligned} \eta \;&=\; \frac{B}{2\sqrt{A}} - i\epsilon \quad , \quad z_{1,2} \;=\; \eta \pm \sqrt{\eta^2 - 1} \mp i\epsilon\,, \\ z_{3,4} \;\equiv\; \kappa_{1,2} \;&=\; -1 + \eta \pm \sqrt{1 + \eta^2 - c} + i\epsilon \\ &=\; -1 + \frac{1}{\sqrt{-sx}}\left[-x + m_e^2 - m_\pi^2 \pm \sqrt{\lambda(x, m_e^2, m_\pi^2)}\right]\,, \\ z_{5,6} \;\equiv\; \kappa_{3,4} \;&=\; 1 + \eta \pm \sqrt{1 + \eta^2 - C} - i\epsilon \\ &=\; 1 + \frac{1}{\sqrt{-sx}}\left[-x + m_e^2 - m_\pi^2 \pm \sqrt{\lambda(x, m_e^2, m_\pi^2)}\right]\,, \end{aligned} \tag{B.42}$$

leads to

$$\begin{aligned} \beta_{12a} \;&=\; \frac{1}{2}\frac{(z - z_1)(z - z_2)}{z - \eta}\,, \\ 1 + \beta_{12a} \;&=\; \frac{1}{2}\frac{(z - z_3)(z - z_4)}{z - \eta}\,,\; 1 - \beta_{12a} \;=\; -\frac{1}{2}\,\frac{(z - z_5)(z - z_6)}{z - \eta}\,, \\ da \;&=\; +\frac{1}{\sqrt{A}}\,\frac{\beta_{12a}}{z - \eta}\,dz\,, \\ z(a = 0) \;&=\; \sqrt{C} \;=\; \beta_\pi\,, \\ z(a = 1) \;&=\; \sqrt{A + B + C} + \sqrt{A} \;=\; \beta_e + 2\sqrt{-\frac{x}{s}}\,. \end{aligned} \tag{B.43}$$

We finally arrive at the following expression for $F(x)$:

$$\begin{aligned} F(x) \;&=\; \int_{\beta_\pi}^{\beta_e + 2\sqrt{-\frac{t}{s}}} d\kappa \left\{ \left[\frac{1}{\kappa - \kappa_1} - \frac{1}{\kappa - \kappa_2} - \frac{1}{\kappa - \kappa_3} + \frac{1}{\kappa - \kappa_4}\right] \right. \\ &\times \quad \left. \left[\log(\kappa - \kappa_1) + \log(\kappa - \kappa_2) - \log(\kappa_3 - \kappa) - \log(\kappa - \kappa_4)\right] \right\}\,. \end{aligned} \tag{B.44}$$

This leads to a sum of different log's and dilog's. One has to keep in mind that

$\kappa_3 > \kappa_4 > \kappa_1 > \kappa_2$. With $\kappa_i = \kappa_i(x)$ $(x = u, t)$ we obtain

$$\begin{aligned} F(x) &= \Big( \Big[ f_1(z_3) - f_1(z_4) - f_1(z_6) + f_2(z_5) - f_3(z_3, z_4) - f_3(z_6, z_3) \\ &+ f_3(z_6, z_4) + f_4(z_4, z_3) + f_4(z_3, z_6) + f_4(z_4, z_6) - f_5(z_5, z_3) \\ &+ f_5(z_5, z_4) - f_5(z_5, z_6) - f_6(z_3, z_5) - f_6(z_4, z_5) + f_6(z_6, z_5) \Big] \Big) \\ &= \Big[ f_1(\kappa_1) - f_1(\kappa_2) - f_1(\kappa_4) + f_2(\kappa_3) - f_3(\kappa_1, \kappa_2) - f_3(\kappa_4, \kappa_1) \\ &+ f_3(\kappa_4, \kappa_2) + f_4(\kappa_2, \kappa_1) + f_4(\kappa_1, \kappa_4) + f_4(\kappa_2, \kappa_4) - f_5(\kappa_3, \kappa_1) \\ &+ f_5(\kappa_3, \kappa_2) - f_5(\kappa_3, \kappa_4) - f_6(\kappa_1, \kappa_3) - f_6(\kappa_2, \kappa_3) + f_6(\kappa_4, \kappa_3) \Big] , \end{aligned} \tag{B.45}$$

with

$$f_1(\eta) = \frac{1}{2} \log^2[b - \eta] - \frac{1}{2} \log^2[a - \eta] , \tag{B.46}$$

$$f_2(\eta) = \frac{1}{2} \log^2[\eta - a] - \frac{1}{2} \log^2[\eta - b] , \tag{B.47}$$

$$\begin{aligned} f_3(\eta_1, \eta_2) &= -\mathrm{Li}_2 \left[ \frac{(b-a)(\eta_1 - \eta_2)}{(b - \eta_1)(a - \eta_2)} \right] + \mathrm{Li}_2 \left( -\frac{b-a}{a - \eta_2} \right) \\ &+ \mathrm{Li}_2 \left( \frac{b-a}{b - \eta_1} \right) + \log(b - \eta_1) \log \left( \frac{b - \eta_2}{a - \eta_2} \right) , \end{aligned} \tag{B.48}$$

$$\begin{aligned} f_4(\eta_1, \eta_2) &= \mathrm{Li}_2 \left[ \frac{(b-a)(\eta_2 - \eta_1)}{(b - \eta_2)(a - \eta_1)} \right] - \mathrm{Li}_2 \left( -\frac{b-a}{a - \eta_1} \right) \\ &- \mathrm{Li}_2 \left( \frac{b-a}{b - \eta_2} \right) + \log(a - \eta_1) \log \left( \frac{b - \eta_2}{a - \eta_2} \right) , \end{aligned} \tag{B.49}$$

$$\begin{aligned} f_5(\eta_1, \eta_2) &= \log[\eta_1 - \eta_2] \log \left( \frac{b - \eta_2}{a - \eta_2} \right) + \mathrm{Li}_2 \left( \frac{a - \eta_2}{\eta_1 - \eta_2} \right) \\ &- \mathrm{Li}_2 \left( \frac{b - \eta_2}{\eta_1 - \eta_2} \right) , \end{aligned} \tag{B.50}$$

$$\begin{aligned} f_6(\eta_1, \eta_2) &= \log[\eta_2 - \eta_1] \log \left( \frac{\eta_2 - b}{\eta_2 - a} \right) + \mathrm{Li}_2 \left( \frac{\eta_2 - a}{\eta_2 - \eta_1} \right) \\ &- \mathrm{Li}_2 \left( \frac{\eta_2 - b}{\eta_2 - \eta_1} \right) , \end{aligned} \tag{B.51}$$

$$a = \beta_\pi(s) , \quad b(x) = \beta_e + 2\sqrt{-\frac{x}{s}} , \tag{B.52}$$

$$\kappa_{1,2}(x) = -1 + \frac{1}{\sqrt{-sx}} \left[ -x + m_e^2 - m_\pi^2 \pm \sqrt{\lambda(x, m_e^2, m_\pi^2)} \right] , \tag{B.53}$$

$$\kappa_{3,4}(x) = 1 + \frac{1}{\sqrt{-sx}} \left[ -x + m_e^2 - m_\pi^2 \pm \sqrt{\lambda(x, m_e^2, m_\pi^2)} \right] , \tag{B.54}$$

$$\lambda(A, B, C) = A^2 + B^2 + C^2 - 2AB - 2AC - 2BC . \tag{B.55}$$

# Appendix C

# Phase-Space Integration

The phase-space integration corresponding to a 3-particle final state as needed for the numerical integration procedure of the A$\phi\rho\omega$DITE program will be considered. Let us begin with the 2-particle phase-space integration.

## C.1 2-Particle Phase-Space

Consider a scattering process leading to a 2-particle final state with the 4-momenta $k_1$ and $k_2$ ($q = k_1 + k_2$, $s = q^2$) which are chosen in the center of mass system of particle 1 and 2:

$$k_1 = E_1(1, \beta_1 \sin\theta, 0, \beta_1 \cos\theta) \ , \ k_2 = E_2(1, -\beta_2 \sin\theta, 0, -\beta_2 \cos\theta) \ ,$$
$$q = \sqrt{s}\ (1,0,0,0) \ , \quad \text{with} \quad \beta_{1,2} = \sqrt{1 - \frac{m_{1,2}^2}{E_{1,2}^2}} \ .$$

For the subsequent phases-pace calculations it is convenient to use a Lorentz-invariant expression for the velocities $\beta_{1,2}$. Using energy and momentum conservation,

$$E_1 + E_2 = \sqrt{s} \ , \quad E_1\beta_1 - E_2\beta_2 = 0 \ , \tag{C.1}$$

a straight forward calculation yields

$$\beta_{1,2} = \frac{\sqrt{\lambda(s, m_1^2, m_2^2)}}{2\sqrt{s}\ E_{1,2}} \ , \quad \text{with} \quad E_{1.2} = \frac{\sqrt{s}}{2} + \frac{m_{1,2}^2 - m_{2,1}^2}{2\sqrt{s}} \tag{C.2}$$
$$\text{and} \qquad \lambda(a,b,c) = a^2 + b^2 + c^2 - 2ab - 2ac - 2bc \ .$$

Using this Lorentz invariant expression for $\beta_{1,2}$ we obtain for the two particle phase-space integral

$$\begin{aligned} Ph_2 &= \int \frac{d^3k_1}{2E_1}\,\frac{d^3k_2}{2E_2}\,\delta^4(q-k_1-k_2)\,\ldots \\ &= \int \frac{d^3k_1}{2E_1}\,d^4k_2\,\delta(k_2^2-m_2^2)\,\delta^4(q-k_1-k_2)\,\ldots \\ &= \int \frac{d^3k_1}{2E_1}\,\delta(q^2-2k_1q+m_1^2-m_2^2)\,\ldots \\ &= \int d|\vec{k}_1|\,\frac{|\vec{k}_1|^2}{2E_1}\,d\Omega\,\delta(s-2\sqrt{s}E_1+m_1^2-m_2^2)\,\ldots \\ &= \int \beta_1\,dE_1\,\frac{E_1}{2}\,d\Omega\,\frac{1}{2\sqrt{s}}\,\delta(E_1-\frac{\sqrt{s}}{2}-\frac{m_1^2-m_2^2}{2\sqrt{s}})\,\ldots \\ &= \beta_1\,\frac{E_1}{2}\int d\Omega\,\frac{1}{2\sqrt{s}}\,\ldots\,=\,\frac{\sqrt{\lambda(s,m_1^2,m_2^2)}}{8s}\int d\Omega\,\ldots\,. \end{aligned} \tag{C.3}$$

Here $\Omega$ is the solid angle of particle 1 in a center of mass system of particle 1 and particle 2. For equal masses ($m_1 = m_2 = m$) we get

$$\begin{aligned} &\lambda(s,m^2,m^2) = s(s-4m^2),\ E_1 = E_2 = \sqrt{s}/2\ , \\ &\beta_1 = \beta_2 = \sqrt{1-\frac{4m^2}{s}}\ , \\ \Longrightarrow\qquad &\int \frac{d^3k_1}{2E_1}\,\frac{d^3k_2}{2E_2}\,\delta^4(q-k_1-k_2)\cdots = \frac{1}{8}\,\sqrt{1-\frac{4m^2}{s}}\,\int d\Omega\ldots\,. \end{aligned} \tag{C.4}$$

## C.2 3- and 4-Particle Phase-Space

The 3-particle phase-space integration is needed e.g. for $\pi^+\pi^-$ pair production including one radiated photon. $k_1$, $k_2$ can then be identified with the momenta of the two pions, $k_3 = k$ with the momentum of the bremsstrahlung photon. It turns out to be useful to express the 3-particle phase-space integral

$$Ph_3 \;=\; \int \frac{d^3k_1}{2E_1}\,\frac{d^3k_2}{2E_2}\,\frac{d^3k_3}{2E_3}\,\delta^4(q-k_1-k_2-k_3)\ldots \tag{C.5}$$

in terms of two Lorentz-invariant 2-particle phase-space integrations and a subsequent integration over the invariant mass of the sub-system of particle 1 and 2, $s_{12} = q_{12}^2 = (k_1+k_2)^2$. We can easily obtain such an expression by inserting the following identities

$$\mathbf{1} = \int d^4q_{12}\,\delta^4(q_{12}-k_1-k_2) \quad\text{and}\quad \mathbf{1} = \int ds_{12}\,\delta(s_{12}-q_{12}^2) \tag{C.6}$$

into eq. (C.5). This yields

$$\begin{aligned} Ph_3 &= \int \frac{d^3k_1}{2E_1}\,\frac{d^3k_2}{2E_2}\,\frac{d^3k_3}{2E_3}\,d^4q_{12}\,ds_{12}\,\delta^4(q_{12}-k_1-k_2)\,\delta(s_{12}-q_{12}^2) \\ &\qquad\qquad \times \delta^4(q-k_1-k_2-k_3)\,\ldots \\ &= \int ds_{12}\int \frac{d^3k_3}{2E_3}\,\frac{d^3q_{12}}{2q_{12}^0}\,\delta^4(q-q_{12}-k_3) \\ &\quad \times \int \frac{d^3k_1}{2E_1}\,\frac{d^3k_2}{2E_2}\,\delta^4(q_{12}-k_1-k_2)\,\ldots\,. \end{aligned} \tag{C.7}$$

The phase-space integrations can now conveniently be carried out in the center of mass system of the corresponding 2-particle sub-systems.

The procedure of dividing up the phase-space integrals into subsequent 2-particle phase-space integrations can be generalized to arbitrary n-particle final states. Let us finally give the result for the 4-particle phase space:

$$\begin{aligned} Ph_4 &= \int \frac{d^3k_1}{2E_1}\,\frac{d^3k_2}{2E_2}\,\frac{d^3k_3}{2E_3}\,\frac{d^3k_4}{2E_4}\,\delta^4(q-k_1-k_2-k_3-k_4)\,\ldots \\ &= \int ds_{12}\int ds_{34}\int \frac{d^3q_{12}}{2q_{12}^0}\,\frac{d^3q_{34}}{2q_{34}^0}\,\delta^4(q-q_{12}-q_{34}) \\ &\times \int \frac{d^3k_1}{2E_1}\,\frac{d^3k_2}{2E_2}\,\delta^4(q_{12}-k_1-k_2)\int \frac{d^3k_3}{2E_3}\,\frac{d^3k_4}{2E_4}\,\delta^4(q_{34}-k_3-k_4)\,\ldots\,, \end{aligned} \tag{C.8}$$

where $q_{ij}=k_i+k_j$ and $s_{ij}=q_{ij}^2$.

## C.3 A $2\to 3$ process

Consider now the scattering of two particles into a 3-particle final state $[a_1(p_1)+a_2(p_2)\to a_3(p_3)+a_4(p_4)+a_5(p_5)]$. Here we assume that the initial state particles $a_1$ and $a_2$ have equal masses ($m_1=m_2$) which is true for $e^+e^-$-collision experiments.

### C.3.1 $L_1$-frame: $\vec{p}_1$ pointing up

Let us define the laboratory system $L_1$ to be the center of mass system of the initial state particles $a_1$ and $a_2$ ($\vec{p}_1+\vec{p}_2=0$) with the momentum $\vec{p}_1$ of particle $a_1$ pointing into the positive $z$-direction. Using eq. (C.2) we obtain the corresponding 4-momenta of $a_1$ and $a_2$:

$$p_1^{L_1} = \left(\sqrt{s}/2,0,0,pp_1\right)\,,\quad p_2^{L_1} = \left(\sqrt{s}/2,0,0,-pp_1\right)\,,\ \text{where} \tag{C.9}$$

$$pp_1 = \frac{\sqrt{\lambda(s,m_1^2,m_1^2)}}{2\sqrt{s}}\,,\quad s=q^2\,,\quad q\equiv p_1+p_1=(\sqrt{s},0,0,0)\,. \tag{C.10}$$

The momentum $\vec{p}_3$ of particle $a_3$ is chosen in the x-z plane:

$$p_3^{L_1} = (\sqrt{pp_3^2 + m_3^2}, pp_3 \sin\theta_{13}^L, 0, pp_3 \cos\theta_{13}^L) \text{ , where} \tag{C.11}$$

$$pp_3 = \frac{\sqrt{\lambda(s, s_{45}, m_3^2)}}{2\sqrt{s}} , \quad s_{45} = q_{45}^2 , \quad q_{45} = p_4 + p_5 , \tag{C.12}$$

$$q_{45}^{L_1} = (\sqrt{pp_3^2 + s_{45}}, -pp_3 \sin\theta_{13}^L, 0, -pp_3 \cos\theta_{13}^L) . \tag{C.13}$$

Another interesting frame will be the CMS system of particle 4 and 5 (denoted by $*$). Here the spatial components of $q_{45}$ vanish:

$$q_{45}^* = (\sqrt{s_{45}}, 0, 0, 0) . \tag{C.14}$$

We will now try to find a Lorentz transformation from the laboratory frame $L_1$ to the *-frame:

$$q_{45}^{0*} = \gamma(q_{45}^{0L_1} - \hat{n}\vec{q}_{45}^{L_1}\beta) , \tag{C.15}$$

$$\vec{q}_{45}^{*} = \vec{q}_{45}^{L_1} + \hat{n} \left[ (\gamma - 1)(\hat{n}\vec{q}_{45}^{L_1}) - q_{45}^{0L_1}\gamma\beta \right] . \tag{C.16}$$

$\hat{n}$ is a unit vector pointing into the boost direction and $\beta$ and $\gamma = (1 - \beta^2)^{-1/2}$ are the usual boost parameters. From a comparison of eq. (C.16) and eq. (C.14) follows immediately that $\hat{n}$ has to be parallel to $\vec{q}_{45}^{L_1}$. Hence

$$\vec{q}_{45}^{L_1} = -\hat{n}pp_3 = -\vec{p}_3^{L_1} , \quad \hat{n} = (\sin\theta_{13}^L, 0, \cos\theta_{13}^L) , \tag{C.17}$$

$$pp_3 = \left[ -(\gamma - 1)pp_3 - \sqrt{pp_3^2 + s_{45}}\gamma\beta \right] , \tag{C.18}$$

leading to

$$\beta = -\frac{pp_3}{\sqrt{pp_3^2 + s_{45}}} , \quad \gamma = \frac{\sqrt{pp_3^2 + s_{45}}}{\sqrt{s_{45}}} , \tag{C.19}$$

which are Lorentz invariant functions of $s_{45}$. As a check, inserting these results into eq. (C.15) leads to

$$q_{45}^{0*} = \sqrt{s_{45}} . \tag{C.20}$$

The Lorentz transformation is now determined and the momenta that are known in the laboratory frame can easily be transformed into the *-frame:

$$
\begin{aligned}
p_1^{0*} &= \gamma \left(\frac{s}{2} - pp_1\beta\cos\theta_{13}^L\right) , && \text{(C.21)}\\
\vec{p}_1^{\,*} &= \vec{p}_1 + \hat{n} \left[ (\gamma-1)(\hat{n}\vec{p}_1) - p_1^0\gamma\beta \right] \\
&= (0,0,pp_1) + (\sin\theta_{13}^L, 0, \cos\theta_{13}^L) \left[ (\gamma-1)\cos\theta_{13}^L pp_1 - \frac{\sqrt{s}}{2}\gamma\beta \right] , && \text{(C.22)}\\
p_2^{0*} &= \gamma \left( \frac{s}{2} + pp_1\beta\cos\theta_{13}^L \right) , && \text{(C.23)}\\
\vec{p}_2^{\,*} &= \vec{p}_2 + \hat{n} \left[ (\gamma-1)(\hat{n}\vec{p}_2) - p_2^0\gamma\beta \right] = (0,0,-pp_1) \\
&+ (\sin\theta_{13}^L, 0, \cos\theta_{13}^L) \left[ -(\gamma-1)\cos\theta_{13}^L pp_1 - \frac{\sqrt{s}}{2}\gamma\beta \right] , && \text{(C.24)}\\
p_3^{0*} &= \gamma \left( \sqrt{pp_3^2 + m_3^2} - pp_3\beta \right) , && \text{(C.25)}\\
\vec{p}_3^{\,*} &= \hat{n}\gamma \left[ pp_3 - \sqrt{pp_3^2 + m_3^2}\,\gamma\beta \right] \\
&= (\sin\theta_{13}^L, 0, \cos\theta_3)\,\gamma \left[ pp_3 - \sqrt{pp_3^2 + m_3^2}\,\gamma\beta \right] . && \text{(C.26)}
\end{aligned}
$$

This Lorentz boost can be written as a $4 \times 4$ matrix:

$$
\Lambda_{1\nu}^{\mu} = \begin{pmatrix}
\gamma & -\sin\theta_{13}^L\gamma\beta & 0 & -\cos\theta_{13}^L\gamma\beta \\
-\sin\theta_{13}^L\gamma\beta & 1+(\gamma-1)\sin^2\theta_{13}^L & 0 & (\gamma-1)\sin\theta_{13}^L\cos\theta_{13}^L \\
0 & 0 & 1 & 0 \\
-\cos\theta_{13}^L\gamma\beta & (\gamma-1)\sin\theta_{13}^L\cos\theta_{13}^L & 0 & 1+(\gamma-1)\cos^2\theta_{13}^L
\end{pmatrix} . \quad \text{(C.27)}
$$

The inverse boost (from the *-frame back to the $L_1$-frame) is given by

$$
\left(\Lambda_1^{-1}\right)^{\mu}{}_{\nu} = \begin{pmatrix}
\gamma & \sin\theta_{13}^L\gamma\beta & 0 & \cos\theta_{13}^L\gamma\beta \\
\sin\theta_{13}^L\gamma\beta & 1+(\gamma-1)\sin^2\theta_{13}^L & 0 & (\gamma-1)\sin\theta_{13}^L\cos\theta_{13}^L \\
0 & 0 & 1 & 0 \\
\cos\theta_{13}^L\gamma\beta & (\gamma-1)\sin\theta_{13}^L\cos\theta_{13}^L & 0 & 1+(\gamma-1)\cos^2\theta_{13}^L
\end{pmatrix} . \quad \text{(C.28)}
$$

In a next step the vectors in the *-frame are turned around the y axis by the angle $\theta_{13}^L$ (this frame will be denoted by $c$). As a result $\vec{p}_3$ is now pointing into the $z$-direction. The corresponding rotation matrix is given by

$$
\Lambda_{2\nu}^{\mu} = \begin{pmatrix}
1 & 0 & 0 & 0 \\
0 & \cos\theta_{13}^L & 0 & -\sin\theta_{13}^L \\
0 & 0 & 1 & 0 \\
0 & +\sin\theta_{13}^L & 0 & \cos\theta_{13}^L
\end{pmatrix} \quad \text{(C.29)}
$$

and its inverse reads

$$\left(\Lambda_2^{-1}\right)^{\mu}{}_{\nu} = \begin{pmatrix} 1 & 0 & 0 & 0 \\ 0 & \cos\theta_{13}^L & 0 & +\sin\theta_{13}^L \\ 0 & 0 & 1 & 0 \\ 0 & -\sin\theta_{13}^L & 0 & \cos\theta_{13}^L \end{pmatrix} . \tag{C.30}$$

The combined transformation $\Lambda_3$ is defined as

$$\Lambda_{3\nu}^{\mu} = \Lambda_{2\rho}^{\mu}\Lambda_{1\nu}^{\rho} = \begin{pmatrix} \gamma & -\sin\theta_{13}^L\gamma\beta & 0 & -\cos\theta_{13}^L\gamma\beta \\ 0 & \cos\theta_{13}^L & 0 & -\sin\theta_{13}^L \\ 0 & 0 & 1 & 0 \\ -\gamma\beta & \gamma\sin\theta_{13}^L & 0 & \gamma\cos\theta_{13}^L \end{pmatrix} \tag{C.31}$$

and its inverse reads

$$\left(\Lambda_3^{-1}\right)^{\mu}{}_{\nu} = \begin{pmatrix} \gamma & 0 & 0 & \gamma\beta \\ \sin\theta_{13}^L\gamma\beta & \cos\theta_{13}^L & 0 & \gamma\sin\theta_{13}^L \\ 0 & 0 & 1 & 0 \\ \cos\theta_{13}^L\gamma\beta & -\sin\theta_{13}^L & 0 & \gamma\cos\theta_{13}^L \end{pmatrix} . \tag{C.32}$$

### C.3.2 $L_3$-frame: $\vec{p}_3$ pointing up

Now $\vec{p}_3$ is chosen to point into the positive $z$-direction while the initial state momenta are now chosen in the $x$-$z$ plane. Let us call this the $L_3$-frame. This laboratory frame can be obtained from the $L_1$-frame by the rotation $\Lambda_2$ around the $y$ axis:

$$\begin{aligned} p_1^{L_3} &= \left(\sqrt{s}/2, -pp_1\sin\theta_{13}^L, 0, pp_1\cos\theta_{13}^L\right) , \\ p_2^{L_3} &= \left(\sqrt{s}/2, pp_1\sin\theta_{13}^L, 0, -pp_1\cos\theta_{13}^L\right) , \\ p_3^{L_3} &= \left(\sqrt{pp_3^2+m_3^2}, 0, 0, pp_3\right) , \; q_{45}^{L_3} = \left(\sqrt{pp_3^2+s_{45}}, 0, 0, -pp_3\right) . \end{aligned} \tag{C.33}$$

This coordinate system appears to be much easier since the boost direction is now the z axis [$\hat{n} = (0,0,1)$]. $\beta$ and $\gamma$ are the same as before. Now we can boost immediately from the laboratory system to the $c$-frame without any additional rotation. The boost is given by

$$\Lambda_{4\nu}^{\mu} = \begin{pmatrix} \gamma & 0 & 0 & -\gamma\beta \\ 0 & 1 & 0 & 0 \\ 0 & 0 & 1 & 0 \\ -\gamma\beta & 0 & 0 & \gamma \end{pmatrix} . \tag{C.34}$$

Its inverse reads

$$\left(\Lambda_4^{-1}\right)^{\mu}{}_{\nu} = \begin{pmatrix} \gamma & 0 & 0 & +\gamma\beta \\ 0 & 1 & 0 & 0 \\ 0 & 0 & 1 & 0 \\ +\gamma\beta & 0 & 0 & \gamma \end{pmatrix} . \tag{C.35}$$

Hence the momenta in the $c$-frame are related to the corresponding momenta in the $L_3$-frame in the following way:

$$p^{c\mu} \;=\; \Lambda^{\mu}_{4\nu}\, p^{L_3\nu}\;,\; p^{L_3\mu} \;=\; \left(\Lambda_4^{-1}\right)^{\mu}_{\ \nu}\, p^{c\nu}\;. \tag{C.36}$$

Obviously the rotation $\Lambda_2$ followed by the boost $\Lambda_4$ is just the Lorentz transformation $\Lambda_3$:

$$\Lambda^{\mu}_{4\rho}\Lambda^{\rho}_{2\nu} = \Lambda^{\mu}_{3\nu} = \Lambda^{\mu}_{2\rho}\Lambda^{\rho}_{1\nu}\;. \tag{C.37}$$

### C.3.3 Phase-Space Integration

At first we will focus on two inertial systems: the $L_3$-frame and the $c$-frame which can be reached from the $L_3$-frame by the Lorentz boost $\Lambda_4$. In both frames $\vec{p}_3$ is pointing into the $z$-direction and the vectors $\vec{p}_1$ and $\vec{p}_2$ are in the $x$-$z$ plane. In the $c$-frame we have

$$\begin{aligned} q^c_{45} &= (\sqrt{s_{45}}, 0, 0, 0)\;, \\ p^c_4 &= (\sqrt{pp_4^2 + m_4^2}, pp_4 \sin\theta^c_{34}\cos\phi_{34}, pp_4 \sin\theta^c_{34}\sin\phi_{34}, pp_4\cos\theta^c_{34})\;, \\ p^c_5 &= q^c_{45} - p^c_4\;, \end{aligned} \tag{C.38}$$

where

$$pp_4 = \frac{\sqrt{\lambda(s_{45}, m_4^2, m_5^2)}}{2\sqrt{s_{45}}}\;. \tag{C.39}$$

Note that the azimuthal angles are not altered by the Lorentz boost $\Lambda_4$ ($\phi^c_{34} = \phi^L_{34}$). In a $2 \to 3$ process we have four non-trivial phase-space integrations corresponding to four phase-space variables. They are chosen to be[1] $s_{45}$, $\theta^L_{13}$, $\theta^L_{34}$ and $\phi_{34}$. The strategy will be the following: as shown before [see eq. (C.5)] the 3-particle phase-space integral is divided up into two 2-particle phase-space integrals and one integration over $s_{45}$. Then suitable coordinate systems are chosen which are the center of mass

[1] For experimental purposes it is convenient to choose all angles in the laboratory system. The convention is the following: $\theta^L_{ij}$ and $\theta^c_{ij}$ is the angle between the momenta $\vec{p}_i$ and $\vec{p}_j$ of particle $a_i$ and $a_j$ in the laboratory system and the center of mass system respectively.

systems of the 2-particle sub-systems ($L_3$ and $c$):

$$\begin{aligned}
\sigma &= \frac{1}{F}\int \frac{d^3p_3}{(2\pi)^3 2E_3}\frac{d^3p_4}{(2\pi)^3 2E_4}\frac{d^3p_5}{(2\pi)^3 2E_5} \\
&\quad \times (2\pi)^4\,\delta^4(p_1+p_2-p_3-p_4-p_5)\,\overline{|\mathcal{M}|}^2 \\
&= \frac{1}{(2\pi)^5 F}\int ds_{45}\int \frac{d^3p_3}{2E_3}\frac{d^3q_{45}}{2E_{45}}\delta^4(q-p_3-q_{45}) \\
&\quad \times \int \frac{d^3p_4}{2E_4}\frac{d^3p_5}{2E_5}\delta^4(q_{45}-p_4-p_5)\,\overline{|\mathcal{M}|}^2 \\
&= \frac{1}{(2\pi)^4 F}\int ds_{45} f_\lambda \int d\cos\theta_{13}^L \int d\Omega_{34}^c\,\overline{|\mathcal{M}|}^2\ , \\
\text{with}\quad F &= 4\sqrt{s}\,pp_1\ , \quad f_\lambda = \frac{\sqrt{\lambda(s,s_{45},m_3^2)}}{8s}\,\frac{\sqrt{\lambda(s_{45},m_4^2,m_5^2)}}{8s_{45}}\ . \qquad \text{(C.40)}
\end{aligned}$$

In a next step the boost $\Lambda_4^{-1}$ has to be applied to transform particle 4 from the $c$-frame to the-$L_3$ frame. Recall that all integration angles are wanted the $L_3$ frame. Since $p_4^{L_3} = \Lambda_4^{-1}p_4^c$ is still a function of $\theta_{34}^c$, one has to express $\theta_{34}^c$ in terms of $\theta_{34}^L$ which is the angle between $p_3^{L_3}$ and $p_4^{L_3}$ (remember that $\phi_{34}^L = \phi_{34}^c$). Then we can replace $d\Omega_{34}^c$ by $d\Omega_{34}^L$:

$$\int d\Omega_4^c = \int d\phi_{34}\,d\cos\theta_{34}^c = \int d\phi_{34}\,\frac{\partial\cos\theta_{34}^c}{\partial\cos\theta_{34}^L}\,d\cos\theta_{34}^L\ . \qquad \text{(C.41)}$$

Using the expression for $\Lambda_4^{-1}$ in eq. (C.35) and $p_4^c$ in eq. (C.38) yields

$$\begin{aligned}
p_4^{L_3} &= (\gamma\sqrt{pp_4^2+m_4^2}+\gamma\beta pp_4\cos\theta_{34}^c, pp_4\sin\theta_{34}^c\cos\phi_{34}, \qquad \text{(C.42)}\\
&\quad pp_4\sin\theta_{34}^c\sin\phi_{34}, \gamma\beta\sqrt{pp_4^2+m_4^2}+\gamma pp_4\cos\theta_{34}^c)\ .
\end{aligned}$$

We can now determine the polar angle $\theta_{34}^L$ in the laboratory system as a function of the corresponding polar angle in the $c$-frame:

$$\cos\theta_{34}^L = \frac{(p_4^{L_3})_z}{|\vec{p}_4^{L_3}|} = \frac{\gamma\beta\sqrt{pp_4^2+m_4^2}+\gamma pp_4\cos\theta_{34}^c}{\left[pp_4^2(1-\cos\theta_{34}^{c2})+(\gamma\beta\sqrt{pp_4^2+m_4^2}+\gamma pp_4\cos\theta_{34}^c)^2\right]^{1/2}}. \qquad \text{(C.43)}$$

What is actually needed is $\cos\theta_{34}^c$ as a function of $\cos\theta_{34}^L$. So the above equation has to be inverted leading to a quadratic equation in $\cos\theta_{34}^c$ which has the solution

$$\begin{aligned}
\cos\theta_{34}^c &= \frac{-\gamma^2\beta\sqrt{pp_4^2+m_4^2}(1-\cos^2\theta_{34}^L)}{pp_4[\gamma^2(1-\cos^2\theta_{34}^L)+\cos^2\theta_{34}^L]} \\
&\quad \pm \left[\frac{\cos^2\theta_{34}^L[pp_4^2-\gamma^2\beta^2m_4^2(1-\cos^2\theta_{34}^L)]}{pp_4^2\left[\gamma^2(1-\cos^2\theta_{34}^L)+\cos^2\theta_{34}^L\right]^2}\right]^{1/2}\ . \qquad \text{(C.44)}
\end{aligned}$$

The difficulty is now to decide when the plus sign and when the minus sign in front of the square root has to be applied. In fact there are two different cases:

**1.** $\cos\theta_{34}^L$ is running from $-1$ to 1 when $\cos\theta_{34}^c$ is running from $-1$ to 1. This is true when the parameter

$$num_1 := \gamma\beta\sqrt{pp_4^2 + m_4^2} + \gamma pp_4 > 0\,. \tag{C.45}$$

**2.** $\cos\theta_{34}^L$ is running from $-1$ to $-1$ when $\cos\theta_{34}^c$ is running from $-1$ to 1 with an intermediate maximum at

$$\cos\theta_{34}^L = \cos\tilde{\theta}_{34}^L \equiv -\sqrt{1 - \frac{pp_4^2}{\gamma^2\beta^2 m_4^2}}\,, \tag{C.46}$$

which is always $< 0$. This is the case when

$$num_1 \;=\; \gamma\beta\sqrt{pp_4^2 + m_4^2} + \gamma pp_4 < 0\,. \tag{C.47}$$

Eq. (C.46) can be obtained by demanding

$$\frac{\partial\cos\theta_{34}^L}{\partial\cos\theta_{34}^c} \;=\; 0\,, \tag{C.48}$$

which yields

$$\cos\tilde{\theta}_{34}^c \;=\; -\frac{pp_4}{\beta\sqrt{pp_4^2 + m_4^2}} \quad \text{with} \quad |\beta| \;>\; \frac{pp_4}{\sqrt{pp_4^2 + m_4^2}}\,. \tag{C.49}$$

From $num_1 < 0$ follows that $\beta < 0$. Hence

$$\beta \;<\; -\frac{pp_4}{\sqrt{pp_4^2 + m_4^2}}\,. \tag{C.50}$$

It may be checked that $-pp_4^2 + \gamma^2\beta^2 m_4^2 > 0$. Inserting now the expression for $\cos\tilde{\theta}_{34}^c$ in eq. (C.49) into eq. (C.43) and using the above relations yields the expression for $\cos\tilde{\theta}_{34}^L$ in eq. (C.46).

Note that if $\gamma\beta\sqrt{pp_4^2 + m_4^2} + \gamma pp_4 = 0$ then $\cos\tilde{\theta}_{34}^L = 0$ and if $\gamma\beta\sqrt{pp_4^2 + m_4^2} + \gamma pp_4 > 0$ (case 1) then $\cos\tilde{\theta}_{34}^L \notin \Re$ and is therefore not defined. This is consistent with the expectation since only for case 2 an intermediate maximum exists.

For case 1 $\cos\theta_{34}^c$ is a monotonous function of $\cos\theta_{34}^L$ with $\cos\theta_{34}^c(\cos\theta_{34}^L = \pm 1) = \pm 1$. Therefore the second term in eq. (C.44) has to flip sign when going from $\cos\theta_{34}^L = -1$ to $+1$. Since that term vanishes for $\cos\theta_{34}^L = 0$ this has to be the point of the flip. Hence the $\pm$ sign has to be replaced by $-1 + 2\Theta(\cos\theta_{34}^L)$ where $\Theta$ is the Heavyside

step function. Equivalently one overall term $\cos\theta_{34}^L$ can be pulled outside the square root bracket leading to

$$\begin{aligned}\cos\theta_{34}^c &= \frac{-\gamma^2\beta\sqrt{pp_4^2+m_4^2}(1-\cos^2\theta_{34}^L)}{pp_4[\gamma^2(1-\cos^2\theta_{34}^L)+\cos^2\theta_{34}^L]} \\ &+ \cos\theta_{34}^L\left[\frac{pp_4^2-\gamma^2\beta^2m_4^2(1-\cos^2\theta_{34}^L)}{pp_4^2\left[\gamma^2(1-\cos^2\theta_{34}^L)+\cos^2\theta_{34}^L\right]^2}\right]^{1/2}. \qquad \text{(C.51)}\end{aligned}$$

For case 2 $\cos\theta_{34}^c$ is not an ordinary function of $\cos\theta_{34}^L$ since then eq. (C.43) cannot simply be inverted. Now to a given laboratory angle there exist two different center of mass angles corresponding to the cases + and − in eq. (C.44). When integrating a function $f(\cos\theta_{34}^c)$ we get

$$\begin{aligned}\int_{-1}^{1} d\cos\theta_{34}^c\ f(\cos\theta_{34}^c) &= \left(\int_{-1}^{\cos\tilde{\theta}_{34}^c}+\int_{\cos\tilde{\theta}_{34}^c}^{1}\right) d\cos\theta_{34}^c\ f(\cos\theta_{34}^c) \\ = \int_{-1}^{\cos\tilde{\theta}_{34}^L} d\cos\theta_{34}^L &\left(\frac{\partial\cos\theta_{34}^L}{\partial\cos\theta_{34}^c}\right)_-^{-1} f(-) \\ + \int_{\cos\tilde{\theta}_{34}^L}^{-1} d\cos\theta_{34}^L &\left(\frac{\partial\cos\theta_{34}^L}{\partial\cos\theta_{34}^c}\right)_+^{-1} f(+) \\ = \int_{-1}^{\cos\tilde{\theta}_{34}^L} d\cos\theta_{34}^L &\left\{\left[\left(\frac{\partial\cos\theta_{34}^L}{\partial\cos\theta_{34}^c}\right)^{-1} f\right]_- - \left[\left(\frac{\partial\cos\theta_{34}^L}{\partial\cos\theta_{34}^c}\right)^{-1} f\right]_+\right\}, \qquad \text{(C.52)}\end{aligned}$$

where '+' and '−' correspond to the signs in eq. (C.44) for $\cos\theta_{34}^c$. For case 2 the boost from the $c$-frame to the laboratory system produces a momentum flip for a particle flying in boost direction in the $c$-frame. As a consequence in the laboratory frame a part of the angular phase-space is empty. Note that for massless particles only case 1 exists which simplifies the situation a lot.

To obtain the Jacobian $\Delta_L^c$ corresponding to the boost from the $c$-frame to the $L_3$-frame it is more convenient to use eq. (C.43) rather than eq. (C.44) since the expression for the Jacobian in terms of $\cos\theta_{34}^c$ is much shorter than in terms of $\cos\theta_{34}^L$ (the relationship between $\cos\theta_{34}^c$ and $\cos\theta_{34}^L$ is known anyway):

$$\begin{aligned}\Delta_L^c &= \frac{\partial\cos\theta_{34}^c}{\partial\cos\theta_{34}^L} = \frac{1}{\frac{\partial\cos\theta_{34}^L}{\partial\cos\theta_{34}^c}} \\ &= \frac{\left[pp_4^2(1-\cos^2\theta_{34}^c)+\gamma^2\left(pp_4\cos\theta_{34}^c+\beta\sqrt{pp_4^2+m_4^2}\right)^2\right]^{3/2}}{\gamma pp_4^2\left(pp_4+\beta\sqrt{pp_4^2+m_4^2}\cos\theta_{34}^c\right)}. \qquad \text{(C.53)}\end{aligned}$$

Until now the calculation has been completely general. No masses for the final state particles $a_1$, $a_2$ and $a_3$ have been assumed. Now we choose particle 4 and 5 to have

equal masses (e.g. $a_4 = \pi^-$, $a_5 = \pi^+$) and particle 3 is assumed to be massless (e.g. $a_3 = \gamma$). The lower and the upper limit of the $s_{45}$ integral in eq. (C.40) is then $4m_4^2$ and $s$ respectively. Let us now define the function

$$\begin{aligned} f_{\text{cut}} &= \Theta\left[s_{45} - \text{lcut}(s_{45})\right] \times \Theta\left[\text{ucut}(s_{45}) - s_{45}\right] \\ &\times \prod_{i\neq j}\Big\{\Theta\left[\cos\theta_{ij} + \text{cut}(\cos\theta_{ij})\right] \times \Theta\left[\text{cut}(\cos\theta_{ij}) - \cos\theta_{ij}\right]\Big\} \end{aligned} \tag{C.54}$$

which is 0 if $|\cos\theta_{ij}| > \text{cut}(\theta_{ij})$ (for any $i, j \in \{1,2,3,4,5\}$) or $s_{45} < \text{lcut}(s_{45})$ or $s_{45} > \text{ucut}(s_{45})$ and 1 otherwise. Hence by convoluting the phase-space integration with $f_{\text{cut}}$ allows us to apply arbitrary kinematical cuts. We can then write the cross section (with cuts) as

$$\begin{aligned} \sigma &= \frac{1}{(2\pi)^4 F}\int_{4m_4^2}^{s} ds_{45} f_\lambda \int_{-1}^{1} d\cos\theta_{13}^L \int_0^{2\pi} d\phi_{34} \\ &\times \int_{-1}^{1} d\cos\theta_{34}^L \Big\{ f_{\text{cut}}\ \Theta(num_1)\ \Delta_L^c\ \overline{|\mathcal{M}|}^2 + \Theta(-num_1) \\ &\times\Theta(\cos\tilde{\theta}_{34}^L - \cos\theta_{34}^L)\Big[(\Delta_L^c\ \overline{|\mathcal{M}|}^2\ f_{\text{cut}})_- - (\Delta_L^c\ \overline{|\mathcal{M}|}^2\ f_{\text{cut}})_+\Big]\Big\}\ . \end{aligned} \tag{C.55}$$

As before the indices '$-$' and '$+$' correspond to the cases '$-$' and '$+$' in eq. (C.44) respectively. Rotating the $L_3$-momenta by applying $\Lambda_2^{-1}$ [see eq. (C.30)] brings us from the $L_3$-frame to the $L_1$-frame with the momentum $\vec{p}_1$ pointing into the $z$-direction. Since the Jacobian of a rotation is 1 ($\int d\cos\theta_{34} d\phi_{34} \cdots = \int d\cos\theta_{14} d\phi_{14} \ldots$) we only have to express the $L_3$-variables in terms of the $L_1$-variables:

$$\cos\theta_{34}^L = \sin\theta_{13}^L \sin\theta_{14}^L \cos\phi_{14}^L + \cos\theta_{13}^L \cos\theta_{14}^L \tag{C.56}$$

$$\phi_{34} = \arcsin\left[\frac{\sin\theta_{14}^L \sin\phi_{14}^L}{\sin\theta_{34}^L}\right]\ . \tag{C.57}$$

Eq. (C.55) is just the expression which is needed to obtain the differential cross sections or the total cross section with arbitrary kinematical cuts as discussed in chapter 4.

## C.4 Tensor Integration

In eq. (4.24) the squared matrix elements corresponding to the real photon IS, FS and IFS interference corrections to the process $e^-(p_1) + e^+(p_2) \to \pi^-(k_1)\pi^+(k_2)\gamma(k)$ were written as contractions of two tensors respectively: an initial state tensor $E_{\mu\nu\ldots\tau}$ containing the initial state momenta $p_{1,2}^\mu$ and the scalar products $p_{1,2}k$ and a final state tensor $F^{\mu\nu\ldots\tau}$ containing the final state momenta $k_{1,2}^\mu$ and the scalar products $k_{1,2}k$. If we are only interested in the total cross section $\sigma$ or the spectral function $d\sigma/ds'$ ($s' = q'^2$, $q' = k_1 + k_2$) without angular cuts, it appears to be convenient

to use tensor integration for the evaluation of the phase space integral. For this purpose the 3-particle phase space integral is written in the form of eq. (C.7):

$$\begin{aligned} \sigma &= \frac{1}{(2\pi)^5 F} \int ds' \int \frac{d^3k}{2E_\gamma} \frac{d^3q'}{2q'^0}\, \delta^4(q-k-q') \\ &\quad \times \int \frac{d^3k_1}{2E_3} \frac{d^3k_2}{2E_4}\, \delta^4(q'-k_1-k_2)\, \overline{|\mathcal{M}|}^2 \\ \text{with} \quad F &= 4\sqrt{s}\, pp_1 \;=\; 2s\beta_e\;, \quad \beta_e := \sqrt{1-\frac{4m_e^2}{s}}\;. \end{aligned} \tag{C.58}$$

Now we proceed in two steps: first we integrate $F^{\mu\nu\ldots\tau}$ over the momenta $k_1$ and $k_2$ in the $\pi^+\pi^-$ center of mass system where we use a frame in which the photon momentum $\vec{k}$ is pointing into $z$-direction. This frame will be denoted by CMS. Then we contract the integrated tensor $\mathcal{F}^{\mu\nu\ldots\tau}$ with the initial state tensor $E_{\mu\nu\ldots\tau}$ and carry out the remaining integration over the photon angle in the laboratory system $L$. Since we want to integrate over the momenta $k_1$ and $k_2$ completely the integration over the azimuthal angle becomes trivial, leading to an overall factor $2\pi$. What remains is the integration over the polar angle $\theta_\pi$ between the negatively charged pion and the photon in the CMS. We can therefore write [see eq. (C.40)]

$$\begin{aligned} \sigma &= \frac{\beta'_\pi}{16(4\pi)^3} \frac{s-s'}{s^2} \int ds' \int_L d\cos\theta_\gamma \int_{\text{CMS}} d\cos\theta_\pi\, \overline{|\mathcal{M}|}^2\;, \\ \text{with} \quad \beta'_\pi &\equiv \beta_\pi(s') = \sqrt{1-\frac{4m_\pi^2}{s'}}\;. \end{aligned} \tag{C.59}$$

Thus we have two different Lorentz frames in which the phase space integrations are carried out. The first frame denoted by $L$ is the laboratory system which is the center of mass system of the initial state electron and positron, with the electron momentum $\vec{p}_1$ pointing into the positive $z$-direction. The photon momentum is chosen in the x-z-plane forming an angle $\theta_\gamma$ with the z-axis:

$$\begin{aligned} L: \quad q &= p_1+p_2 \;=\; (\sqrt{s},0,0,0)\;, \quad p_1 \;=\; \frac{\sqrt{s}}{2}\,(1,0,0,\beta_e)\;. \\ k &= pp_\gamma\,(1,\sin\theta_\gamma,0,\cos\theta_\gamma)\;, \quad pp_\gamma \;=\; \frac{\sqrt{\lambda(s,s',0)}}{2\sqrt{s}} = \frac{s-s'}{2\sqrt{s}}\;. \end{aligned} \tag{C.60}$$

The second frame (CMS) is the center of mass system of the two pions with the photon flying in the direction of the positive z-axis and the pion momenta in the x-z-plane with the polar angle $\theta_\pi$:

$$\begin{aligned} \text{CMS}: \quad q' &= (\sqrt{s'},0,0,0)\;, \quad k \;=\; pp_{\gamma_C}\,(1,0,0,1)\;, \\ k_1 &= \frac{\sqrt{s'}}{2}(1,\beta'_\pi\sin\theta_\pi,0,\beta'_\pi\cos\theta_\pi)\;, \\ pp_{\gamma_C} &= pp_\gamma\,(\gamma-\gamma\beta)\;. \end{aligned} \tag{C.61}$$

Here $\beta$ and $\gamma = 1/\sqrt{(1-\beta^2)}$ are the boost variables for the Lorentz transformation

$$(\Lambda_a)^{\mu}{}_{\nu} \;=\; \begin{pmatrix} \gamma & -\sin\theta_\gamma\gamma\beta & 0 & -\cos\theta_\gamma\gamma\beta \\ 0 & \cos\theta_\gamma & 0 & -\sin\theta_\gamma \\ 0 & 0 & 1 & 0 \\ -\gamma\beta & \gamma\sin\theta_\gamma & 0 & \gamma\cos\theta_\gamma \end{pmatrix} \tag{C.62}$$

of a 4-vector from the $L$- to the CMS-frame [see eq. (C.19)]:

$$\begin{aligned} \beta \;&=\; -\frac{pp_\gamma}{\sqrt{pp_\gamma^2+s'}} \;=\; -\frac{s-s'}{s+s'}\,, \quad \gamma \;=\; \frac{\sqrt{pp_\gamma^2+s'}}{\sqrt{s'}} \;=\; \frac{s+s'}{2\sqrt{ss'}} \\ \Longrightarrow\; pp_{\gamma_C} \;&=\; pp_\gamma\sqrt{\frac{s}{s'}} \;=\; \frac{s-s'}{2\sqrt{s'}}\,. \end{aligned} \tag{C.63}$$

Consider now the integration of the final state tensor over the pion pair 2-particle phase space:

$$\mathcal{F}^{\mu\nu\ldots\tau} \;=\; \int \frac{d^3k_1}{2E_3}\frac{d^3k_2}{2E_4}\;\delta^4(q'-k_1-k_2)\;F^{\mu\nu\ldots\tau}(k_1^\mu,k_2^\mu,k_1k,k_2k)\,. \tag{C.64}$$

Obviously $\mathcal{F}^{\mu\nu\ldots\tau}$ can be written as the sum over tensors of the following kind:

$$\begin{aligned} I^{\mu\nu\ldots\tau} \;&=\; \int \frac{d^3k_1}{2E_3}\frac{d^3k_2}{2E_4}\;\delta^4(q'-k_1-k_2)\;k_{1(2)}^\mu k_{1(2)}^\nu\ldots k_{1(2)}^\tau\;f(k_1k,k_2k) \\ &=\; \int \frac{d^3k_1}{2E_3}\;\delta(s'-2k_1q')\;k_{1(2)}^\mu k_{1(2)}^\nu\ldots k_{1(2)}^\tau\;f(k_1k,k_2k)\;|_{k_2=q'-k_1}\,. \end{aligned} \tag{C.65}$$

Note that the integral in eq. (C.65) is an integral with a Lorentz-invariant measure over a Lorentz-covariant tensor. Therefore the solution also has to be a Lorentz covariant tensor. Since the integrand only depends on the momenta $k_1^\mu$, $q'^\mu$ and $k^\mu$, where $k_1^\mu$ is integrated over, it is obvious that the solution of this integral can only be a linear combination of tensors containing $g^{\mu\nu}$, $q'^\mu$ and $k^\mu$:

$$I^{\mu\nu\ldots\tau} \;=\; c_1\;g^{\mu\nu}g^{\phi\rho}\ldots g^{\sigma\tau} + c_2\;g^{\mu\nu}g^{\phi\rho}\ldots q'^\tau + \;\ldots\; + c_n\;k^\mu\ldots k^\tau\,. \tag{C.66}$$

Later we will prove that this is in fact the correct ansatz.

As discussed before the integration over the final state tensor is carried out in the CMS. We now have to integrate tensors of different rank in the momentum $k_1^\mu$ over the cosine of the CMS polar angle $\cos\theta_\pi$. In the following useful master integrals are presented which can be used in a FORM program that carries out the integration automatically. We have the scalar integrals

$$\begin{aligned} S_1 \;&:=\; \int d\cos\theta_\pi\;\frac{1}{k_1k}\,, \quad S_2 \;:=\; \int d\cos\theta_\pi\;\frac{1}{(k_1k)^2}\,, \\ S_3 \;&:=\; \int d\cos\theta_\pi\;\frac{1}{(k_1k)(k_2k)}\,, \quad S_4 \;:=\; \int d\cos\theta_\pi\;\frac{k_1k}{k_2k}\,, \\ S_5 \;&:=\; \int d\cos\theta_\pi\;\frac{(k_1k)^2}{k_2k}\,, \quad S_6 \;:=\; \int d\cos\theta_\pi\;\frac{k_1k}{(k_2k)^2}\,. \end{aligned} \tag{C.67}$$

The necessary rank-1 tensor master integrals read

$$\begin{aligned} V_1^\mu &:= \int d\cos\theta_\pi \, \frac{k_1^\mu}{k_1 k} \,, \quad V_2^\mu := \int d\cos\theta_\pi \, \frac{k_1^\mu}{(k_1 k)^2} \,, \\ V_3^\mu &:= \int d\cos\theta_\pi \, \frac{k_1^\mu}{(k_1 k)(k_2 k)} \,. \end{aligned} \tag{C.68}$$

The necessary rank-2 tensor master integrals read

$$\begin{aligned} T_1^{\mu\nu} &:= \int d\cos\theta_\pi \, \frac{k_1^\mu k_1^\nu}{k_1 k} \,, \quad T_2^{\mu\nu} := \int d\cos\theta_\pi \, \frac{k_1^\mu k_1^\nu}{(k_1 k)^2} \,, \\ T_3^{\mu\nu} &:= \int d\cos\theta_\pi \, \frac{k_1^\mu k_1^\nu}{(k_1 k)(k_2 k)} \,. \end{aligned} \tag{C.69}$$

Note that the above rank-2 tensor integrals are symmetric under the exchange of Lorentz indices which makes the integration easier since such integrals can be written as a linear combination of just four linear independent rank-2 tensors. All other necessary integrals can be written as linear combinations of the fundamental integrals listed above. As in the interference case the tensor integrals can be written as linear combinations of tensors only containing the momenta $q'$ and $k$:

$$\begin{aligned} V_1^\mu &:= a_1 \, q'^\mu + a_2 \, k^\mu \,, \\ V_2^\mu &:= b_1 \, q'^\mu + b_2 \, k^\mu \,, \\ V_3^\mu &:= c_1 \, q'^\mu + c_2 \, k^\mu \,, \\ T_1^{\mu\nu} &:= d_1 g^{\mu\nu} + d_2 q'^\mu q'^\nu + d_3 \left( q'^\mu k^\nu + k^\mu q'^\nu \right) + d_4 k^\mu k^\nu \,, \\ T_2^{\mu\nu} &:= e_1 g^{\mu\nu} + e_2 q'^\mu q'^\nu + e_3 \left( q'^\mu k^\nu + k^\mu q'^\nu \right) + e_4 k^\mu k^\nu \,, \\ T_3^{\mu\nu} &:= f_1 g^{\mu\nu} + f_2 q'^\mu q'^\nu + f_3 \left( q'^\mu k^\nu + k^\mu q'^\nu \right) + f_4 k^\mu k^\nu \,. \end{aligned} \tag{C.70}$$

By successively contracting the above equations with the corresponding linear independent covariant tensors we obtain a system of linear equations which allows us to determine the respective constants. First let us give the solution of the scalar

integrals:

$$
\begin{aligned}
S_1 &= \frac{2}{pp_{\gamma_C}\sqrt{s'}\beta'_\pi}\, L'_\pi \quad , \quad S_2 = \frac{8}{pp^2_{\gamma_C} s'(1-\beta'^2_\pi)} = \frac{2}{pp^2_{\gamma_C} m^2_\pi} \, , \\
S_3 &= \frac{4}{pp^2_{\gamma_C} s'\beta'_\pi}\, L'_\pi \quad , \quad S_4 = 2\left[-1+\frac{1}{\beta'_\pi}L'_\pi\right] , \\
S_5 &= pp_{\gamma_C}\sqrt{s'}\left[-3+\frac{2}{\beta'_\pi}L'_\pi\right] , \\
S_6 &= \frac{2}{pp_{\gamma_C}\sqrt{s'}(1-\beta'^2_\pi)}\left[4-\frac{1}{\beta'_\pi}L'_\pi(1-\beta'^2_\pi)\right] \\
&= \frac{2\sqrt{s'}}{pp_{\gamma_C} m^2_\pi}\left[1-\frac{m^2_\pi}{s'\beta'_\pi}L'_\pi\right] , \\
\text{with} \quad L'_\pi &= \log\left(\frac{1+\beta'_\pi}{1-\beta'_\pi}\right) . \qquad \text{(C.71)}
\end{aligned}
$$

Proceeding as described above, to obtain the rank-1 tensor integrals we have to solve the following three linear equation systems:

$$
\begin{aligned}
a_1 s' + a_2\sqrt{s'}pp_{\gamma_C} &= \frac{s'}{2}\, S_1 \, , \quad a_1\sqrt{s'}pp_{\gamma_C} = 2 \qquad \text{(C.72)} \\
b_1 s' + b_2\sqrt{s'}pp_{\gamma_C} &= \frac{s'}{2}\, S_2 \, , \quad b_1\sqrt{s'}pp_{\gamma_C} = S_1 \qquad \text{(C.73)} \\
c_1 s' + c_2\sqrt{s'}pp_{\gamma_C} &= \frac{s'}{2}\, S_3 \, , \quad c_1\sqrt{s'}pp_{\gamma_C} = S_1 \qquad \text{(C.74)}
\end{aligned}
$$

The solutions are

$$
\begin{aligned}
a_1 &= \frac{2}{pp_{\gamma_C}\sqrt{s'}} \quad , \quad a_2 = -\frac{1}{2pp^2_{\gamma_C}}\left[4-pp_{\gamma_C}\sqrt{s'}\, S_1\right] , \qquad \text{(C.75)} \\
b_1 &= \frac{S_1}{pp_{\gamma_C}\sqrt{s'}} = \frac{S_1}{2}a_1 \quad , \quad b_2 = -\frac{1}{2pp^2_{\gamma_C}}\left[2S_1-pp_{\gamma_C}\sqrt{s'}\, S_2\right] , \qquad \text{(C.76)} \\
c_1 &= \frac{S_1}{pp_{\gamma_C}\sqrt{s'}} = \frac{S_1}{2}a_1 \quad , \quad c_2 = -\frac{1}{2pp^2_{\gamma_C}}\left[2S_1-pp_{\gamma_C}\sqrt{s'}\, S_3\right] . \qquad \text{(C.77)}
\end{aligned}
$$

For the rank-2 tensor integrals we get the following three linear equation systems:

$$\begin{array}{llll} 4d_1 & +d_2\ s' & +d_3\ 2pp_{\gamma_C}\sqrt{s'} & = m_\pi^2 S_1 \\ d_1\ s' & +d_2\ s'^2 & +d_3\ 2s'pp_{\gamma_C}\sqrt{s'} \quad +d_4\ pp_{\gamma_C}^2 s' & = s'^2/4\ S_1 \\ d_1\ pp_{\gamma_C}\sqrt{s'} & +d_2\ s'pp_{\gamma_C}\sqrt{s'} & +d_3\ pp_{\gamma_C}^2 s' & = \ s' \\ & d_2\ pp_{\gamma_C}^2 s' & & = \sqrt{s'}pp_{\gamma_C} \end{array} \tag{C.78}$$

$$\begin{array}{llll} 4e_1 & +e_2\ s' & +e_3\ 2pp_{\gamma_C}\sqrt{s'} & = m_\pi^2 S_2 \\ e_1\ s' & +e_2\ s'^2 & +e_3\ 2s'pp_{\gamma_C}\sqrt{s'} \quad +e_4\ pp_{\gamma_C}^2 s' & = s'^2/4\ S_2 \\ e_1\ pp_{\gamma_C}\sqrt{s'} & +e_2\ s'pp_{\gamma_C}\sqrt{s'} & +e_3\ pp_{\gamma_C}^2 s' & = \ s'/2\ S_1 \\ & e_2\ pp_{\gamma_C}^2 s' & & = 2 \end{array} \tag{C.79}$$

$$\begin{array}{llll} 4f_1 & +f_2\ s' & +f_3\ 2pp_{\gamma_C}\sqrt{s'} & = m_\pi^2 S_3 \\ f_1\ s' & +f_2\ s'^2 & +f_3\ 2s'pp_{\gamma_C}\sqrt{s'} \quad +f_4\ pp_{\gamma_C}^2 s' & = s'^2/4\ S_3 \\ f_1\ pp_{\gamma_C}\sqrt{s'} & +f_2\ s'pp_{\gamma_C}\sqrt{s'} & +f_3\ pp_{\gamma_C}^2 s' & = \ s'/2\ S_1 \\ & f_2\ pp_{\gamma_C}^2 s' & & = S_4 \end{array} \tag{C.80}$$

The solutions for the constants are

$$\begin{aligned} d_1 &= -\frac{\sqrt{s'}}{2pp_{\gamma_C}} + \frac{m_\pi^2}{2} S_1\ , \\ d_2 &= \frac{1}{pp_{\gamma_C}\sqrt{s'}} \ \equiv\ \frac{a_1}{2}\ , \\ d_3 &= -\frac{1}{pp_{\gamma_C}\sqrt{s'}} \left[ -\frac{\sqrt{s'}}{2pp_{\gamma_C}} + \frac{m_\pi^2}{2} S_1 \right] \ \equiv\ -d_1 d_2\ , \\ d_4 &= \frac{1}{pp_{\gamma_C}^2} \left[ \frac{s' + 2m_\pi^2}{4} S_1 - \frac{3}{2} \frac{\sqrt{s'}}{pp_{\gamma_C}} \right]\ , \end{aligned} \tag{C.81}$$

$$\begin{aligned} e_1 &= \frac{1}{pp_{\gamma_C}^2} + \frac{m_\pi^2}{2}\ S_2 - \frac{1}{2} \frac{\sqrt{s'}}{pp_{\gamma_C}}\ S_1\ , \\ e_2 &= \frac{2}{pp_{\gamma_C}^2 s'} \ \equiv\ 2\ d_2^2\ , \\ e_3 &= -\frac{1}{pp_{\gamma_C}^2 \sqrt{s'}} \left[ \frac{3}{pp_{\gamma_C}} + \frac{pp_{\gamma_C}}{2} m_\pi^2\ S_2 - \sqrt{s'}\ S_1 \right]\ , \\ e_4 &= \frac{1}{pp_{\gamma_C}^2} \left[ \frac{s' + 2m_\pi^2}{4}\ S_2 + \frac{3}{pp_{\gamma_C}^2} - \frac{3}{2} \frac{\sqrt{s'}}{pp_{\gamma_C}}\ S_1 \right]\ , \end{aligned} \tag{C.82}$$

$$
\begin{aligned}
f_1 &= \frac{1}{pp_{\gamma C}^2}\,\frac{S_4}{2} + \frac{m_\pi^2}{2}\,S_3 - \frac{1}{2}\frac{\sqrt{s'}}{pp_{\gamma C}}\,S_1\ , \\
f_2 &= \frac{S_4}{pp_{\gamma C}^2 s'} \;\equiv\; S_4\,d_2^2\ , \\
f_3 &= -\frac{1}{pp_{\gamma C}^2\sqrt{s'}}\left[\frac{3}{pp_{\gamma C}}\,\frac{S_4}{2} + \frac{pp_{\gamma C}}{2}m_\pi^2\,S_3 - \sqrt{s'}\,S_1\right]\ , \\
f_4 &= \frac{1}{pp_{\gamma C}^2}\left[\frac{s'+2m_\pi^2}{4}\,S_3 + \frac{3}{pp_{\gamma C}^2}\,\frac{S_4}{2} - \frac{3}{2}\frac{\sqrt{s'}}{pp_{\gamma C}}\,S_1\right]\ .
\end{aligned}
\tag{C.83}
$$

We will now write some other necessary tensor integrals as linear combinations of the master integrals presented above:

$$
\begin{aligned}
\int d\cos\theta_\pi \frac{k_1^\mu}{k_2 k} &= q'^\mu\,S_1 - V_1^\mu\ ,\ \int d\cos\theta_\pi \frac{k_1^\mu}{(k_2k)^2} \;=\; q'^\mu\,S_2 - V_2^\mu\ , \\
\int d\cos\theta_\pi \frac{k_1^\mu k_2^\nu}{k_1 k} &= q'^\nu\,V_1^\mu - T_1^{\mu\nu}\ ,\ \int d\cos\theta_\pi \frac{k_1^\mu k_2^\nu}{(k_1k)^2} \;=\; q'^\nu\,V_2^\mu - T_2^{\mu\nu}\ , \\
&\int d\cos\theta_\pi \frac{k_1^\mu k_2^\nu}{(k_1k)(k_2k)} \;=\; q'^\nu\,V_3^\mu - T_3^{\mu\nu}\ .
\end{aligned}
\tag{C.84}
$$

Note that the tensor integration method can easily be extended to other scattering processes also with more final state particles. The above results can also be used for fermion pair production in QED. If we want to consider parity-violating processes like fermion pair production in electroweak theory, in addition we have to take integrals over $\varepsilon$-tensors into account ($\theta_\pi \to \theta_f$):

$$
\int d\cos\theta_f\,\frac{\varepsilon(k_1,k_2,k,\mu)k_1^\nu}{(k_1k)(k_2k)} = T_3^{\alpha\nu}\varepsilon(\alpha,q',k,\mu)\ , \tag{C.85}
$$

$$
\int d\cos\theta_f\,\frac{\varepsilon(k_1,k_2,k,\mu)k_2^\nu}{(k_1k)(k_2k)} = T_3^{\beta\nu}\varepsilon(q',\beta,k,\mu)\ , \tag{C.86}
$$

$$
\int d\cos\theta_f\,\frac{\varepsilon(k_1,k_2,\mu,\nu)}{(k_1k)^2} = \varepsilon(V_2,q',\mu,\nu)\ , \tag{C.87}
$$

$$
\int d\cos\theta_f\,\frac{\varepsilon(k_1,k_2,\mu,\nu)}{(k_1k)(k_2k)} = \varepsilon(V_3,q',\mu,\nu)\ , \tag{C.88}
$$

$$
\int d\cos\theta_f\,\frac{\varepsilon(k_1,k_2,\mu,\nu)}{k_1k} = \varepsilon(V_1,q',\mu,\nu)\ , \tag{C.89}
$$

$$
\int d\cos\theta_f\,\frac{\varepsilon(k_1,k,\mu,\nu)}{(k_1k)(k_2k)} = \varepsilon(V_3,k,\mu,\nu)\ , \tag{C.90}
$$

$$
\int d\cos\theta_f\,\frac{\varepsilon(k_1,k,\mu,\nu)}{(k_2k)^2} = S_2\,\varepsilon(q',k,\mu,\nu) - \varepsilon(V_2,k,\mu,\nu)\ , \tag{C.91}
$$

$$
\int d\cos\theta_f\,\frac{\varepsilon(k_1,k,\mu,\nu)}{k_2k} = S_1\,\varepsilon(q',k,\mu,\nu) - \varepsilon(V_1,k,\mu,\nu)\ . \tag{C.92}
$$

The tensor integration method was also used in [112] to obtain the real photon IFS interference contribution to the spectral function of fermion pair production. Making the exchange $k_1 \leftrightarrow k_2$ does not change all the integrals discussed above.

We will show now that the solution of the tensor integrals can always be written in the form of eq. (C.66) which means that no contribution from possible linear independent tensors have been forgotten. Recall eq. (C.65). From Lorentz invariance and Lorentz covariance follows that the solution for $I^{\mu\nu\ldots\tau}$ has to be true in any coordinate system. It is therefore possible to choose the CMS ($\vec{q'} = 0$). In addition $\vec{k}_1$ will be chosen to point into the positive $z$-direction. The momentum $\vec{k}$ can always be chosen in the $x$-$z$ plane, forming the angle $\theta_\pi$ with $\vec{k}_1$:

$$\begin{aligned} q^{'\mu} &= \sqrt{s'}(1,0,0,0)\ , \quad k_1^\mu = \frac{\sqrt{s'}}{2}(1.0,0,\beta'_\pi)\ , \\ k^\mu &= pp_\gamma(1,-\sin\theta_\pi,0,\cos\theta_\pi)\ . \end{aligned} \tag{C.93}$$

Since $k_2 = q' - k_1$, the integrand in eq. (C.65) can be written as a covariant tensor containing only $q'$ and $k_1$. In the CMS the integral is then of the form:

$$\begin{aligned} I^{\mu\nu\ldots\tau} &\propto \int_{\mathrm{CMS}} d\cos\theta_\pi\ q^{'\mu}\ldots q^{'\rho} k_1^\sigma \ldots k_1^\tau\ f(k_1k)\ , \\ &= q^{'\mu}\ldots q^{'\rho} \int_{\mathrm{CMS}} d\cos\theta_\pi\ k_1^\sigma \ldots k_1^\tau\ f(k_1k)\ . \end{aligned} \tag{C.94}$$

Thus, since in the CMS by definition $q'$ does not depend on any angles, it can be pulled in front of the integral. This leaves us an integral over a tensor only containing the momentum $k_1^\mu$. Therefore it is sufficient to prove that the tensor-ansatz (C.66) is correct for integrals of the following type:

$$J^{\mu\ldots\tau} = \int_{\mathrm{CMS}} d\cos\theta_\pi\ k_1^\mu \ldots k_1^\tau\ f(k_1k)\ . \tag{C.95}$$

Note that this integral is now symmetric under the exchange of Lorentz indices. Obviously if the ansatz in eq. (C.66) is correct we can now make the ansatz to write the integral in eq. (C.95) as a linear combination of all linear independent, covariant tensors of the same rank as $J^{\mu\ldots\tau}$, containing the metric tensor $g^{\mu\nu}$ as well as $q^{'\mu}$ and $k^\mu$ which are symmetric under the exchange of Lorentz indices:

$$\begin{aligned} J^{\mu\ldots\tau} &\equiv T^{\mu\ldots\tau}\ , \quad \text{with} \\ T^{\mu\ldots\tau} &= a_1\ g^{\mu\nu}\ldots g^{\sigma\tau} + \ldots\ldots\ldots + a_n\ k^\mu \ldots k^\tau\ . \end{aligned} \tag{C.96}$$

To prove that this is really the most general ansatz let us assume that there are additional tensor contributions that have to be taken into account, containing an arbitrary 4-vector $A^\mu$ which cannot be written as a linear combination of $q^{'\mu}$ and $k^\mu$. Hence $A^\mu$ is also independent of the angular integration. For our choice of the

coordinate system also the scalar products $A_\mu k_1^\mu$ and $q'_\mu k_1^\mu$ do not depend on the angular integration. Let us now make the modified ansatz:

$$J^{\mu\ldots\tau} = T^{\mu\ldots\tau}(q'^\mu, k^\mu) + \tilde{T}^{\mu\ldots\tau}(q'^\mu, k^\mu, A^\mu) , \tag{C.97}$$

where $\tilde{T}^{\mu\ldots\tau}$ is the additional contribution, depending on $A^\mu$. If in eq. (C.96) the ansatz is correct this additional contribution has to vanish. Contracting eq. (C.97) successively with $A_\mu$ and $q'_\mu$ leads to the following two equations:

$$\frac{Ak_1}{q'k_1}\, q'_\mu J^{\mu\ldots\tau} = A_\mu(T^{\mu\ldots\tau} + \tilde{T}^{\mu\ldots\tau}) \tag{C.98}$$

$$q'_\mu J^{\mu\ldots\tau} = q'_\mu(T^{\mu\ldots\tau} + \tilde{T}^{\mu\ldots\tau}) . \tag{C.99}$$

In eq. (C.98) it was used that the scalar products $A_\mu k_1^\mu$ and $q'_\mu k_1^\mu$ are not affected by the angular integration. Multiplying now eq. (C.99) by $Ak_1/q'k_1$ and subtracting (C.99) from (C.98) yields:

$$\left(A_\mu - \frac{Ak_1}{q'k_1} q'_\mu\right)(T^{\mu\ldots\tau} + \tilde{T}^{\mu\ldots\tau}) = 0 . \tag{C.100}$$

Since $A^\mu$ was assumed to be linear independent of $q'^\mu$ eq. (C.100) can only be valid if

$$J^{\mu\ldots\tau} = 0 , \tag{C.101}$$

which is obviously in general not the case. Hence a necessary condition for the modified ansatz in eq. (C.97) to be correct is

$$A_\mu - \frac{Ak_1}{q'k_1} q'_\mu = 0 , \tag{C.102}$$

which is in contradiction to the assumption that $A^\mu$ is linear independent of $q'^\mu$. This finally proves that the tensor-ansatz in eq. (C.66) is indeed the correct ansatz and no additional linear independent tensors contribute to the tensor integral. □

# Bibliography


[1] S. Tomonaga. *Prog. Theor. Phys.*, 1:27, 1946.

[2] S. Tomonaga. *Phys. Rev.*, 74:224, 1948.

[3] J. Schwinger. *Phys. Rev.*, 75:651, 1949.

[4] J. Schwinger. *Phys. Rev.*, 76:790, 1949.

[5] R. P. Feynman. *Phys. Rev.*, 76:749–759, 1949.

[6] R. P. Feynman. *Phys. Rev.*, 76:769–789, 1949.

[7] S. Laporta and E. Remiddi. The electron (g(e)-2) and the value of alpha: A check of qed at 1 ppb. *Acta Phys. Polon.*, B28:959, 1997.

[8] V. W. Hughes and T. Kinoshita. Anomalous g values of the electron and muon. *Rev. Mod. Phys.*, 71:S133, 1999.

[9] R. S. Van Dyck, P. B. Schwinberg, and H. G. Dehmelt. New high precision comparison of electron and positron g factors. *Phys. Rev. Lett.*, 59:26–29, 1987.

[10] P. J. Mohr and B.N. Taylor. *Rev. Mod. Phys.*, 72:351, 2000.

[11] Toichiro Kinoshita. The fine structure constant. *Rept. Prog. Phys.*, 59:1459–1492, 1996.

[12] H. N. Brown et al. Precise measurement of the positive muon anomalous magnetic moment. *Phys. Rev. Lett.*, 86:2227–2231, 2001.

[13] J. Bailey et al. Final report on the cern muon storage ring including the anomalous magnetic moment and the electric dipole moment of the muon, and a direct test of relativistic time dilation. *Nucl. Phys.*, B150:1, 1979.

[14] Andrzej Czarnecki and William J. Marciano. Lepton anomalous magnetic moments: A theory update. 1998.

[15] S. Laporta and E. Remiddi. The analytical value of the electron (g-2) at order alpha 3 in qed. *Phys. Lett.*, B379:283–291, 1996.

[16] T. Kinoshita, B. Nizic, and Y. Okamoto. Eighth order qed contribution to the anomalous magnetic moment of the muon. *Phys. Rev.*, D41:593–610, 1990.

[17] T. Kinoshita, B. Nizic, and Y. Okamoto. Hadronic contributions to the anomalous magnetic moment of the muon. *Phys. Rev.*, D31:2108, 1985.

[18] S. Eidelman and F. Jegerlehner. Hadronic contributions to g-2 of the leptons and to the effective fine structure constant alpha (m(z)**2). *Z. Phys.*, C67:585–602, 1995.

[19] Fred Jegerlehner. Hadronic contributions to the photon vacuum polarization and their role in precision physics. 2001.

[20] Johan Bijnens, Elisabetta Pallante, and Joaquim Prades. Analysis of the hadronic light-by-light contributions to the muon $g-2$. *Nucl. Phys.*, B474:379–420, 1996.

[21] M. Hayakawa and T. Kinoshita. Pseudoscalar pole terms in the hadronic light-by-light scattering contribution to muon g-2. *Phys. Rev.*, D57:465–477, 1998.

[22] R. Jackiw and S. Weinberg. Weak interaction corrections to the muon magnetic moment and to muonic atom energy levels. *Phys. Rev.*, D5:2396–2398, 1972.

[23] G. Altarelli, N. Cabibbo, and L. Maiani. The drell-hearn sum rule and the lepton magnetic moment in the weinberg model of weak and electromagnetic interactions. *Phys. Lett.*, B40:415, 1972.

[24] I. Bars and M. Yoshimura. Muon magnetic moment in a finite theory of weak and electromagnetic interaction. *Phys. Rev.*, D6:374–376, 1972.

[25] W. A. Bardeen, R. Gastmans, and B. Lautrup. Static quantities in weinberg's model of weak and electromagnetic interactions. *Nucl. Phys.*, B46:319–331, 1972.

[26] Andrzej Czarnecki, Bernd Krause, and William J. Marciano. Electroweak fermion loop contributions to the muon anomalous magnetic moment. *Phys. Rev.*, D52:2619–2623, 1995.

[27] T. V. Kukhto, E. A. Kuraev, Z. K. Silagadze, and A. Schiller. The dominant two loop electroweak contributions to the anomalous magnetic moment of the muon. *Nucl. Phys.*, B371:567–596, 1992.

[28] Santiago Peris, Michel Perrottet, and Eduardo de Rafael. Two loop electroweak corrections to the muon g-2: A new class of hadronic contributions. *Phys. Lett.*, B355:523–530, 1995.

[29] Stephan Narison. Muon and tau anomalies updated. *Phys. Lett.*, B513:53–70, 2001.

[30] J. F. De Troconiz and F. J. Yndurain. Precision determination of the pion form factor and calculation of the muon g-2. 2001.

[31] Gorazd Cvetic, Taekoon Lee, and Ivan Schmidt. Resummations with renormalon effects for the leading hadronic contribution to the muon (g-2). 2001.

[32] Andrzej Czarnecki and William J. Marciano. The muon anomalous magnetic moment: A harbinger for 'new physics'. 2001.

[33] Michel Davier and Andreas Hocker. New results on the hadronic contributions to alpha(m(z)**2) and to (g-2)(mu). *Phys. Lett.*, B435:427–440, 1998.

[34] Kirill Melnikov. On the theoretical uncertainties in the muon anomalous magnetic moment. 2001.

[35] F. J. Yndurain. Disagreement between standard model and experiment for muon g-2? 2001.

[36] J. A. Grifols and A. Mendez. Constraints on supersymmetric particle masses from (g-2) mu. *Phys. Rev.*, D26:1809, 1982.

[37] John Ellis, John Hagelin, and D. V. Nanopoulos. Spin 0 leptons and the anomalous magnetic moment of the muon. *Phys. Lett.*, B116:283, 1982.

[38] R. Barbieri and L. Maiani. The muon anomalous magnetic moment in broken supersymmetric theories. *Phys. Lett.*, B117:203, 1982.

[39] David A. Kosower, Lawrence M. Krauss, and Norisuke Sakai. Low-energy supergravity and the anomalous magnetic moment of the muon. *Phys. Lett.*, B133:305, 1983.

[40] T. C. Yuan, R. Arnowitt, A. H. Chamseddine, and Pran Nath. Supersymmetric electroweak effects on g-2 (mu). *Zeit. Phys.*, C26:407, 1984.

[41] R. M. Francis, M. Frank, and C. S. Kalman. Anomalous magnetic moment of the muon arising from the extensions of the supersymmetric standard model based on left-right symmetry. *Phys. Rev.*, D43:2369–2385, 1991.

[42] Takeo Moroi. The muon anomalous magnetic dipole moment in the minimal supersymmetric standard model. *Phys. Rev.*, D53:6565–6575, 1996.

[43] Andrea Brignole, Elena Perazzi, and Fabio Zwirner. On the muon anomalous magnetic moment in models with a superlight gravitino. *JHEP*, 09:002, 1999.

[44] M. Carena, G. F. Giudice, and C. E. M. Wagner. Constraints on supersymmetric models from the muon anomalous magnetic moment. *Phys. Lett.*, B390:234–242, 1997.

[45] Debrupa Chakraverty, Debajyoti Choudhury, and Anindya Datta. A non-supersymmetric resolution of the anomalous muon magnetic moment. 2001.

[46] T. Huang, Z. H. Lin, L. Y. Shan, and X. Zhang. Muon anomalous magnetic moment and lepton flavor violation. 2001.

[47] S. N. Gninenko and N. V. Krasnikov. The muon anomalous magnetic moment and a new light gauge boson. 2001.

[48] Ernest Ma and Martti Raidal. Neutrino mass, muon anomalous magnetic moment, and lepton flavor nonconservation. 2001.

[49] Zhao-Hua Xiong and Jin Min Yang. Muon anomalous magnetic moment in technicolor models. 2001.

[50] Athanasios Dedes and Howard E. Haber. Can the higgs sector contribute significantly to the muon anomalous magnetic moment? 2001.

[51] John Ellis, D. V. Nanopoulos, and Keith A. Olive. Combining the muon anomalous magnetic moment with other constraints on the cmssm. 2001.

[52] Xavier Calmet, Harald Fritzsch, and Dirk Holtmannspotter. The anomalous magnetic moment of the muon and radiative lepton decays. 2001.

[53] Stephen P. Martin and James D. Wells. Muon anomalous magnetic dipole moment in supersymmetric theories. 2001.

[54] K. Agashe, N. G. Deshpande, and G. H. Wu. Can extra dimensions accessible to the sm explain the recent measurement of anomalous magnetic moment of the muon? 2001.

[55] Howard Baer, Csaba Balazs, Javier Ferrandis, and Xerxes Tata. Impact of muon anomalous magnetic moment on supersymmetric models. 2001.

[56] L. Michel C. Bouchiat. *J. Phys. Radium 22*, 1961.

[57] M. Gourdin and E. De Rafael. Hadronic contributions to the muon g-factor. *Nucl. Phys.*, B10:667–674, 1969.

[58] N. Cabibbo and R. Gatto. Electron positron colliding beam experiments. *Phys. Rev.*, 124:1577–1595, 1961.

[59] F. Jegerlehner. Hadronic contributions to electroweak parameter shifts: A detailed analysis. *Z. Phys.*, C32:195, 1986.

[60] T. Kinoshita, B. Nizic, and Y. Okamoto. Improved theory of the muon anomalous magnetic moment. *Phys. Rev. Lett.*, 52:717, 1984.

[61] Ricard Alemany, Michel Davier, and Andreas Hocker. Improved determination of the hadronic contribution to the muon (g-2) and to alpha(m(z)**2) using new data from hadronic tau decays. *Eur. Phys. J.*, C2:123–135, 1998.

[62] F. Jegerlehner. Hadronic effects in (g-2)(mu) and alpha(qed)(m(z)): Status and perspectives. 1999.

[63] M. N. Achasov et al. Experiments at vepp-2m with snd detector. 1998.

[64] R. R. Akhmetshin et al. Measurement of $e^+e^- \to \pi^+\pi^-$ cross- section with cmd-2 around $\rho$ meson. 1999.

[65] M. N. Achasov et al. Resent results from snd detector at vepp-2m. 2000.

[66] Zhi-Peng Zheng. Results from the bes. *Int. J. Mod. Phys.*, A15:4723–4737, 2000.

[67] H. Czyz and J. H. Kuhn. Four pion final states with tagged photons at electron positron colliders. *Eur. Phys. J.*, C18:497–509, 2001.

[68] (ed. ) L. Maiani, (ed. ) G. Pancheri, and (ed. ) N. Paver. The daphne physics handbook. vol. 1, 2. Frascati, Italy: INFN (1992) 611 p.

[69] (ed. ) L. Maiani, (ed. ) G. Pancheri, and (ed. ) N. Paver. The second daphne physics handbook. vol. 1, 2. Frascati, Italy: INFN (1995) 1202 p.

[70] A. Antonelli. Hadronic physics at daphne with the kloe detector. Prepared for 3rd Biennial Conference on Low-Energy Antiproton Physics (LEAP 94), Bled, Slovenia, 12-17 Sep 1994.

[71] M. Benayoun, S. I. Eidelman, V. N. Ivanchenko, and Z. K. Silagadze. Spectroscopy at b-factories using hard photon emission. *Mod. Phys. Lett.*, A14:2605–2614, 1999.

[72] J. Z. Bai et al. Measurements of the cross section for e+ e –¿ hadrons at center-of-mass energies from 2-gev to 5-gev. 2001.

[73] G. S. Huang. New r values in 2-gev - 5-gev from the beijing spectrometer. 2001.

[74] S. Spagnolo. The hadronic contribution to the muon g-2 from hadron production in initial state radiation events at the e+ e- collider daphne. *Eur. Phys. J.*, C6:637, 1999.

[75] G. Cataldi, A. Denig, W. Kluge, S. Muller, and G. Venanzoni. Measurement of the hadronic cross section with kloe using a radiated photon in the initial state.

[76] S. Binner, J. H. Kuhn, and K. Melnikov. Measuring sigma(e+ e- –¿ hadrons) using tagged photon. *Phys. Lett.*, B459:279, 1999.

[77] A. B. Arbuzov, E. A. Kuraev, N. P. Merenkov, and L. Trentadue. Hadronic cross-sections in electron positron annihilation with tagged photon. *JHEP*, 12:009, 1998.

[78] M. I. Konchatnij and N. P. Merenkov. Scanning of hadron cross-section at daphne by analysis of initial-state radiative events. *JETP Lett.*, 69:811, 1999.

[79] V. A. Khoze et al. Radiative corrections to the hadronic cross-section measurement at daphne. *Eur. Phys. J.*, C18:481–490, 2001.

[80] F. A. Berends, W. L. van Neerven, and G. J. H. Burgers. Higher order radiative corrections at lep energies. *Nucl. Phys.*, B297:429, 1988.

[81] A. Hoefer, J. Gluza, and F. Jegerlehner. Pion pair production with higher order radiative corrections in low energy e+ e- collisions. 2001.

[82] F. Bloch and A. Nordsieck. Note on the radiation field of the electron. *Phys. Rev.*, 52:54–59, 1937.

[83] D. R. Yennie, S. C. Frautschi, and H. Suura. The infrared divergence phenomena and high-energy processes. *Ann. Phys.*, 13:379–452, 1961.

[84] S. Pokorski. Gauge field theories. Cambridge, Uk: Univ. Pr. ( 1987) 394 P. ( Cambridge Monographs On Mathematical Physics).

[85] Fred Jegerlehner. Renormalizing the standard model. Lectures given at the Theoretical Advanced Study Institute in Elementary Particle Physics, (TASI), Boulder, Colo., Jun 3-29, 1990.

[86] J. C. Collins. Renormalization. an introduction to renormalization, the renormalization group, and the operator product expansion. Cambridge, Uk: Univ. Pr. ( 1984) 380p.

[87] M. E. Peskin and D. V. Schroeder. An introduction to quantum field theory. Reading, USA: Addison-Wesley (1995) 842 p.

[88] G. Bonneau and F. Martin. Hard photon emission in e+ e- reactions. *Nucl. Phys.*, B27:381–397, 1971.

[89] Bastian Kubis and Ulf-G. Meissner. Virtual photons in the pion form factors and the energy- momentum tensor. *Nucl. Phys.*, A671:332–356, 2000.

[90] G. J. Gounaris and J. J Sakurai. Finite width corrections to the vector meson dominance prediction for rho → e+ e-. *Phys. Rev. Lett.*, 21:244, 1968.

[91] J. H. Kuhn and A. Santamaria. Tau decays to pions. *Z. Phys.*, C48:445–452, 1990.

[92] M. Benayoun et al. New results in $\rho^0$ meson physics. *Eur. Phys. J.*, C2:269, 1998.

[93] J. A. Casas, C. Lopez, and F. J. Yndurain. Hadronic contributions to the g - 2 of the muon. *Phys. Rev.*, D32:736–742, 1985.

[94] Francisco Guerrero and Antonio Pich. Effective field theory description of the pion form factor. *Phys. Lett.*, B412:382–388, 1997.

[95] J. Bijnens, G. Colangelo, and P. Talavera. The vector and scalar form factors of the pion to two loops. *JHEP*, 05:014, 1998.

[96] G. Colangelo, J. Gasser, and H. Leutwyler. pi pi scattering. *Nucl. Phys.*, B603:125–179, 2001.

[97] A. B. Arbuzov et al. Radiative corrections for pion and kaon production at e+ e- colliders of energies below 2-gev. *JHEP*, 10:006, 1997.

[98] J. A. M. Vermaseren. The symbolic manipulation program form. KEK-TH-326.

[99] A. Quenzer et al. Pion form-factor from 480-mev to 1100-mev. (talk). *Phys. Lett.*, B76:512–516, 1978.

[100] T. Kinoshita. Mass singularities of feynman amplitudes. *J. Math. Phys.*, 3:650–677, 1962.

[101] T. D. Lee and M. Nauenberg. Degenerate systems and mass singularities. *Phys. Rev.*, 133:B1549, 1964.

[102] Julian S. Schwinger. Particles, sources, and fields. vol. 3. REDWOOD CITY, USA: ADDISON-WESLEY (1989) 318 P. (ADVANCED BOOK CLASSICS SERIES).

[103] Manuel Drees and Ken-ichi Hikasa. Scalar top production in e+ e- annihilation. *Phys. Lett.*, B252:127–134, 1990.

[104] Guido Montagna, Oreste Nicrosini, and Fulvio Piccinini. The qed radiator at order alpha**3. *Phys. Lett.*, B406:243–248, 1997.

[105] B. A. Kniehl, M. Krawczyk, J. H. Kuhn, and R. G. Stuart. Hadronic contributions to o (alpha**2) radiative corrections in e+ e- annihilation. *Phys. Lett.*, B209:337, 1988.

[106] A. B. Arbuzov. Light pair corrections to electron positron annihilation at lep/slc. 1999.

[107] M. Skrzypek. *Acta. Phys. Pol.*, B23:135, 1992.

[108] S. Jadach, B. F. L. Ward, and Z. Was. The precision monte carlo event generator kk for two- fermion final states in e+ e- collisions. *Comput. Phys. Commun.*, 130:260, 2000.

[109] German Rodrigo, Aude Gehrmann-De Ridder, Marc Guilleaume, and Johann H. Kuhn. Nlo qed corrections to isr in e+ e- annihilation and the measurement of sigma(e+ e- –¿ hadrons) using tagged photons. 2001.

[110] G. Kopp and F. Kruger. Introduction to quantum electrodynamics. (in german). Stuttgart, Germany: Teubner (1997) 373 p.

[111] P. Van Nieuwenhuizen. Muon-electron scattering cross section to order alpha-to- the-third. *Nucl. Phys.*, B28:429–454, 1971.

[112] M. Jack, A. Hoefer, A. Leike, and T. Riemann. Predictions for fermion pair production at e+ e- colliders. *Nucl. Phys. Proc. Suppl.*, 89:15, 2000.

# Acknowledgements

In the first place I would like to thank my advisor Prof. Dr. Fred Jegerlehner for his personal and technical support and very interesting and illuminating discussions during my stay at DESY Zeuthen.

I am grateful to Prof. Dr. Ulrich Wolff for kindly acting as the official supervisor of my thesis.

I would like to thank the DESY institute for giving me the opportunity to prepare my thesis at DESY Zeuthen.

Many thanks also to my collaborator Dr. Janusz Gluza for the very nice and productive time we were working together. We were a good team!

I would like to thank Dr. Tord Riemann for numerous very useful discussions from which I profited a lot.

Many thanks also to my colleagues Dr. Jochen Biebel, Dr. Claus-Jochen Biebl, Dr. Johannes Blümlein, Thomas Chiarappa, Dr. Christopher Ford, Dr. Marco Guagnelli, Dr. Stefan Herrlich, Dr. Francesco Knechtli, Dr. José Illana, Dr. Mark Jack, Dr. Karl Jansen, Dr. Hans Kaiser, Dr. Mikhail Kalmykov, Dr. Hiroyuki Kawamura, Dr. Martin Kurth, Stefan Kurth, Alejandro Lorca, Heiko Molke, Silvia Necco, Dr. Andreas Nyffeler, Dr. Kurt Riesselmann, Dr. Stephan Riemersma, Dr. Hubert Simma, Dr. Rainer Sommer, Dr. Oleg Tarasov, Dr. Avto Tkabladze, Dr. Ravindran Vajravelu, Dr. Oleg Veretin, Dr. Alessandro Vicini, Dr. Gerhard Weigt and Dr. Anja Werthenbach for interesting discussions and a nice time together in Zeuthen.

I also would like to thank Dr. Arnd Leike with whom I had the pleasure to collaborate in a small project together with Tord Riemann and Mark Jack.

Christopher Ford I would like to thank for reading the manuscript.

Finally I would like to thank my parents for their moral support.

# Curriculum Vitae

| | |
|---|---|
| Name | Axel Hoefer |
| Geburtstag | 10.2.1970 |
| Geburtsort | Ekeren (Belgien) |
| 09/76 - 07/83 | Besuch der Deutschen Schule Antwerpen (Belgien) |
| 09/83 - 07/88 | Besuch der Europäischen Schule Mol (Belgien) |
| | Abschluss: Abitur |
| 09/80 - 06/90 | Besuch der Muziekakademie Ekeren-Antwerpen |
| | Abschluss: Diplom (Instrument: Violine) |
| 10/88 - 07/96 | Physikstudium an der RWTH Aachen |
| 9/93 - 10/95 | Diplomarbeit bei Prof. Dr. L. M. Sehgal |
| 07/96 | Abschluss: Diplom (Gesamturteil “sehr gut”) |
| Seit 10/96 | Doktorand bei Prof. Dr. U. Wolff, Humbold-Universität zu Berlin |
| | und Prof. Dr. F. Jegerlehner, DESY Zeuthen |

# Publications

**1.** Axel Hoefer and Lalit Mohan Sehgal,
"Pair production and correlated decay of heavy Majorana neutrinos in $e^+e^-$ collisions",
*Phys. Rev.*, **D54**:1944–1954, 1996
(hep-ph/9603240).

**2.** Axel Hoefer,
"On the possibilities of distinguishing Majorana from Dirac neutrinos",
1997 (hep-ph/9705362).

**3.** Mark Jack, Axel Hoefer, Arnd Leike and Tord Riemann,
"Predictions for fermion pair production at $e^+e^-$ colliders",
*Nucl. Phys. Proc. Suppl.*, 89:15, 2000,
(hep-ph/0007046).

**4.** Axel Hoefer, Janusz Gluza and Fred Jegerlehner,
"Pion pair production with higher order radiative corrections in low energy $e^+e^-$ collisions",
2001 (to be published in *Eur. Phys. J.* **C**),
(hep-ph/0107154).